Analytic Representations of Finite Quantum Systems on a Torus

Muna Jabuni

Submitted for the Degree
of Doctor of Philosophy

Department of Computing
University of Bradford

2010

Abstract

Quantum systems with a finite Hilbert space, where position x and momentum p take values in $\mathbb{Z}(d)$ (integers modulo d), are studied. An analytic representation of finite quantum systems is considered. Quantum states are represented by analytic functions on a torus. This function has exactly d zeros, which define uniquely the quantum state. The analytic function of a state can be constructed using its zeros. As the system evolves in time, the d zeros follow d paths on the torus. Examples of the paths $\zeta_n(t)$ of the zeros, for various Hamiltonians, are given. In addition, for given paths $\zeta_n(t)$ of the d zeros, the Hamiltonian is calculated. Furthermore, periodic finite quantum systems are considered. Special cases where $\mathfrak{M}$ of the zeros follow the same path are also studied, and general ideas are demonstrated with several examples. Examples of the path with multiplicity $\mathfrak{M} = 1, 2, 3, 4, 5$ are given. It is evidenced within the study that a small perturbation of the initial values of the zeros splits a path with multiplicity $\mathfrak{M}$ into $\mathfrak{M}$ different paths.

Dedicated to my loving Mum ...

keeps inspiring me!

Acknowledgements

My deepest thanks firstly go to God, who created me, helps me and has given me the ability to reach this stage.

I would like to thank Professor Apostolos Vourdas, my advisor, for his great support and guidance during this research. His inspiring suggestions and constant encouragement have had a great effect on my study, and I count myself fortunate to have been given the valuable opportunity to work under his supervision throughout this journey.

I would also like to thank all members of the Quantum Information research group in the school. Many thanks go also to my research colleagues for their invaluable discussions, as well as the School of Computing, Informatics and Media at the University of Bradford for the financial and technical support and all the staff who helped me during my study.

I should also mention that my research study in the UK was sponsored totally by Libyan Cultural Affairs.

Finally, I give gratitude to my loving mum for her encouragement, support and patience.

Declaration

Some parts of the work presented in this thesis have been published in the following article:

M. Tubani, A. Vourdas, S. Zhang "Zeros in analytic representations of finite quantum systems on a torus",Phys. Scr., to appear (2010)

Table of Contents

Chapter 1

Introduction

This thesis is devoted to the study of zeros of analytic representations for finite quantum systems on a torus (the phase space is $\mathbb{Z}_d \times \mathbb{Z}_d$) and the time evolution of these zeros. Various Hamiltonians and initial states are considered.

Analytic functions have been used in various contexts in quantum mechanics [1, 2, 3]. The Bargmann function in the complex plane [4, 5, 6] is perhaps the most popular of these, and is an important tool for studying the overcompleteness of coherent states [7] and has been used in the context of semiclassical methods [8, 9, 10, 11] and chaotic systems [12]. Especially the zeros of Bargmann functions, which are also the zeros of the Q or Husimi function (sometimes called 'Husimi zeros' or 'stellar representation'), have been used in the study of several models [13, 14, 15, 16, 17, 18, 19]. Recently, there has been a lot of work on quantum systems whereby the position and momentum take values in $\mathbb{Z}_d$ (the integers modulo d). A review with many references is given in [20]. Ref [21, 22] studied an analytic representation for

these systems on a torus, using Theta functions. It was shown that the analytic function representing a quantum state has exactly d number of zeros in any such square region (which obey a constraint), and that these zeros define uniquely the quantum state. In this thesis, we extend this work.

We consider the time evolution of the system and the motion of the d zeros on the torus. The d paths $\zeta_n(t)$ of the d zeros define completely the finite quantum system. For example, from the $\zeta_n(t)$ we can calculate the Hamiltonian and the quantum states. In this sense, the paths of the zeros provide an alternative description for the standard quantum formalism, for finite quantum systems. In infinite dimensional systems, the paths of the zeros do not define uniquely the quantum system (this is related to Hadamard's theorem [2]). We demonstrate these general ideas with various concrete examples. Further, we consider various Hamiltonians and initial states, and we calculate the d paths of the zeros. Using its zeros, the analytic function of a state can be constructed. We also consider the inverse problem, where the paths of the zeros are given, and we calculate the Hamiltonian.

An important special case relates to periodic systems. The Hamiltonians in periodic systems have commensurate eigenvalues. In this case, the paths of the zeros are closed paths. Interesting results show that in some cases $\mathfrak{M}$ of d zeros follow the same path, in which instance we say that this path has multiplicity $\mathfrak{M}$. We consider this in more detail and show that after a period the zeros exchange their positions.

Furthermore, we give a brief introduction to the Symplectic transformations into the $\mathbb{Z}_d \times \mathbb{Z}_d$ phase space of a finite quantum system. We consider the effect of a change in the basis on the zeros using Symplectic transforma-

tions.

1.1 Structure of this thesis

This thesis consists of six chapters. This first chapter is an introduction to the thesis.

Chapter 2 gives a review on phase space methods for quantum particles on a real line. A number of fundamental aspects in quantum systems with a continuous Hilbert space are discussed. The Wigner and Weyl functions are introduced, while the Bargmann analytic representation in the complex plane is studied. In addition the Husimi function is introduced.

Chapter 3 gives a brief introduction to finite quantum systems. We discuss the analytic representation and its zeros, after which various Hamiltonians and initial states are considered.

Chapter 4 discusses periodic systems and discusses examples where two or more zeros follow the same path.

In chapter 5, The Symplectic transformations into the $\mathbb{Z}_d \times \mathbb{Z}_d$ phase space of a finite quantum system are introduced. The effect of a change in the basis on the zeros using Symplectic transformations is studied. various examples have been given.

Finally, we conclude in Chapter 6 with a discussion of our results.

Chapter 2

Quantum Systems on a Real Line

2.1 Introduction

In this chapter, we consider the phase space methods used to describe the states of quantum particles on a real plane $\mathbb{R}$. The standard Dirac notation $|\psi\rangle$ is used for a quantum state in this case.

Quantum mechanics for a particle on a real line is defined in terms of a pair of hermitian operators $\hat{x}$ (position operator) and $\hat{p}$ (momentum operator), which satisfy the canonical commutation relation

$$[\hat{x}, \hat{p}] \;=\; i. \tag{2.1}$$

We are going to set Planck's constant $\hbar = 1$ for simplicity. The position operator $\hat{x}$ and momentum operator $\hat{x}$ obey the relation

$$\hat{x}\psi(x) = x\psi(x), \quad \hat{p}\psi(x) = -i\frac{\partial}{\partial x}\psi(x), \tag{2.2}$$

where $\psi(x)$ is the wave function of the particle in the position representation. The position and momentum take real values, so the phase space is a $\mathbb{R} \times \mathbb{R}$ plane.

In the next section, we introduce basic formalism of the $\mathbb{R} \times \mathbb{R}$ phase space.

Section 2.3 gives a brief introduction to the basic formalism of a one-dimensional linear harmonic oscillator, including expressions of some special states such as number states, displacement and parity operators, coherent states, and the Wigner and Weyl functions.

In section 2.4, we give a brief introduction to the Bargmann analytic representation in the complex plane, which is defined by the Glaubar coherent states, including a brief introduction to the P and Q functions.

2.2 Position and Momentum

In this section, we investigate the position operator $\hat{x}$ and the momentum operator $\hat{p}$ in more detail. These operators satisfy the Dirac quantum condition in Eq. (2.1), as it is well known that the eigenstates of $\hat{x}$ and $\hat{p}$ form the basis for the representation of a quantum system. Let $|x\rangle$ be the position eigenstates and $|p\rangle$ the momentum eigenstates, they satisfy

$$\hat{x}|x\rangle = x|x\rangle, \tag{2.3}$$

$$\hat{p}|p\rangle = p|p\rangle, \tag{2.4}$$

where x and p are real numbers (their operators are hermitian). They both form orthogonal (not normalised) bases for the Hilbert space $L^2(\mathbb{R})$ and they satisfy

$$\langle x|x^{'}\rangle = \delta(x - x^{'}), \tag{2.5}$$

$$\langle p|p^{'}\rangle = \delta(p - p^{'}), \tag{2.6}$$

here $\delta(x)$ is the Dirac delta function. The eigenstates of the position operator $|x\rangle$ satisfy the completeness relation

$$\int_{-\infty}^{\infty} |x\rangle\langle x|dx = \hat{\mathbf{1}}. \tag{2.7}$$

We can then expand any quantum state $|\psi\rangle$ into position states

$$|\psi\rangle = \int_{-\infty}^{\infty} |x\rangle\langle x|\psi\rangle dx \equiv \int_{-\infty}^{\infty} \psi(x)|x\rangle dx, \tag{2.8}$$

where we define

$$\psi(x) \equiv \langle x|\psi\rangle. \tag{2.9}$$

The eigenstates of the momentum operator $|p\rangle$ also satisfy the completeness relation

$$\int_{-\infty}^{\infty} |p\rangle\langle p|dp = \hat{\mathbf{1}}. \tag{2.10}$$

and we expand $|\psi\rangle$ as

$$|\psi\rangle = \int_{-\infty}^{\infty} |p\rangle\langle p|\psi\rangle dp \equiv \int_{-\infty}^{\infty} \tilde{\psi}(p)|p\rangle dp, \tag{2.11}$$

and define

$$\tilde{\psi}(p) \equiv \langle p|\psi\rangle. \tag{2.12}$$

We call the two wave functions $\psi(x)$ and $\tilde{\psi}(p)$ – the position representation and momentum representation of the state $|\psi\rangle$, respectively, which satisfy

$$\int_{-\infty}^{\infty} |\psi(x)|^2 dx = 1, \tag{2.13}$$

$$\int_{-\infty}^{\infty} |\tilde{\psi}(p)|^2 dp = 1, \tag{2.14}$$

where $|\psi(x)|^2$ and $|\tilde{\psi}(p)|^2$ are the position and momentum probability of the state $|\psi\rangle$, respectively. The position representation and momentum representation of state $|\psi\rangle$ are related to each other through the Fourier transform: by inserting Eq. (2.10) we can see that

$$\psi(x) = (2\pi)^{-1/2} \int_{-\infty}^{\infty} exp\,(ixp)\,\tilde{\psi}(p) dp, \tag{2.15}$$

$$\tilde{\psi}(p) = (2\pi)^{-1/2} \int_{-\infty}^{\infty} exp\,(-ixp)\,\psi(x) dx. \tag{2.16}$$

The state vectors $|x\rangle$ and $|p\rangle$ are related to each other by Fourier transform

$$|x\rangle = (2\pi)^{-1/2} \int_{-\infty}^{\infty} exp\,(-ixp)\,|p\rangle dp, \tag{2.17}$$

$$|p\rangle = (2\pi)^{-1/2} \int_{-\infty}^{\infty} exp\,(ixp)\,|x\rangle dx. \tag{2.18}$$

By using an important property of the delta function

$$\delta\,(x - x_1) \;\; = \;\; \frac{1}{2\pi} \int_{-\infty}^{\infty} exp\,[-i(x - x_1)p]\,dp, \tag{2.19}$$

we can prove the inner product between $|x\rangle$ and $|p\rangle$

$$\langle x|p\rangle \;\; = \;\; (2\pi)^{-1/2} exp\,(ixp)\,. \tag{2.20}$$

We can represent the Fourier transform by an unitary operator $\hat{F}$, which is called the Fourier operator and defined as

$$\hat{F} \equiv \int_{-\infty}^{\infty} |\xi\rangle_{px}\langle\xi| d\xi, \tag{2.21}$$

where $|\xi\rangle_x$ means the position eigenstate corresponding to the eigenvalue ξ. The Fourier operator obeys

$$\hat{F}|\xi\rangle_x = |\xi\rangle_p, \qquad \hat{F}|\xi\rangle_p = |-\xi\rangle_x, \tag{2.22}$$

$$\hat{F}^\dagger \hat{x} \hat{F} = \hat{p}, \qquad \hat{F}^\dagger \hat{p} \hat{F} = -\hat{x}. \tag{2.23}$$

It is easy to see that

$$\hat{F}^4 = \hat{\mathbf{1}}. \tag{2.24}$$

We have seen that the position and momentum are real, then the phase space is $\mathbb{R} \times \mathbb{R}$.

2.3 Quantum harmonic oscillator

In this section, we consider the special case of a quantum system on a real line, namely a one-dimensional linear harmonic oscillator. The potential energy of the system at position x is given as

$$V(x) = \frac{1}{2}kx^2, \tag{2.25}$$

where k is the constant force. For simplicity, let $k = 1$ and assume that the mass $m = 1$ and angular frequency $\omega = 1$.

The Hamiltonian of the harmonic oscillator in the position and momentum operators is

$$\hat{H} \;=\; \frac{1}{2}\left(\hat{x}^2 + \hat{p}^2\right). \tag{2.26}$$

2.3.1 Number State

We introduce the annihilation operator a and creation operator $a^\dagger$, which are defined as

$$\begin{aligned} a &= (2)^{-1/2}\left(\hat{x} + i\hat{p}\right), \\ a^\dagger &= (2)^{-1/2}\left(\hat{x} - i\hat{p}\right). \end{aligned} \tag{2.27}$$

These two operators obey the canonical commutation relation

$$[a, a^\dagger] = I. \tag{2.28}$$

The Hamiltonian operator in Eq. (2.26) can be expressed as

$$\hat{H} = a^\dagger a + \frac{1}{2}. \tag{2.29}$$

We derive the following commutator relations:

$$[a, \hat{H}] = a, \tag{2.30}$$

$$[a^\dagger, \hat{H}] = -a^\dagger. \tag{2.31}$$

The eigenstates $|n\rangle$ of the Hamiltonian operator $\hat{H}$ are known as the number states satisfying

$$\hat{H}|n\rangle = (n + 1/2)|n\rangle, \quad n = 0, 1, 2, ... \tag{2.32}$$

here the non-negative integers n characterise the energy spectrum of the linear harmonic oscillator. The vacuum state $|0\rangle$ is defined as

$$\hat{a}|0\rangle = 0, \quad \langle 0|0\rangle = 1. \tag{2.33}$$

The position representation of the number states is

$$\psi_n(x) \;=\; \langle x|n\rangle \;=\; \left(\frac{1}{\sqrt{\pi}2^n n!}\right)^{1/2} exp\left(-\frac{x^2}{2}\right) H_n(x), \tag{2.34}$$

where $H_n(x)$ are the Hermite polynomials of order n. The number states $|n\rangle$ form an orthonormal basis of a Hilbert space

$$\begin{aligned} \langle m|n\rangle &= \delta_{mn}, \\ \sum_{n=0}^{\infty} |n\rangle\langle n| &= \hat{\mathbf{1}}. \end{aligned} \tag{2.35}$$

For the normalised eigenkets $|n\rangle$, the operators $a^\dagger, a$ act on the number state as follows:

$$\begin{aligned} \hat{a}^\dagger|n\rangle &= \sqrt{n+1}|n+1\rangle, \\ \hat{a}|n\rangle &= \sqrt{n}|n-1\rangle. \end{aligned} \tag{2.36}$$

It is evident that the operator $a^\dagger$ creates one quantum of energy by raising the system from $|n\rangle$ to $|n+1\rangle$. Thus, the operator $a^\dagger$ is known as the creation operator or the rising operator. Where the operator $\hat{a}$ destroys one quantum of energy by lowering the system from $|n\rangle$ to $|n-1\rangle$, the operator a is called the annihilation operator or the destruction operator. For proof, see [23].

The number operator $\hat{n}$ is defined as

$$\hat{n} = \sum_{n=0}^{\infty} n|n\rangle\langle n|, \quad \hat{n}|n\rangle = n|n\rangle. \tag{2.37}$$

Using the definition (2.27), the position and momentum operators can be defined as follows:

$$\begin{aligned} \hat{x} &= \frac{(\hat{a} + \hat{a}^\dagger)}{\sqrt{2}}, \\ \hat{p} &= \frac{i(\hat{a}^\dagger - \hat{a})}{\sqrt{2}}. \end{aligned} \tag{2.38}$$

2.3.2 Displacement operator and parity operator

The displacement operators can be defined as

$$\hat{D}(\alpha) = exp\left(\alpha\hat{a}^\dagger - \alpha^*\hat{a}\right), \tag{2.39}$$

where α is a complex number and can be written in terms of x and p as

$$\alpha = (x + ip)/\sqrt{2}.$$

The displacement operator can be expressed in terms of the position and momentum operators $\hat{x}, \hat{p}$ as

$$\hat{D}(x_0, p_0) = exp\left(ip_0\hat{x} - ix_0\hat{p}\right). \tag{2.40}$$

We also define the parity operator as

$$\hat{U_0} \equiv \int_{-\infty}^{\infty} |-x\rangle\langle x|dx = \int_{-\infty}^{\infty} |-p\rangle\langle p|dp. \tag{2.41}$$

This parity operator, acting on the position and momentum operator and their eigenstates, changes them into their inverses

$$\hat{U_0}\hat{x}\hat{U_0}^{\dagger} = -\hat{x}, \quad \hat{U_0}\hat{p}\hat{U_0}^{\dagger} = -\hat{p}, \tag{2.42}$$

$$\hat{U_0}|x\rangle = |-x\rangle, \quad \hat{U_0}|p\rangle = |-p\rangle, \tag{2.43}$$

and also changes the signs of the parameters of the displacement operator

$$\hat{U_0}\hat{D}(x_0, p_0)\hat{U_0}^{\dagger} = \hat{D}(-x_0, -p_0). \tag{2.44}$$

2.3.3 Coherent state

The Glauber coherent state [24, 25, 26, 27, 28, 29, 30, 31] is defined as the eigenstate of the destruction operator $\hat{a}$

$$\hat{a}|\alpha\rangle = \alpha|\alpha\rangle, \tag{2.45}$$

where α is a complex number. It is generated by acting the displacement operator on the vacuum state

$$|\alpha\rangle = \hat{D}(\alpha)|0\rangle. \tag{2.46}$$

The coherent state can be written in terms of number states

$$|\alpha\rangle \;=\; exp\left(-\frac{|\alpha|^2}{2}\right)\sum_{n=0}^{\infty}\frac{\alpha^n}{\sqrt{n!}}\,|n\rangle. \tag{2.47}$$

Eq. (2.46) shows that the coherent state is a displaced vacuum state in the phase space. The average photon number of $\langle n \rangle$ in the coherent state is equal to $|\alpha|^2$.

$$\langle n \rangle = \langle \alpha | n | \alpha \rangle = |\alpha|^2, \tag{2.48}$$

$$\Delta^2 n = \langle n^2 \rangle - \langle n \rangle^2 = \left(|\alpha|^4 + |\alpha|^2 \right) - |\alpha|^4 = |\alpha|^2 = \langle n \rangle. \tag{2.49}$$

The position representation of the coherent state is a Gaussian function

$$\langle x | \alpha \rangle = \pi^{-1/4} exp \left(-\frac{x^2}{2} + \sqrt{2}\alpha x - \alpha \alpha_R \right), \tag{2.50}$$

where $\alpha = \alpha_R + i\alpha_I$.

The momentum representation of the coherent state is

$$\langle p | \alpha \rangle = \pi^{-1/4} exp \left(-\frac{p^2}{2} - \sqrt{2}\alpha i p + \alpha \alpha_I i \right). \tag{2.51}$$

We can obtain the expectation value of $\hat{x}$ and $\hat{p}$ from Eqs. (2.50) and (2.51)

$$\langle x \rangle = \langle \alpha | \hat{x} | \alpha \rangle = \sqrt{2}\alpha_R, \quad \langle p \rangle = \langle \alpha | \hat{p} | \alpha \rangle = \sqrt{2}\alpha_I. \tag{2.52}$$

The variances of $\hat{x}$ and $\hat{p}$ are equal

$$(\Delta x)^2 = (\Delta p)^2 = \frac{1}{2}. \tag{2.53}$$

The inner product of two coherent states $|\alpha\rangle$ and $|\beta\rangle$ is

$$\langle\beta|\alpha\rangle \;=\; exp\left(-\frac{1}{2}|\alpha|^2 - \frac{1}{2}|\beta|^2 + \alpha\beta^*\right). \tag{2.54}$$

The completeness relation for the coherent states is

$$\frac{1}{\pi}\int_{\mathbb{C}} |\alpha\rangle\langle\alpha| d^2\alpha = \hat{\mathbf{1}}, \tag{2.55}$$

where $\mathbb{C}$ is the complex plane.

2.3.4 Wigner function and Weyl function

The Wigner function was described by E. Wigner in 1932 [32]. It is a quasi-probability distribution function in the phase space, and it shows important properties of the quantum state described by a density operator. The Wigner function [33, 34, 35, 36] can be viewed as the intermediate between two representations and is defined as

$$W_\rho(x,p) \equiv \frac{1}{2\pi}\int_{-\infty}^{\infty} exp(ipX)\left\langle x - \frac{X}{2}\right|\hat{\rho}\left|x + \frac{X}{2}\right\rangle\, dX \tag{2.56}$$

$$W_\rho(x,p) \equiv \frac{1}{2\pi}\int_{-\infty}^{\infty} exp(-iPx)\left\langle p - \frac{P}{2}\right|\hat{\rho}\left|p + \frac{P}{2}\right\rangle\, dP, \tag{2.57}$$

where X and P are the position and momentum increments. This is also written in terms of the displaced parity operator as

$$W_\rho(x,p) = \frac{1}{\pi}\mathrm{Tr}\left[\hat{\rho}\hat{U}(x,p)\right]. \tag{2.58}$$

The Wigner function corresponding to the density matrix is real, i.e.

$$W_\rho(x,p) = W_\rho^*(x,p).$$

In addition, it can be defined for an arbitrary operator $\hat{A}$ by replacing the density matrix $\hat{\rho}$ with $\hat{A}$

$$W_A(x,p) = \frac{1}{\pi}\mathrm{Tr}\left[\hat{A}\hat{U}(x,p)\right]. \tag{2.59}$$

The Wigner distribution for a density operator may contain some negative values.

The Weyl function is defined as

$$\begin{aligned}\tilde{W}_\rho(X,P) &\equiv \int_{-\infty}^{\infty} exp\,(iPx)\left\langle x-\frac{X}{2}\right|\hat{\rho}\left|x+\frac{X}{2}\right\rangle\,dx \\ &= \int_{-\infty}^{\infty} exp\,(-ipX)\left\langle p-\frac{P}{2}\right|\hat{\rho}\left|p+\frac{P}{2}\right\rangle\,dp. \end{aligned}\tag{2.60}$$

and is expressed in terms of the displacement operator as

$$\tilde{W}_\rho(X,P) = \mathrm{Tr}\left[\hat{\rho}\hat{D}(X,P)\right]. \tag{2.61}$$

The Wigner and weyl functions are related to each other through the two-dimensional Fourier transform

$$W_\rho(x,p) = \frac{1}{4\pi^2}\int_{-\infty}^{\infty}\int_{-\infty}^{\infty}\tilde{W}_\rho(X,P)\,exp\left[-i(Xp-Px)\right]\,dX\,dP. \tag{2.62}$$

2.3.5 Examples of the Wigner and Weyl functions

To highlight some examples, we derive the Wigner representation and Weyl representation of number states and coherent states:

- The Wigner representation of the number states $|n\rangle$ is

$$W_n(x,p) = \frac{(-1)^n}{\pi} exp\left(-x^2-p^2\right) L_n\left[2(x^2+p^2)\right], \quad (2.63)$$

  where $L_n(x)$ are the Laguerre polynomials.

  The corresponding Weyl function is

$$\tilde{W}_n(x,p) = exp\left[-\frac{x^2+p^2}{4}\right] L_n\left[\frac{x^2+p^2}{2}\right]. \quad (2.64)$$

- The Wigner representation of the coherent states $|\alpha\rangle$ is

$$W_\alpha(x,p) = \frac{1}{\pi} exp\left[-\left(x-\sqrt{2}\alpha_R\right)^2 - \left(p-\sqrt{2}\alpha_I\right)^2\right], \quad (2.65)$$

  Correspondingly, the Weyl function is

$$\tilde{W}_\alpha(x,p) = exp\left[-\left(\frac{x}{2}+\sqrt{2}i\alpha_I\right)^2 - \left(\frac{p}{2}-\sqrt{2}i\alpha_R\right)^2 - 2|\alpha|^2\right]. \quad (2.66)$$

In Fig. 2.1 we show the Wigner representation of the number states $|3\rangle$, whereas in Fig. 2.2 we show the Wigner representation of the coherent states $|2+2i\rangle$.

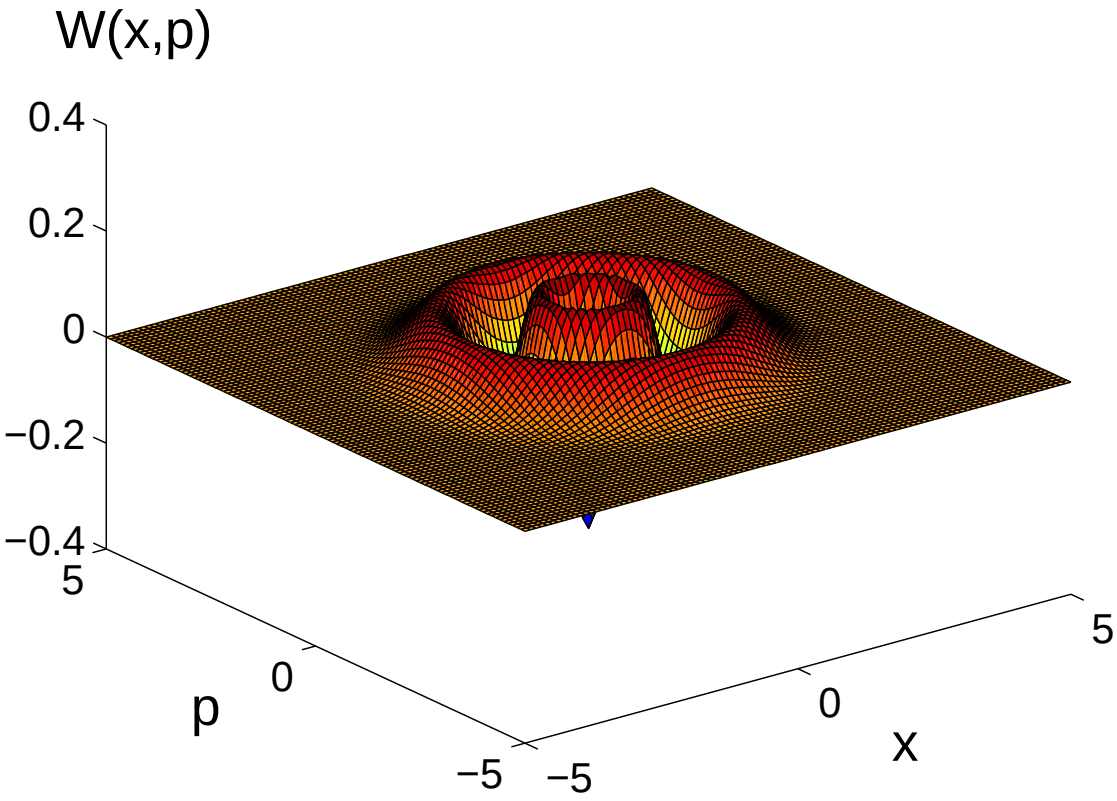

Figure 2.1: The Wigner representation of the number states $|3\rangle$.

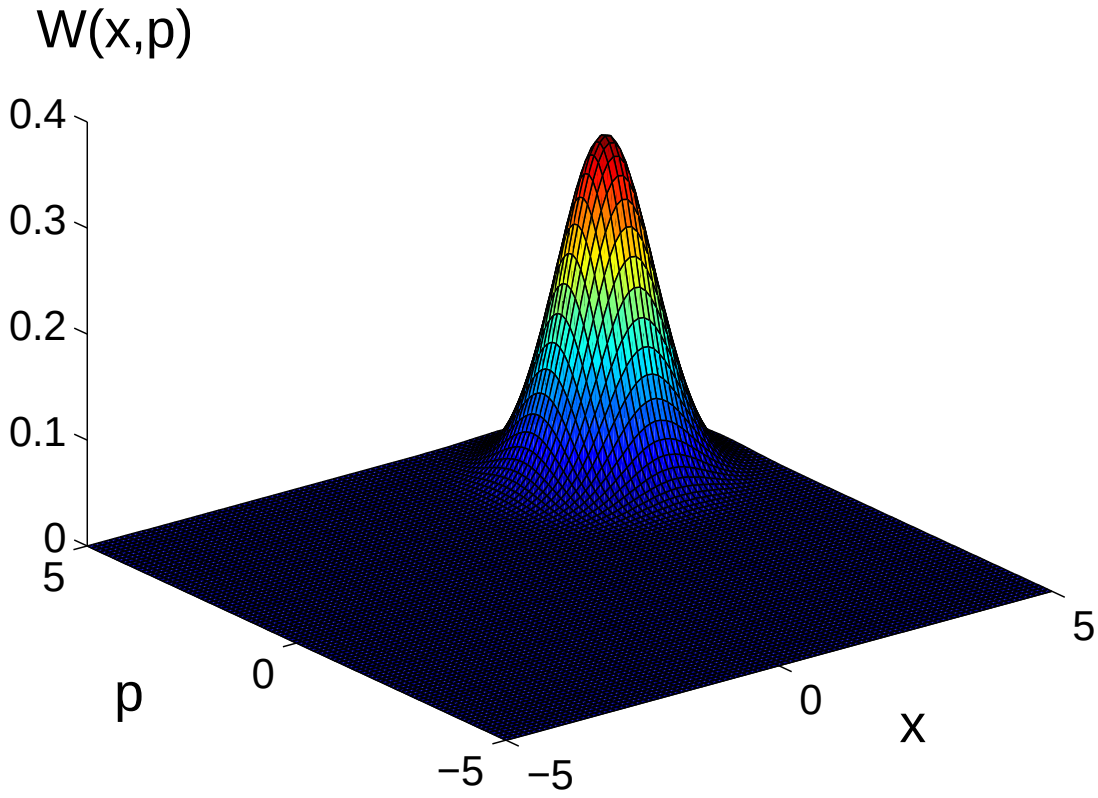

Figure 2.2: The Wigner representation of the coherent state $|2+2i\rangle$.

2.4 Bargmann analytic representation

We have seen in section 2.3.3 that the coherent states are defined on a complex plane, and in addition they obey the completeness relation (2.55).

In this section, we introduce the Bargmann analytic representation in the complex plane defined by the Glaubar coherent state. The space of the Bargmann representation is a space of entire functions, which has no singularities in the complex plane. The growth of an analytic function is characterised by its order and type [37, 38, 39, 40].

2.4.1 Definition

We consider an arbitrary $|f\rangle$ state

$$|f\rangle = \sum_{n=0}^{\infty} f_n |n\rangle, \tag{2.67}$$

$$\sum_{n=0}^{\infty} |f_n|^2 = 1. \tag{2.68}$$

We then use the notation

$$|f^*\rangle = \sum_{n=0}^{\infty} f_n^* |n\rangle, \tag{2.69}$$

$$\sum_{n=0}^{\infty} |f_n|^2 = 1. \tag{2.70}$$

In the Bargmann representation [4, 5, 6, 41], the state $|f\rangle$ is represented by

$$f(z) \;=\; exp\left(\frac{|z|^2}{2}\right)\langle z^*|f\rangle = \sum_{n=0}^{\infty}\frac{f_n\, z^n}{\sqrt{n!}}, \tag{2.71}$$

which is an entire function (i.e. analytic function in the complex plane $\mathbb{C}$).

If we let $f(\zeta)=0$ (i.e. ζ is a zero of $f(z)$), then the coherent state $|\zeta\rangle$ is orthogonal to $|f^*\rangle$.

The inner product of the two states is given by

$$\langle f|g\rangle \;=\; \frac{1}{\pi}\int_{\mathbb{C}}[f(z)]^*\; g(z)\; exp\left(-|z|^2\right)\; d^2z. \tag{2.72}$$

If we let $\hat{\Omega}$ be an arbitrary operator

$$\hat{\Omega} \;=\; \sum_{m,n=0}^{\infty}\Omega_{mn}\,|m\rangle\langle n|, \tag{2.73}$$

we can represent this by the two variable analytic functions in the Bargmann analytic representation

$$\begin{aligned}\Omega(z,\zeta^*) \;&=\; exp\left(\frac{1}{2}|z|^2+\frac{1}{2}|\zeta|^2\right)\langle z^*|\;\hat{\Omega}\;|\zeta^*\rangle, \\ &=\; exp\left(\frac{1}{2}|z|^2+\frac{1}{2}|\zeta|^2\right)\sum_{m,n=0}^{\infty}\frac{\Omega_{mn}\,z^m\,\zeta^{*n}}{\sqrt{m!\;n!}},\end{aligned} \tag{2.74}$$

here $|z^*\rangle$ and $|\zeta^*\rangle$ are coherent states.

Following this, we can express the action of an operator on a state in terms of its analytic function. As an example

$$|g\rangle = \hat{\Omega}\;|f\rangle,$$

it is evident that

$$g(z) = \int_{\mathbb{C}} d^2\zeta \; exp(-|\zeta|^2) \; \Omega(z, \zeta^*) \; f(\zeta). \tag{2.75}$$

The Bargmann analytic representation of the creation and annihilation operator is

$$\begin{aligned} a &\longrightarrow \partial_z; \\ a^\dagger &\longrightarrow z. \end{aligned} \tag{2.76}$$

2.4.2 The growth of Bargmann analytic functions

The growth of an analytic function $f(z)$ is characterised by its order ρ and type σ [37, 38, 39, 40], where

$$\rho = \lim_{R\to\infty} sup \; \frac{lnlnM(R)}{lnR}, \qquad \sigma = \lim_{R\to\infty} sup \; \frac{lnM(R)}{R^\rho}. \tag{2.77}$$

Here $M(R)$ is the maximum value of $f(z)$ on $|z| = R$. We shall denote as $H(\rho, \sigma)$ the space of functions of an order not exceeding ρ and of a type not exceeding σ if of order ρ.

We say that $H(\rho, \sigma)$ is a subspace of $H(\rho^{'}, \sigma^{'})$ if $\rho < \rho^{'}$ or both $\rho = \rho^{'}$ and $\sigma < \sigma^{'}$.

Using the convergence of the scalar product of Eq. (2.72) we conclude that the space of a Bargmann analytic function is a subspace of $H(2, \frac{1}{2})$ [40].

We can now derive the Bargmann analytic representation of some quantum states as examples.

- The number state $|n\rangle$ is represented as

$$f(z) = \frac{z^n}{\sqrt{n!}}, \tag{2.78}$$

and is of order 0.

- The coherent state $|\alpha\rangle$ is represented as

$$f(z) = exp\left(\alpha\ z - \frac{1}{2}|\alpha|^2\right), \tag{2.79}$$

which is of order $\rho = 1$ and type $|\alpha|$.

2.4.3 P and Q (Husimi) functions

The P function [42] of a density operator $\hat{\rho}$ is defined as

$$\hat{\rho} = \int P(\alpha)\ |\alpha\rangle\ \langle\alpha|\ d^2\alpha \tag{2.80}$$

where $|\alpha\rangle$ are the Glauber states. The trace of a density operator $\hat{\rho}$ is given by

$$\begin{aligned} Tr\hat{\rho} &= Tr \int_{\mathbb{C}} d^2\alpha\ P(\alpha)\ |\alpha\rangle\ \langle\alpha| \\ &= \int_{\mathbb{C}} d^2\ \alpha P(\alpha) = 1. \end{aligned} \tag{2.81}$$

If we let $|\psi\rangle$ be an arbitrary state, the Q function or Husimi function [43, 44] is defined by

$$Q(\alpha) = \frac{|\langle\alpha|\psi\rangle|^2}{\pi} \tag{2.82}$$

with

$$\int_{\mathbb{C}} d^2\alpha \; Q(\alpha) = 1 \tag{2.83}$$

Various examples of the Husimi function are given below as follows:

The Husimi function of the coherent state $|\beta\rangle$ is

$$Q(\alpha) = \frac{1}{\pi}|\langle\alpha|\beta\rangle|^2 = \frac{1}{\pi}\, exp\left(-|\alpha-\beta|^2\right). \tag{2.84}$$

The Husimi function of the number state $|n\rangle$ is

$$Q(\alpha) = \frac{1}{\pi}|\langle\alpha|n\rangle|^2 = \frac{1}{\pi}\, exp\left(-|\alpha|^2\right)\; \frac{|\alpha|^{2n}}{n!}. \tag{2.85}$$

In Fig. 2.3 we plot the Husimi representation of the coherent state $|2+2i\rangle$, whereas in Fig. 2.4 we plot the Husimi representation of the number state $|2\rangle$.

2.4.4 Zeros of the Husimi functions

The Husimi function and Bargmann function $f(z)$ are related to each other as follows:

$$Q(z,z^*) = exp\left(-|z|^2\right)\; |f(z)|^2, \tag{2.86}$$

so they have the same zeros (i.e ζ is a zero of $f(z)$ providing ζ is a zero of the Husimi function).

The number state $|n\rangle$ has exactly n zeros, it has the zero $\zeta = 0$ (with

multiplicity n). As an example we consider the function

$$f(z) = \sum_{n=0}^{14} \frac{f_n \, z^n}{\sqrt{n!}}. \tag{2.87}$$

The coefficients f_n are given in Table. 2.1.

i	f_i	i	f_i
0	0.14-0.62i	8	0.54-0.09i
1	0.91+0.79i	9	0.41-0.52i
2	0.95+0.65i	10	0.18-0.30i
3	0.03-0.84i	11	-0.18+0.61i
4	0.93-0.67i	12	0.46+0.78i
5	0.27-0.04i	13	-0.04-0.29i
6	0.78+0.04i	14	-0.02-0.25i
7	0.28+0.04i		

Table 2.1: The coefficients f_n

In Fig. 2.5 we plot the zeros of function $f(z)$ which is polynomial of order 14 and has 14 zeros.

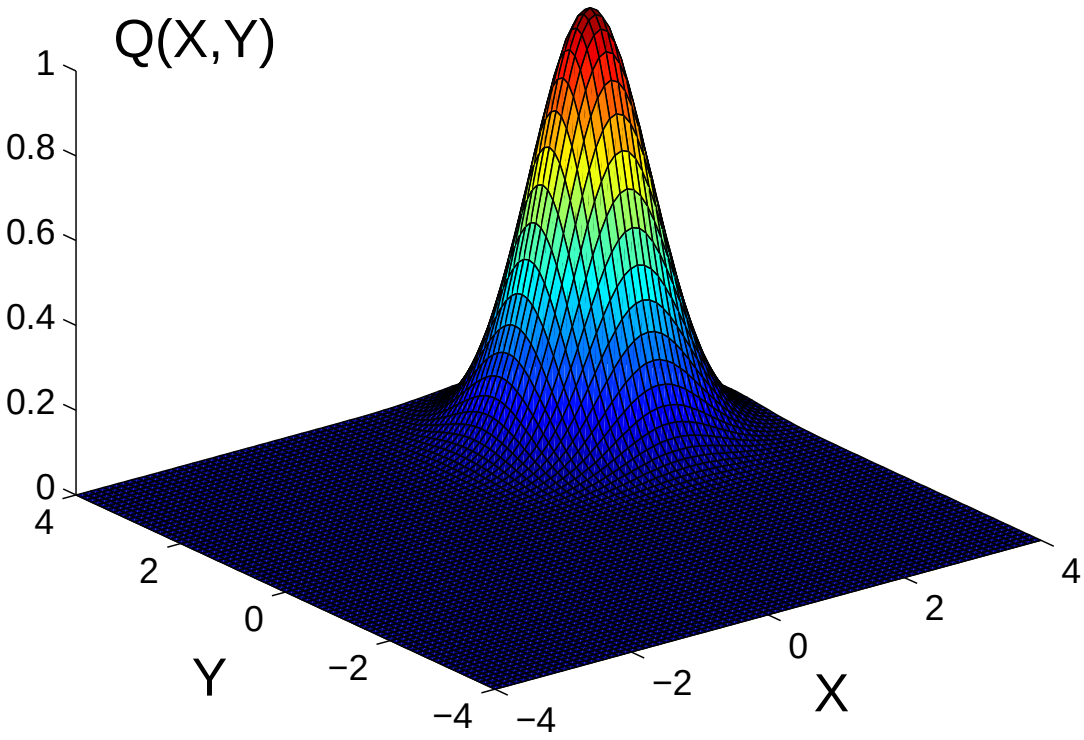

Figure 2.3: The Husimi representation of the coherent state $|2+2i\rangle$.

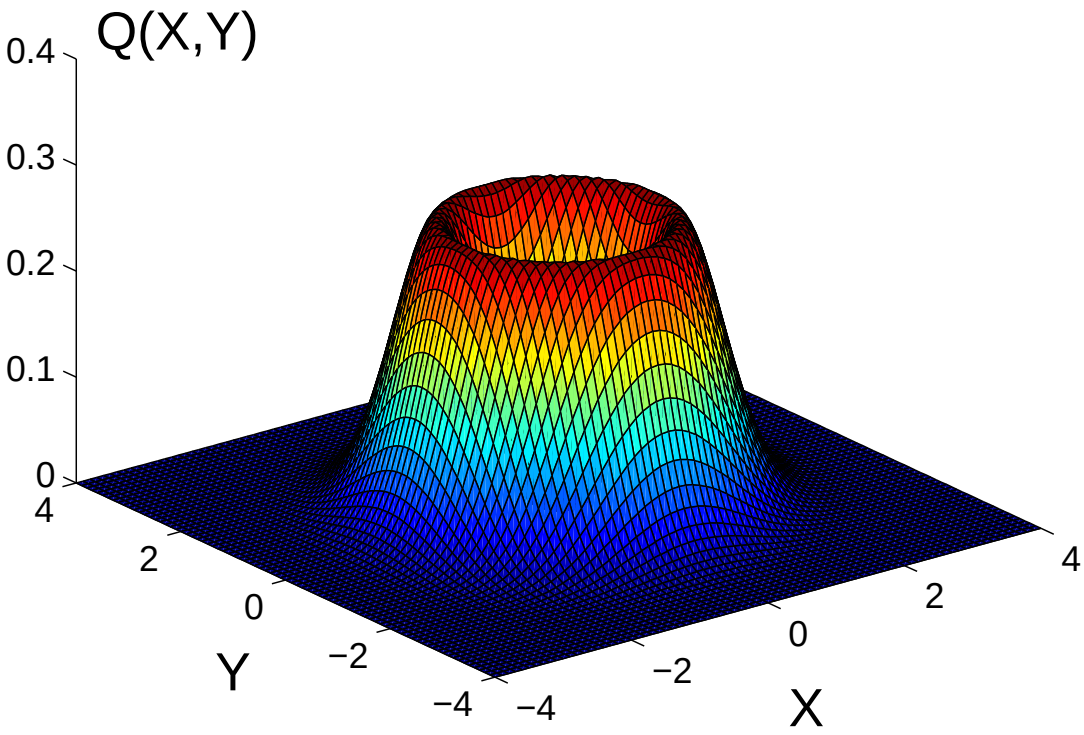

Figure 2.4: The Husimi representation of the number state $|2\rangle$.

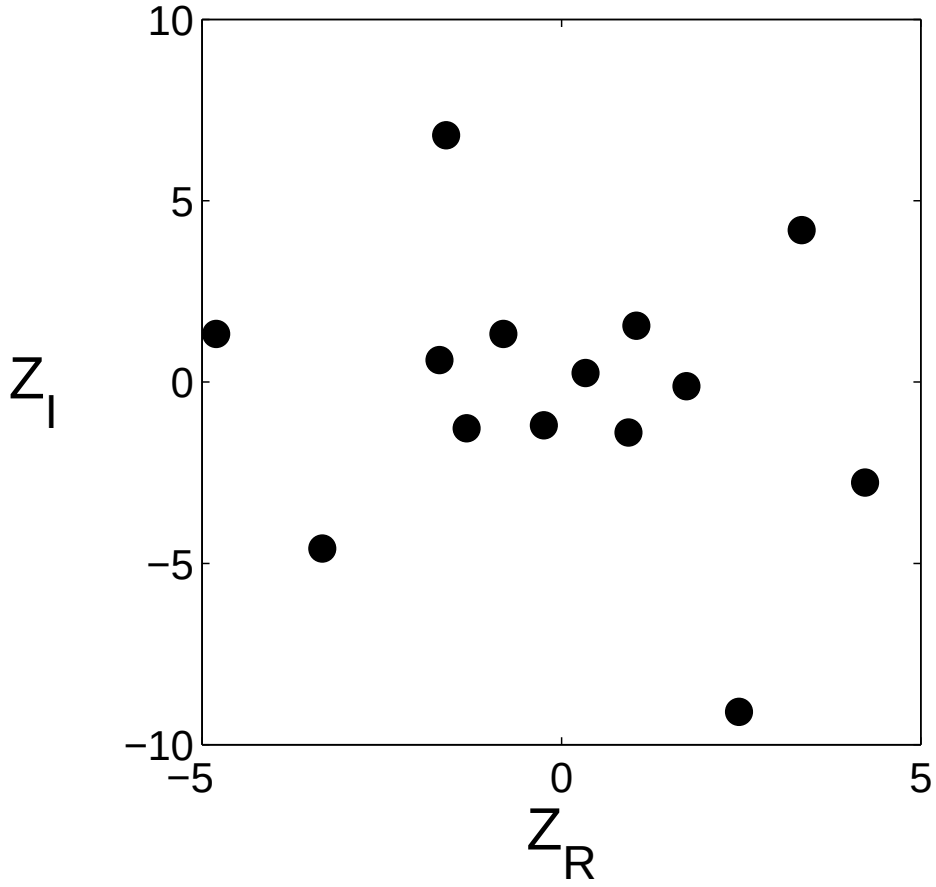

Figure 2.5: The distributions of zeros of function $f(z)$ of Eq. (2.87). The coefficients f_n are give in Table. 2.1

2.5 Summary

In this chapter, we undertook a review of the phase space methods for quantum particles on a real line $\mathbb{R}$, and the basic formalisms of this phase space were introduced. Some special states such as number states, displacement, parity operators and coherent states were studied, and the most popular functions used in phase space – the Wigner function and the Weyl function methods – were described. The Bargmann analytic representation in the complex plane, which was defined by the Glaubar coherent states, was considered.

Finally, we briefly introduced the P and Q functions.

Chapter 3

Analytic Representations of Finite Quantum Systems

3.1 Introduction

Finite quantum systems, with the position and momentum take values in $\mathbb{Z}_d$ (the integers modulo d) [45, 46, 47], have been studied by many authors. A review with many references is given in [20]. The Wigner function in this phase space has been defined by [48], this definition has been discussed by [49, 50]. A slightly different definition given by [51]. Both methods have been applied in different fields, such as quantum computing [52, 53] and quantum optics [54]. When d is a prime number, $\mathbb{Z}_d$ is a Galois field [20]. In such case, a group of discrete symplectic transformations are well defined [55, 56, 57]. The wigner functions are defined in this Galois field phase space [58, 59, 60]. Analytic functions have been used in various contexts in quantum mechanics [1, 2, 3]. Ref [21, 61] studied an analytic representation for these systems

on a torus, using Theta functions. It was shown that the analytic function representing a quantum state has exactly d zeros (which obey a constraint). We derive some examples within this chapter to show the zero distributions of various states. Ref [21] constructed the function $f(z)$ from its zeros. In this chapter, we study the time evolution of the system and the motion of the d zeros on the torus. We study various Hamiltonians and various initial states, and we calculate the d paths of the zeros. The zeros of this analytic representation define uniquely the quantum state. In addition, we consider the inverse problem and we calculate the Hamiltonian for given zeros, We assume that the paths $\zeta_n(t)$ of the zeros are given and we calculate the Hamiltonian.

3.2 Finite Quantum Systems

We consider a quantum system with a $d-$dimensional Hilbert space $\mathcal{H}$, where position and momentum take values in $\mathbb{Z}_d$. We use the notation $|f\rangle$ for the states in this particular Hilbert space $L^2(\mathbb{Z}_d)$.

3.2.1 Position and Momentum States

Let $|\mathcal{X};m\rangle$ and $|\mathcal{P};m\rangle$, where $m \in \mathbb{Z}_d$ (the integers modulo d), are both orthonormal bases of $L^2(\mathbb{Z}_d)$, which we call position states and momentum states correspondingly.

$$\langle \mathcal{X};m|\mathcal{X};n\rangle = \delta_{mn}, \qquad \langle \mathcal{P};m|\mathcal{P};n\rangle = \delta_{mn}; \tag{3.1}$$

$$\sum_{m=0}^{d-1} |\mathcal{X}; m\rangle\langle\mathcal{X}; m| = \sum_{m=0}^{d-1} |\mathcal{P}; m\rangle\langle\mathcal{P}; m| = \hat{\mathbf{1}}. \tag{3.2}$$

δ_{mn} in Eq. 3.1 is the Kronecker Delta satisfying

$$\delta_{mn} = \begin{cases} 0 \quad if \quad m \neq n; \\ \\ 1 \quad if \quad m = n. \end{cases} \tag{3.3}$$

The position and momentum states are related to each other through the finite Fourier transformation

$$|\mathcal{P}; n\rangle = d^{-1/2} \sum_{m=0}^{d-1} \omega(mn)|\mathcal{X}; m\rangle. \tag{3.4}$$

where

$$\omega(\alpha) = exp\left(\frac{2\pi i\alpha}{d}\right). \tag{3.5}$$

The position and momentum operators are given by

$$\hat{x} \;=\; \sum_{n=0}^{d-1} n|\mathcal{X}; n\rangle\langle\mathcal{X}; n|; \qquad \hat{p} \;=\; \sum_{n=0}^{d-1} n|\mathcal{P}; n\rangle\langle\mathcal{P}; n|; \tag{3.6}$$

The Fourier operator is a unitary operator defined as

$$\hat{\mathcal{F}} = d^{-1/2} \sum_{m,n=0}^{d-1} \omega(mn)|\mathcal{X}; m\rangle\langle\mathcal{X}; n|; \tag{3.7}$$

and satisfies

$$\hat{\mathcal{F}}\hat{x}\hat{\mathcal{F}}^{\dagger} = \hat{p}; \quad \hat{\mathcal{F}}\hat{p}\hat{\mathcal{F}}^{\dagger} = -\hat{x}; \tag{3.8}$$

and

$$\hat{\mathcal{F}}|\mathcal{X};m\rangle = |\mathcal{P};m\rangle; \quad \hat{\mathcal{F}}|\mathcal{P};m\rangle = |\mathcal{X};-m\rangle; \tag{3.9}$$

therefore

$$|\mathcal{X};m\rangle \xrightarrow{\mathcal{F}} |\mathcal{P};m\rangle \xrightarrow{\mathcal{F}} |\mathcal{X};-m\rangle \xrightarrow{\mathcal{F}} |\mathcal{P};-m\rangle \xrightarrow{\mathcal{F}} |\mathcal{X};m\rangle; \tag{3.10}$$

$$\hat{x} \xrightarrow{\mathcal{F}} \hat{p} \xrightarrow{\mathcal{F}} -\hat{x} \xrightarrow{\mathcal{F}} -\hat{p} \xrightarrow{\mathcal{F}} \hat{x} \tag{3.11}$$

$$\hat{\mathcal{F}}^4 = \hat{\mathbf{1}}. \tag{3.12}$$

3.2.2 Displacement Operators

In the finite quantum system, the position and momentum are both integers modulo d, therefore, the phase space is the toroidal lattice $\mathbb{Z}_d \times \mathbb{Z}_d$.

The displacement operators in this particular phase space are defined as

$$\hat{Z} = exp\left(i\frac{2\pi}{d}\hat{x}\right); \quad \hat{X} = exp\left(-i\frac{2\pi}{d}\hat{p}\right). \tag{3.13}$$

These operators perform displacements along the $\mathcal{P}$ and $\mathcal{X}$ axes in the $\mathbb{Z}_d \times \mathbb{Z}_d$ phase space, obeying the relations

$$\hat{X}^d = \hat{Z}^d = \hat{\mathbf{1}}; \quad \hat{X}^\beta \hat{Z}^\alpha = \hat{Z}^\alpha \hat{X}^\beta \omega(-\alpha\beta). \tag{3.14}$$

where α, β are integers in $\mathbb{Z}_d$.

$$\hat{Z}^\alpha|P;m\rangle = |P;m+\alpha\rangle; \quad \hat{Z}^\alpha|X;m\rangle = \omega(\alpha m)|X;m\rangle; \tag{3.15}$$

$$\hat{X}^\beta|P;m\rangle = \omega(-m\beta)|P;m\rangle; \quad \hat{X}^\beta|X;m\rangle = |X;m+\beta\rangle. \tag{3.16}$$

The general displacement operators are defined as

$$\hat{D}(\alpha,\beta) = \hat{Z}^\alpha\hat{X}^\beta\omega(-2^{-1}\alpha\beta) = \hat{X}^\beta\hat{Z}^\alpha\omega(2^{-1}\alpha\beta). \tag{3.17}$$

with

$$\hat{D^\dagger} = \hat{D}(-\alpha,-\beta). \tag{3.18}$$

It is easy to see that

$$\hat{D}(\alpha,\beta)|X;m\rangle = \omega(2^{-1}\alpha\beta+\alpha m)|X;m+\beta\rangle; \tag{3.19}$$

$$\hat{D}(\alpha,\beta)|P;m\rangle = \omega(-2^{-1}\alpha\beta-\beta m)|P;m+\alpha\rangle. \tag{3.20}$$

3.3 Zak Transform

We introduce a map between states in the infinite dimensional Hilbert space H and the d-dimensional Hilbert space $\mathcal{H}$ as follows

$$\Phi(x) \in H \longrightarrow \Phi_m = \mathcal{N}^{-1/2}\sum_{\omega=-\infty}^{\infty}\Phi\left[x=\left(\frac{2\pi}{d}\right)^{1/2}(m+d\,\omega)\right] \in \mathcal{H}; \tag{3.21}$$

where $m \in \mathbb{Z}_d$. $\mathcal{N}$ is a normalisation factor given by

$$\mathcal{N} \;=\; \sum_{m=0}^{d-1} \left\{ \sum_{\omega=-\infty}^{\infty} \Phi^* \left[x = \left(\frac{2\pi}{d}\right)^{1/2} (m + d\,\omega) \right] \right\} \left\{ \sum_{\omega'=-\infty}^{\infty} \Phi \left[x = \left(\frac{2\pi}{d}\right)^{1/2} (m + d\,\omega') \right] \right\}. \tag{3.22}$$

Then $\Phi_{m+d} = \Phi_m$.

We consider the coherent states $|z\rangle$, whose wave function is

$$f(x,z) \;=\; \langle x|z\rangle \;=\; \pi^{-1/4}\, exp\left(-\frac{1}{2}x^2 + z\,x - \frac{1}{2}z_R\,z\right), \tag{3.23}$$

where $z = z_R + iz_I$.

We use Eq. (3.21) to find the corresponding state $|z\rangle_{finite}$ in $\mathcal{H}$:

$$|z\rangle_{finite} = \sum_{m=0}^{d-1} f_m(z)\; |\mathcal{X}; m\rangle; \tag{3.24}$$

where

$$f_m(z) \;=\; \mathcal{N}(z)^{-1/2}\, \pi^{-1/4}\, d^{-1/2}\, exp\left(\frac{i}{2}z_I z\right)\; \vartheta_3\left[\frac{\pi m}{d} - z\,\left(\frac{\pi}{2d}\right)^{1/2}; \frac{i}{d}\right]. \tag{3.25}$$

Here ϑ_3 is the Jacobi Theta functions [64, 65], defined as

$$\vartheta_3(u;\tau) = \sum_{n=-\infty}^{\infty} exp\left(i\pi\tau n^2 + i2nu\right), \tag{3.26}$$

and τ is a complex number with positive imaginary parts.

3.4 Analytic Representation

3.4.1 Definition of an Analytic Representation

We consider an arbitrary pure normalised state $|F\rangle$

$$|F\rangle = \sum_{m=0}^{d-1} F_m \, |X; m\rangle; \quad \sum_{m=0}^{d-1} |F_m|^2 = 1. \tag{3.27}$$

We will use the notation

$$|F^*\rangle \; = \; \sum_{m=0}^{d-1} F_m^* \, |X; m\rangle; \quad \langle F| \; = \; \sum_{m=0}^{d-1} F_m^* \langle X; m|; \quad \langle F^*| \; = \; \sum_{m=0}^{d-1} F_m \, \langle X; m|. \tag{3.28}$$

Using Eq. (3.25), we define the analytic representation of $|F\rangle$ as:

$$\begin{aligned} f(z) \; &= \; [\mathcal{N}(z)]^{1/2} \; d^{1/2} \; exp\left(\frac{-i}{2} \; z_I \; z\right) \; {}_{finite}\langle z^*|F\rangle \\ &= \; \pi^{-1/4} \; \sum_{m=0}^{d-1} \; F_m \; \vartheta_3[\frac{\pi m}{d} - z \; (\frac{\pi}{2d})^{1/2} \; ; \frac{i}{d}]. \end{aligned} \tag{3.29}$$

The function $f(z)$ satisfies

$$\begin{aligned} f\left[z + (2\pi d)^{1/2}\right] \; &= \; f(z), \\ f\left[z + i \; (2\pi d)^{1/2}\right] \; &= \; f(z) \; exp\left[\pi d - i \; (2\pi d)^{1/2} \; z\right]. \end{aligned} \tag{3.30}$$

$f(z)$ is defined on a square area S on the complex plane

$$S = [a, a + (2\pi d)^{1/2}) \times [b, b + (2\pi d)^{1/2}); \qquad a, b \in \mathbb{R}. \tag{3.31}$$

The scalar product is given by

$$\langle F^*|G\rangle \;=\; (2\pi)^{-1/2}d^{-3/2}\int_S d^2\ z\ exp(-z_I^2)\ f(z)\ g(z^*); \qquad (3.32)$$

where

$$z = z_R + iz_I; \qquad z = dz_R\ dz_I. \qquad (3.33)$$

The orthogonality relation

$$\begin{aligned} 2^{-1/2}\pi^{-1}d^{-3/2} \;&\int_S\; d^2z\ \exp\left(-z_I^2\right)\ \vartheta_3\left[\pi n d^{-1} - z\pi^{1/2}(2d)^{-1/2}; id^{-1}\right] \\ &\times\; \vartheta_3\left[\pi m d^{-1} - z^*\pi^{1/2}(2d)^{-1/2}; id^{-1}\right] \;=\; \delta(m,n), \end{aligned} \qquad (3.34)$$

where $m, n \in \mathbb{Z}_d$, is proved as follows:

Using the definition of Theta functions:

$$\vartheta_3(u;\tau) \;=\; \sum_{n=-\infty}^{\infty} \exp(i\pi\tau n^2 + i2nu), \qquad (3.35)$$

we rewrite the right-hand side R of Eq. (3.34) as:

$$R \;=\; 2^{-1/2}\pi^{-1}d^{-3/2}\sum_{k,\ell}\exp\left[\frac{i2\pi(km+\ell n)}{d}\right]R_1$$

$$\times\int_0^{(2\pi d)^{1/2}} dz_I\ \exp\left[-z_I^2 + \left(\frac{2\pi}{d}\right)^{1/2}(k-\ell)z_I - \left(\frac{\pi}{d}\right)(k^2+\ell^2)\right]; \qquad (3.36)$$

where

$$R_1 = \int_0^{(2\pi d)^{1/2}} dz_R \, \exp\left[-i\left(\frac{2\pi}{d}\right)^{1/2}(k+\ell)z_R\right] = (2\pi d)^{1/2}\,\delta(k,-\ell). \quad (3.37)$$

Inserting Eq. (3.37) into Eq. (3.36), we get:

$$\begin{aligned} R &= \pi^{-1/2}d^{-1}\sum_{k=-\infty}^{\infty}\exp\left[\frac{i2\pi k(m-n)}{d}\right] \\ &\times \int_0^{(2\pi d)^{1/2}} dz_I \exp\left\{-\left[z_I-\left(\frac{2\pi}{d}\right)^{1/2}k\right]^2\right\}. \end{aligned} \quad (3.38)$$

We can rewrite k as $k = k_0 + dN$, where $0 \le k_0 \le d-1$ and N is an integer. Then

$$\begin{aligned} R &= \pi^{-1/2}d^{-1}\sum_{k=0}^{d-1}\exp\left[\frac{i2\pi k_0(m-n)}{d}\right] \\ &\times \sum_{N=-\infty}^{\infty}\int_0^{(2\pi d)^{1/2}} dz_I \, \exp\left\{-\left[z_I-\left(\frac{2\pi}{d}\right)^{1/2}(Nd+k_0)\right]^2\right\}. \end{aligned} \quad (3.39)$$

However

$$\sum_{N=-\infty}^{\infty}\int_0^{(2\pi d)^{1/2}} dz_I \exp\left\{-\left[z_I-\left(\frac{2\pi}{d}\right)^{1/2}(Nd+k_0)\right]^2\right\}$$

$$= \int_{-\infty}^{\infty} dz_I \, \exp\left\{-\left[z_I-\left(\frac{2\pi}{d}\right)^{1/2}k_0\right]^2\right\} = \pi^{1/2}. \quad (3.40)$$

Therefore

$$R \;=\; d^{-1}\sum_{k=0}^{d-1}\exp\left[\frac{i2\pi k_0(m-n)}{d}\right]=\delta(m,n). \qquad \Box$$

Using this, we can prove that

$$F_m \;=\; 2^{-1/2}\,\pi^{-1}\,d^{-3/2}\int_S d^2z\; exp\left(-z_I^2\right)\vartheta_3\left[\frac{\pi m}{d}-z\,(\frac{\pi}{2d})^{1/2};\frac{i}{d}\right]f(z^*). \quad (3.41)$$

We derive the analytic representations of position eigenstates $|\mathcal{X};m\rangle$ and momentum eigenstates $|\mathcal{P};m\rangle$ as follows

$$|\mathcal{X};m\rangle \;\longrightarrow\; \pi^{-1/4}\,\vartheta_3\left[\frac{\pi m}{d}-z\left(\frac{\pi}{2d}\right)^{1/2};\frac{i}{d}\right]; \quad (3.42)$$

$$|\mathcal{P};m\rangle \;\longrightarrow\; \pi^{-1/4}\,exp\left(-\frac{1}{2}z^2\right)\;\vartheta_3\left[\frac{\pi m}{d}-z\,i\left(\frac{\pi}{2d}\right)^{1/2};\frac{i}{d}\right]. \quad (3.43)$$

correspondingly. We consider an example where $d=5$ and the $|F\rangle$ at $t=0$ are described through the coefficients

$$F_0=0.14+i0.42; \qquad F_1=0.91+i0.79; \qquad F_2=0.95+i0.65;$$
$$F_3=0.03+i0.84; \qquad F_4=0.93-i0.67. \quad (3.44)$$

In Fig. 3.1 we plot the real part of the function (3.29), where $d=5$ and the $|F\rangle$ are described through the coefficients in Eq. (3.44). In Fig. 3.2 we plot the imaginary part of the function (3.29), where $d=5$ and the $|F\rangle$ are described through the coefficients in Eq. (3.44).

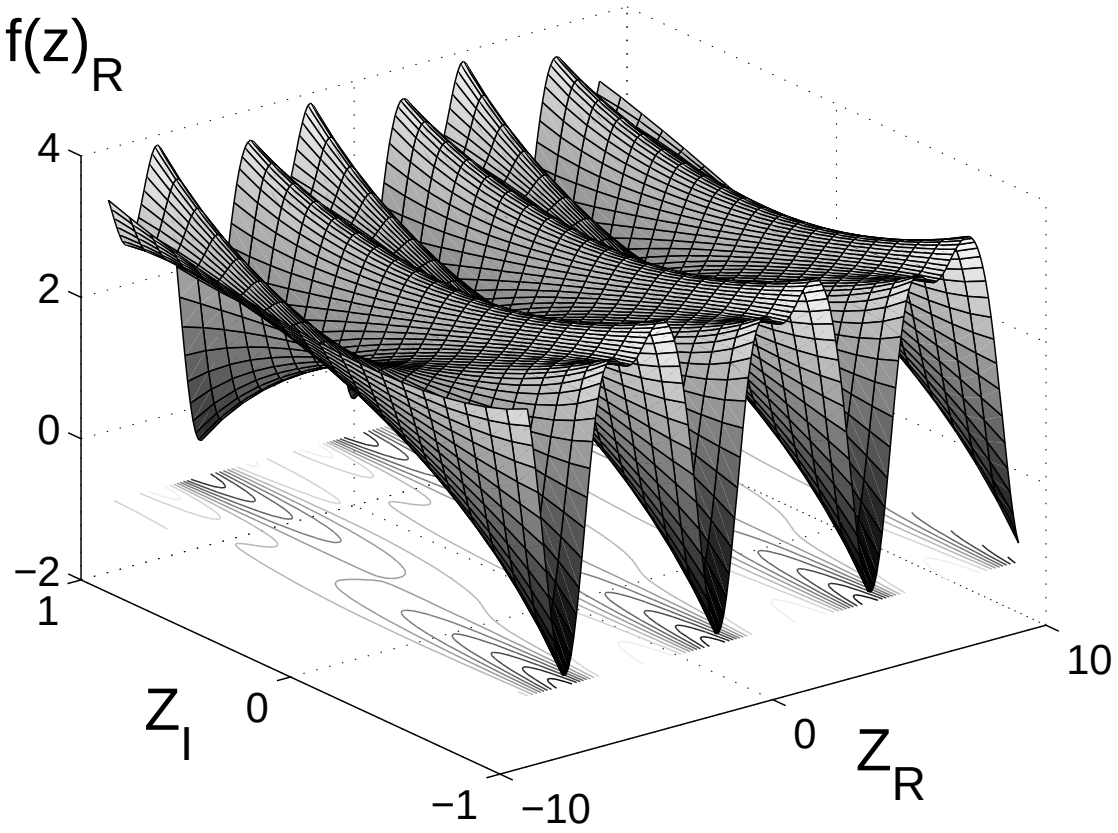

Figure 3.1: The real part of the function $f(z)$ of Eq. (3.29). $d = 5$ and the $|F\rangle$ is described through the coefficients in Eq. (3.44).

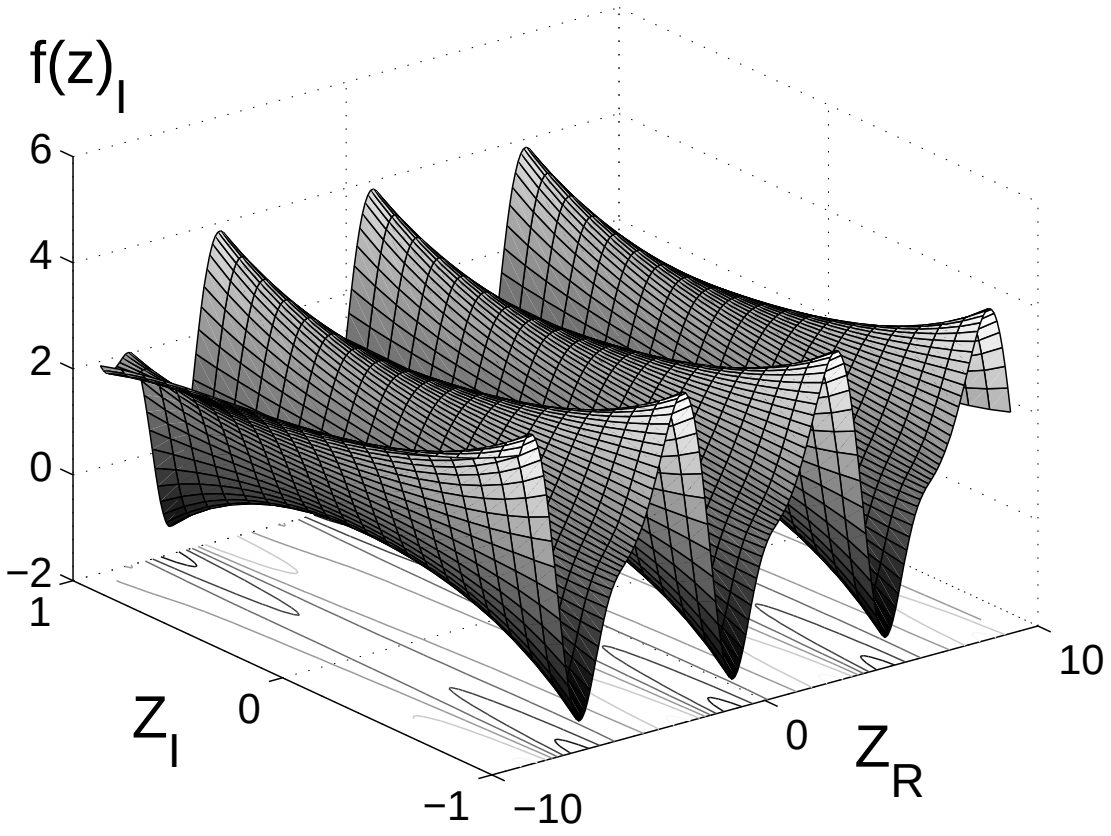

Figure 3.2: The imaginary part of the function $f(z)$ of Eq. (3.29). $d = 5$ and the $|F\rangle$ is described through the coefficients in Eq. (3.44).

3.5 Zeros of the functions $f(z)$

We shall now denote as ζ_n the zeros of $f(z)$, i.e. $f(\zeta_n) = 0$.

Let $f(z)$ be an analytic function. We consider the integrals

$$J_0 \;=\; \oint_\ell \frac{dz}{2\pi i}\frac{\partial_z f(z)}{f(z)}; \quad J_1 \;=\; \oint_\ell \frac{dz}{2\pi i}\frac{\partial_z f(z)}{f(z)} z. \tag{3.45}$$

J_0 is equal to the number of zeros of this function (with the multiplicities taken into account), inside the contour ℓ.

J_1 is equal to the sum of these zeros.

The analytic function $f(z)$ satisfies the quasi-periodicity of Eq. (3.30).

Using the quasi-periodicity of Eq. (3.30) we prove that the integral J_0, for a contour along the boundary of the cell S, is equal to d. Therefore the analytic functions $f(z)$ have exactly d zeros, within each cell S.

Using the quasi-periodicity of Eq. (3.30) we also prove that

$$\oint_\ell \frac{dz}{2\pi i}\frac{\partial_z f(z)}{f(z)}\, z \;=\; (2\pi)^{1/2}\, d^{3/2}\, (M + iN) \;+\; \left(\frac{\pi}{2}\right)^{1/2} d^{3/2}\, (1+i). \tag{3.46}$$

In the plane which acts as the covering surface of the torus, each cell is characterised by a pair of integers (M, N).

Integration on the contour along the boundary of the cell characterised by $(0,0)$, gives $\left(\frac{\pi}{2}\right)^{1/2}\, d^{3/2}\, (1+i)$.

Integration on the contour along the boundary of the cell characterised by (M,N), gives $\left(\frac{\pi}{2}\right)^{1/2}\, d^{3/2}\, (1+i) + (2\pi)^{1/2}\, d^{3/2}\, (M + iN)$.

Therefore, the sum of the zeros ζ_n of $f(z)$ is

$$\sum_{n=1}^{d} \zeta_n \;=\; (2\pi)^{1/2}\, d^{3/2}\, (M + iN) + \left(\frac{\pi}{2}\right)^{1/2} d^{3/2}\, (1 + i). \qquad (3.47)$$

In order to provide some examples, we demonstrate the distributions of zeros for three different cases

• In Fig. 3.3 we show the distributions of zeros for case $d = 3$, and the $|F(t)\rangle$ is described through the coefficients

$$F_0(0) = 0.23 + i0.13;\;\; F_1(0) = 0.67 - i0.04;\;\; F_2(0) = 0.67 - i0.09. \qquad (3.48)$$

• In Fig. 3.4 we show the distributions of zeros for case $d = 5$, and the $|F(t)\rangle$ at $t = 0$ is described through the coefficients in Eq. (3.44).

• In Fig. 3.5 we show the distributions of zeros for case $d = 5$, and the $|F(t)\rangle$ at $t = 0$ is described through the coefficients

$$F_0(0) = 0.84;\; F_1(0) = 0.33;\; F_2(0) = 0.18;\; F_3(0) = 0.18;\; F_4(0) = 0.33; \quad (3.49)$$

where we see only one zero(because the five zeros are **identical**).

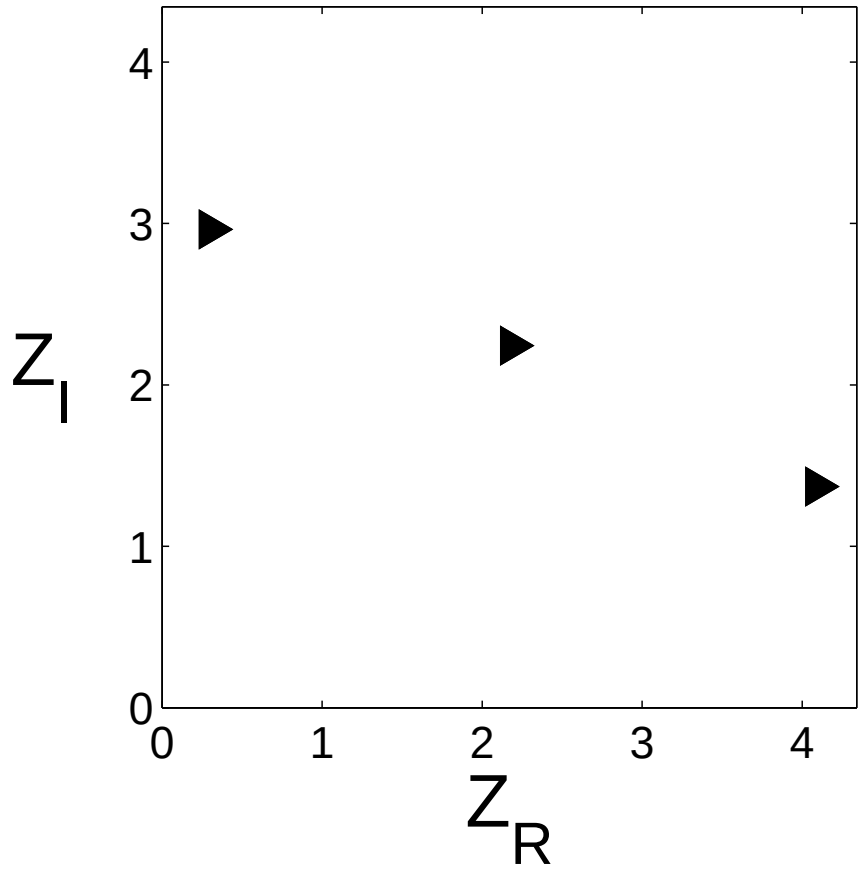

Figure 3.3: The zeros of function $f(z)$ for case $d = 3$. The $|F(t)\rangle$ at $t = 0$ is described through the coefficients in Eq. (3.48).

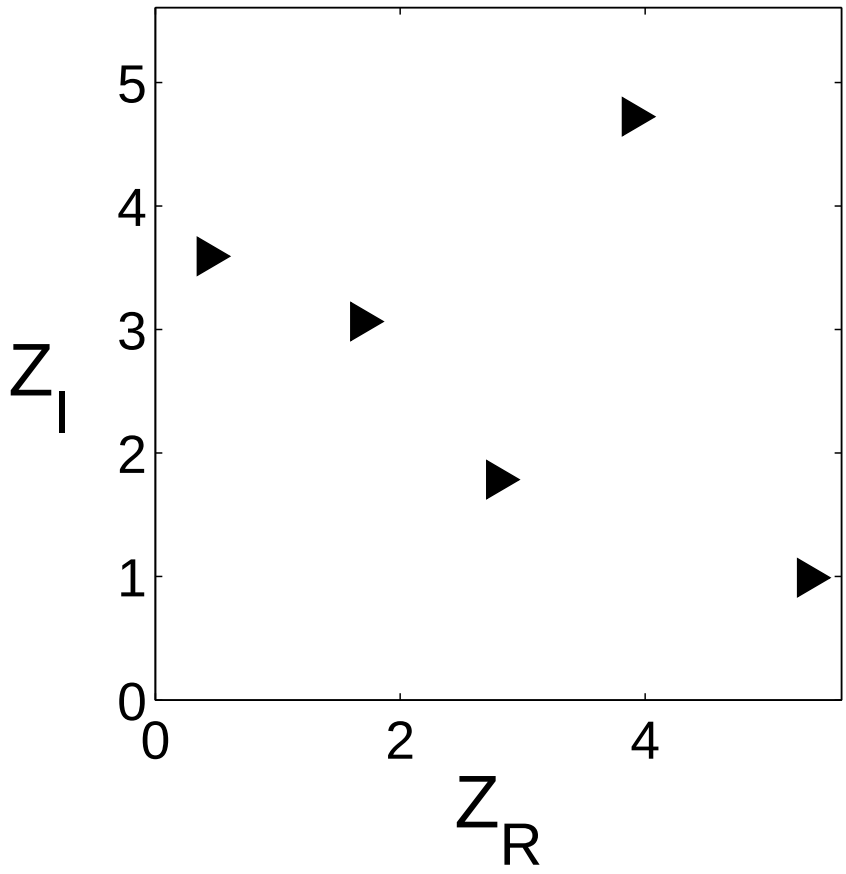

Figure 3.4: The zeros of function $f(z)$ for case $d = 5$. The $|F(t)\rangle$ at $t = 0$ is described through the coefficients in Eq. (3.44).

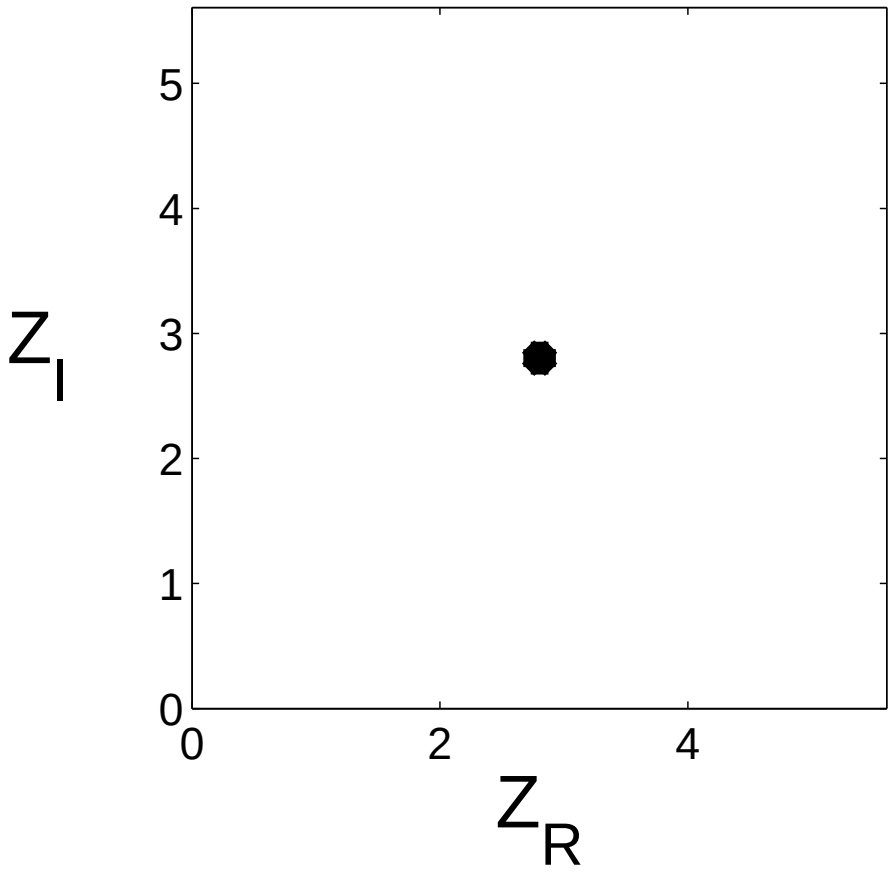

Figure 3.5: The zeros of function $f(z)$ for case $d = 5$. The $|F(t)\rangle$ at $t = 0$ is described through the coefficients in Eq. (3.49).

3.5.1 Construction of the analytic representation from its zeros

We suppose that d zeros ζ_n in the cell S are given, and that they satisfy the constraint of Eq. (3.47). In other words, $d-1$ zeros are given and the last is found through the constraint of Eq. (3.47).

We consider the function

$$\varphi(z) \;=\; \prod_{n=1}^{d} \vartheta_3 \left[\left(\frac{\pi}{2d}\right)^{1/2} (z-\zeta_n) + \frac{\pi(1+i)}{2};\; i \right]; \tag{3.50}$$

It is evident that $\varphi(z)$ has the given zeros. The entire function $f(z)/\varphi(z)$ has no zeros, which means it is the exponential of entire function:

$$f(z) \;=\; \varphi(z) exp\left(\phi(z)\right). \tag{3.51}$$

If we take into account the periodicity constraints of Eq. (3.30) we find

$$\begin{aligned} \phi\left[z+\sqrt{2\pi d}\,\right] &= \phi(z) + i2\pi\mathcal{N}; \\ \phi\left[z+i\sqrt{2\pi d}\,\right] &= \phi(z) + 2\pi\,(N+i\mathcal{M}); \end{aligned} \tag{3.52}$$

where $\mathcal{N};\mathcal{M}$ are arbitrary integers and N is the integer entering the constraint of Eq. (3.47). The growth of $f(z)$ is of order 2. The order of $\varphi(z)$ is 2; which means that the $\phi(z)$ is a polynomial of maximum possible degree 2. From Eq. (3.52) we find that

$$\phi(z) \;=\; -\left(\frac{2\pi}{d}\right)^{1/2} Nzi + \Lambda, \tag{3.53}$$

here Λ is a constant. Therefore the function $f(z)$ is given by

$$\begin{aligned} f(z) &= exp(\Lambda)\, exp\left[-\left(\frac{2\pi}{d}\right)^{1/2} Nzi\right]\varphi(z); \\ &= C\exp\left[-i\left(\frac{2\pi}{d}\right)^{1/2} Nz\right]\prod_{n=1}^{d}\vartheta_3\left[w_n(z);\ i\right]; \\ w_n(z) &= \left(\frac{\pi}{2d}\right)^{1/2}(z-\zeta_n)+\frac{\pi(1+i)}{2}; \end{aligned} \tag{3.54}$$

where $N \in \mathbb{Z}$ in the constraint of Eq. (3.47), and C is a constant determined by the normalisation condition.

3.5.2 Numerical Example

Analytically, using Eq. (3.41) we can calculate the coefficients F_m.

Numerically, we insert d arbitrary values $z_0, ..., z_{d-1}$ and solve the system of d equations with d unknowns:

$$f(z_j) = \pi^{-1/4}\sum_{m=0}^{d-1} F_m\,\vartheta_3\left[\pi\, m\, d^{-1} - z_j\,\pi^{1/2}\,(2d)^{-1/2}; i\, d^{-1}\right]. \tag{3.55}$$

We take the normalisation coefficients equal to one, and after the calculation we normalise the vector F_m.

As an example, let $d = 3$ and $\zeta_0;\ \zeta_1$ be given as follows:

$$\zeta_0 = 0.26 + 2.95i; \quad \zeta_1 = 2.16 + 2.22i. \tag{3.56}$$

Using Eq. (3.47), we get $\zeta_2 = 4.09 + 1.34i$.

We choose three arbitrary values $0, 1, -1$ and insert them with $\zeta_0; \zeta_1; \zeta_2$

in Eq. (3.54). We then find $f(0), f(1), f(-1)$ to insert them in Eq. (3.55) and solve the system of three equations with three unknowns, in which case we get

$$\begin{pmatrix} F_0 \\ F_1 \\ F_2 \end{pmatrix} = \begin{pmatrix} 0.2349 + 0.1301i \\ 0.6778 - 0.0490i \\ 0.6760 - 0.0952i \end{pmatrix}$$

3.6 Paths of the Zeros

Using the Hamiltonian H, the state $|F(0)\rangle = \sum F_m(0)|X;m\rangle$ at $t = 0$ evolves at time t into

$$|F(t)\rangle = \exp(itH)|F(0)\rangle = \sum_{m=0}^{d-1} F_m(t)|X;m\rangle. \tag{3.57}$$

Let $f(z;t)$ be the analytic function corresponding to $\exp(itH)|f\rangle$ (where $f(z;0) = f(z)$) and $\zeta_n(t)$ the zeros.

We consider the evolution operators

$$\begin{aligned} U_A(t) &= \exp(itH_A); \quad H_A = \frac{x^2}{2} + \frac{p^2}{2}, \\ U_B(t) &= \exp(itH_B); \quad H_B = -i \ln \left[\exp\left(\frac{ix^2}{2}\right) \exp\left(\frac{ip^2}{2}\right) \right], \\ U_C(t) &= \exp(itH_C); \quad H_C = F H_B F^\dagger = -i \ln \left[\exp\left(\frac{ip^2}{2}\right) \exp\left(\frac{ix^2}{2}\right) \right]. \end{aligned} \tag{3.58}$$

Each of these is the analogue of a harmonic oscillator evolution operator with Hamiltonian $H = 1/2x^2 + 1/2p^2$. Here, there is no analogous formula to the Baker-Campbell-Hausdorff relation, and therefore there is no simple relation

between them.

Below, we show the eigenvalues of the $d \times d$ matrices H_A, H_B, H_C. The H_B, H_C have the same eigenvalues, because they are related with a unitary transformation.

Mathematically, the eigenvalues of H_B, H_C are defined modulo $2\pi N$, because there is a multivaluedness associated with the logarithms in H_B, H_C.

Physically, the eigenvalues of H_B should be close to the eigenvalues of H_A, because in the semiclassical limit these Hamiltonians are the same.

This physical requirement defines which of the logarithms should be chosen.

3.6.1 Eigenvalues of the Hamiltonians H_A, H_B, H_C

We calculate the eigenvalues of the Hamiltonians H_A, H_B, H_C for the case $d = 5$. The calculation of the eigenvalues A_i of H_A (labelled in ascending order) is straightforward, and the results are shown in Table 3.1.

The eigenvalues B_i of H_B are defined modulo $2\pi N$, and as we explained we chose those close to the eigenvalues A_i of H_A, because in the semiclassical limit the corresponding Hamiltonians are the same.

In order to do this, we express A_i as

$$A_i = A'_i + 2\pi N_i \ (\mathrm{mod}\ 2\pi); \qquad 0 \leq A'_i < 2\pi \tag{3.59}$$

We then calculate the eigenvalues of the matrix $\exp(iH_B) = \exp\left(\frac{ix^2}{2}\right)\exp\left(\frac{ip^2}{2}\right)$, which are $\mathcal{B}_i = \exp(iB_i)$. From $\mathcal{B}_i$, we calculate the values of $B'_i = -i\ln\mathcal{B}_i$ such that $0 \leq B'_i < 2\pi$ (the B'_i are labelled in ascending order). We then

add $2\pi N_i$ (calculated in Eq. (3.59)) to B_i' and we get the B_i. In Table 3.1, we show the B_i, which are eigenvalues of both H_B, H_C.

H_A	H_B, H_C
12.82	12.90
8.15	8.46
5.17	4.44
2.87	3.41
0.96	0.77

Table 3.1: The eigenvalues of H_A, H_B, H_C

As an example, we consider the case where

• $d = 5$ and the state $|F(0)\rangle$ at $t = 0$ are described through the coefficients in Eq. (3.44). We calculate the coefficients $F_m(t)$ for the three cases of Hamiltonians H_A, H_B, H_C in Eq. (3.58), and we further calculate the corresponding $f(z;t)$ using Eq. (3.29). Following this, we find numerically the zeros $\zeta_n(t)$ using MATLAB.

In Fig. 3.6 we show the plot of the five curves $\zeta_n(t)$ for the Hamiltonians H_A (solid line), H_B (broken lines) and H_C (dotted line) of Eq. (3.58). We plot part of these curves in the adjacent cells only (these curves should appear in the original cell also, although through periodicity). In Fig. 3.7 we show the plot of the real part of one of the zeros as a function of time t.

• $d = 3$ and the state $|F(0)\rangle$ at $t = 0$ are described through the coefficients

$$F_0(0) = 0.51 - 0.33i; \quad F_1(0) = 0.22 - 0.21i; \quad F_2(0) = 0.23 - 0.22i; \qquad (3.60)$$

We calculate the coefficients $F_m(t)$ for the Hamiltonian H_B in Eq. (3.58), and we further calculate the corresponding $f(z;t)$ using Eq. (3.29), from

which we find numerically the zeros $\zeta_n(t)$ using MATLAB. In Fig. 3.8 we show the plot of the three curves $\zeta_n(t)$ for the Hamiltonian H_A of Eq. (3.58).

• $d = 3$ and the state $|F(0)\rangle$ at $t = 0$ are described through the coefficients

$$F_0(0) = 0.8881; \quad F_1(0) = 0.3250; \quad F_2(0) = 0.3250. \tag{3.61}$$

We calculate the coefficients $F_m(t)$ for the Hamiltonian H_C in Eq. (3.58), and further calculate the corresponding $f(z;t)$ using Eq. (3.29). In this case, we find numerically three **Identical** zeros using MATLAB.

$$\zeta_0(0) = \zeta_1(0) = \zeta_2(0) = 2.1708 + 2.1708i. \tag{3.62}$$

In Fig. 3.9 we show the plot of the three curves $\zeta_n(t)$ for the Hamiltonian H_B of Eq. (3.58).

• In Fig. 3.10 we consider the case where $d = 3$ and the state $|F(0)\rangle$ at $t = 0$ are described through the coefficients

$$F_0(0) = 0.84 + 0.09i; \quad F_1(0) = 0.36 - 0.04i; \quad F_2(0) = 0.36 - 0.04i. \tag{3.63}$$

We calculate the coefficients $F_m(t)$ for the Hamiltonian

$$H_D = \begin{pmatrix} 1 & 1-i & 0 \\ 1+i & 1 & 0 \\ 0 & 0 & 2.5 \end{pmatrix} \tag{3.64}$$

which has the eigenvalues $-0.41, 2.41, 2.5$ and we calculate the corresponding

$f(z;t)$ using Eq. (3.29).

• In Fig. 3.11 we consider the case where $d = 4$ and the state $|F(0)\rangle$ at $t = 0$ are described through the coefficients

$$F_0(0) = 0.03 + 0.25i; \qquad F_1(0) = 0.53 + 0.05i;$$
$$F_2(0) = 0.74 - 0.22i; \qquad F_3(0) = 0.12 - 0.16i. \tag{3.65}$$

We calculate the coefficients $F_m(t)$ for the Hamiltonian

$$H_E = \begin{pmatrix} 1 & -i & 0 & 0 \\ i & 1 & 0 & 0 \\ 0 & 0 & 1/2 & 0 \\ 0 & 0 & 0 & 1/2 \end{pmatrix} \tag{3.66}$$

which has the eigenvalues $0, 0.5, 0.5, 2$ and we calculate the corresponding $f(z;t)$ using Eq. (3.29).

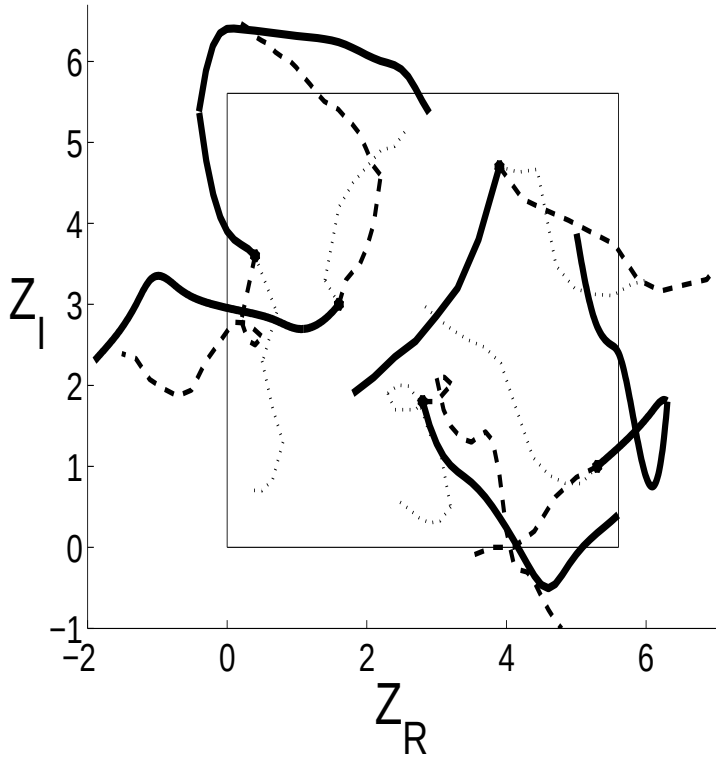

Figure 3.6: The zeros $\zeta_n(t)$ for state $|F(t)\rangle$, which at $t = 0$ are described in Eq. (3.44). We consider the three Hamiltonians H_A (solid line), H_B (broken lines) and H_C (dotted line) of Eq. (3.58). For clarity, parts of these curves are plotted in the adjacent cells only (although through periodicity they should appear in the original cell also).

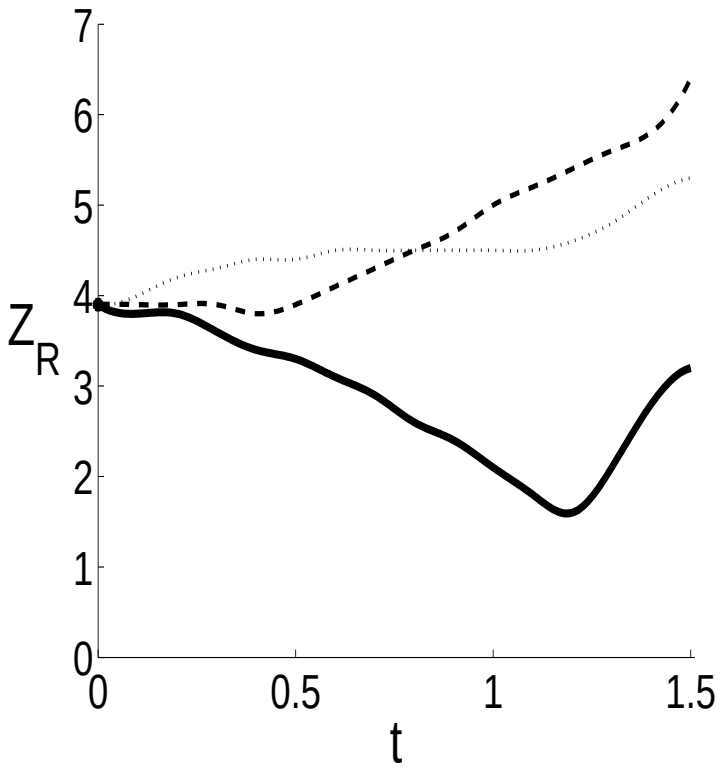

Figure 3.7: The real part of one of the zeros as a function of time t for the state $|F(t)\rangle$, which at $t = 0$ is described in Eq. (3.44). We consider the three Hamiltonians H_A (solid line), H_B (broken lines) and H_C (dotted line) of Eq. (3.58).

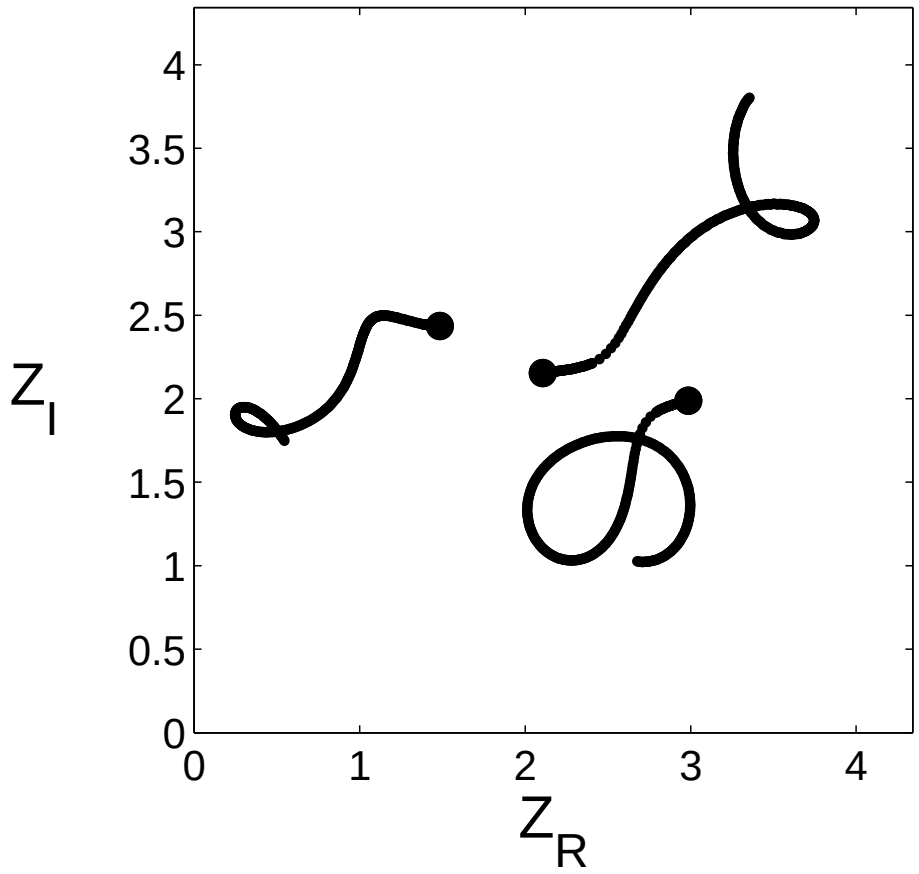

Figure 3.8: The zeros $\zeta_n(t)$ for the state $|F(t)\rangle$, which at $t = 0$ are described in Eq. (3.60). We consider the Hamiltonian H_B of Eq. (3.58).

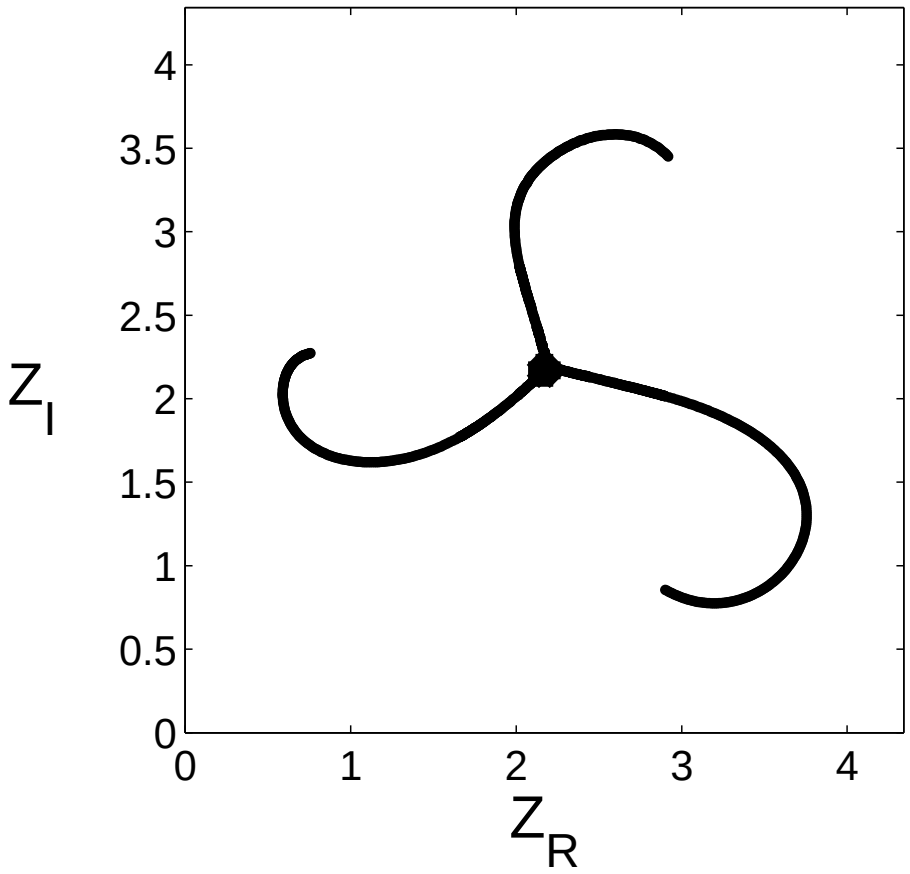

Figure 3.9: The zeros $\zeta_n(t)$ for the state $|F(t)\rangle$, which at $t = 0$ are described in Eq. (3.61). We consider the Hamiltonian H_C of Eq. (3.58).

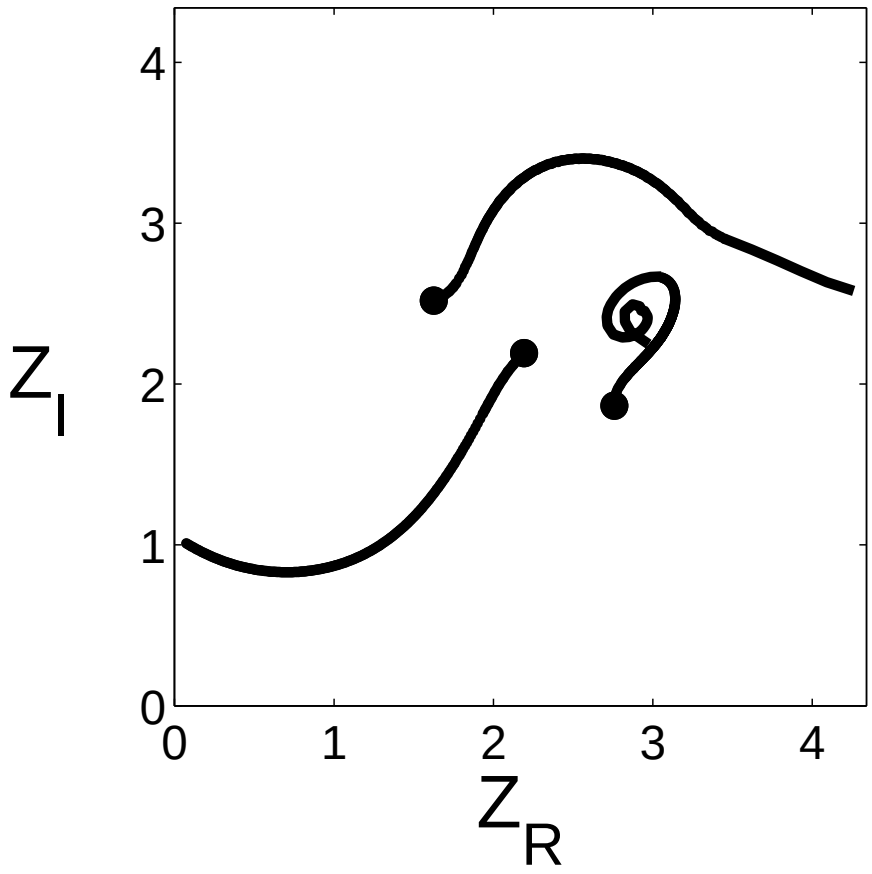

Figure 3.10: The zeros $\zeta_n(t)$ for the state $|F(t)\rangle$, which at $t = 0$ are described in Eq. (3.63). We consider the Hamiltonian H_D of Eq. (3.64).

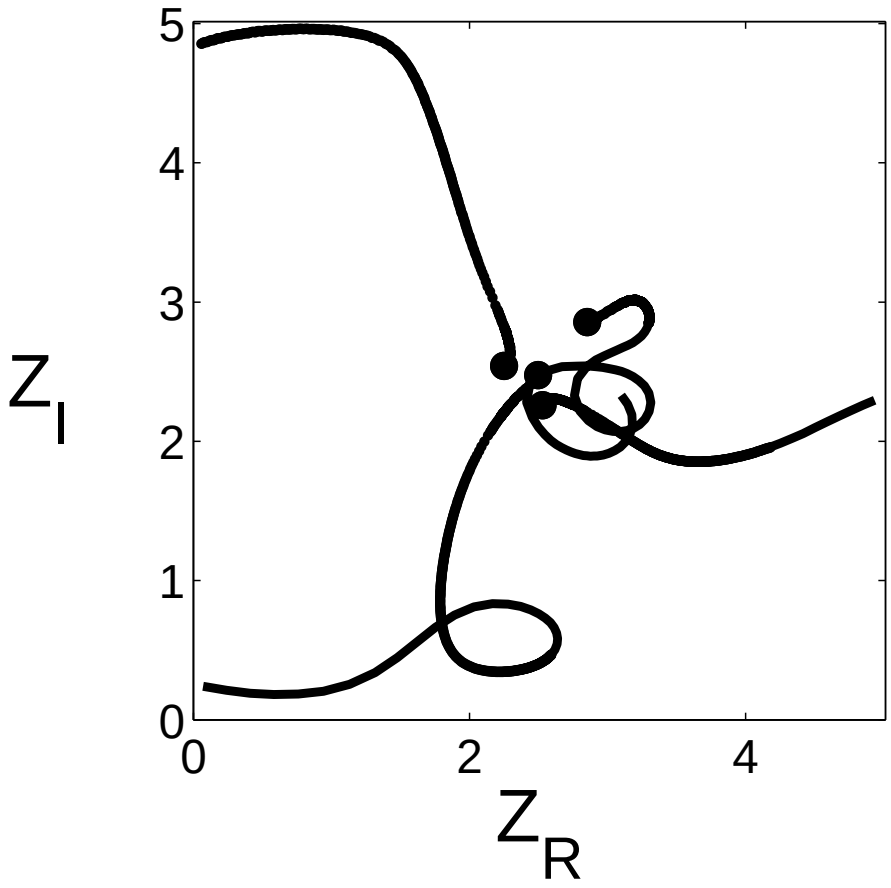

Figure 3.11: The zeros $\zeta_n(t)$ for the state $|F(t)\rangle$, which at $t = 0$ are described in Eq. (3.65). We consider the Hamiltonian H_E of Eq. (3.66).

3.7 Calculation of the Hamiltonian from the paths of the zeros

In Eq. (3.54) we explained how, from the zeros ζ_n, we can calculate the state $f(z)$ in the analytic representation. In section 3.6 we assumed that the Hamiltonian was given, and we then calculated the paths $\zeta_n(t)$ of the d zeros which define completely a finite quantum system. In this section, we consider the inverse problem inasmuch that we calculate the Hamiltonian for a given path $\zeta_n(t)$ of the d zeros. We use Eq. (3.54) to calculate the $f(z;t)$ and then solve the system of Eq. (3.55) to calculate the $F_m(t)$. The Hamiltonian is a $d \times d$ Hermitian matrix, with d^2 real variables, which in general are time-dependent.

For small time intervals δt, we can write the evolution operator

$$U(t) = \exp(iHt)$$

approximately as

$$U_{mn}(\delta t) \approx \delta_{mn} + iH_{mn}\delta t; \qquad m, n = 0, ..., d-1 \tag{3.67}$$

The above equation involves a truncation and is approximate.

We calculate the $F_m(0), F_m(\delta t), ..., F_m(N\delta t)$. We then solve the linear system

$$F_m\left[(j+1)\delta t\right] = F_m(j\delta t) + \sum_{n=0}^{d-1} i\delta t H_{mn}(j\delta t) F_n(j\delta t); \quad j = 0, ..., (N-1). \tag{3.68}$$

We obtain d^2 real unknowns (the degrees of freedom of the matrix H), so we

therefore need ($\mathcal{K} > d^2$) real independent equations. The equations corresponding to each interval (e.g. from $t = 0$ to δt) give d complex equations, i.e. $2d$ real equations, in which case we need at least $d/2$ intervals (or $(d+1)/2$ if d is an odd number). We assume that the Hamiltonian is constant for the small time interval. We then solve the overdetermined system of equations (we use more equations than unknowns).

We here rewrite the system of Eq. (3.68) as $AX = B$, where A is a $\mathcal{K} \times d^2$ matrix, X is the Hamiltonian written as a $d^2 \times 1$ vector and B is a $\mathcal{K} \times 1$ vector. Using a numerical method we minimise $||AX - B||$. We can find many numerical techniques for such systems, and the advantage is that we find stable solutions. A change to δt or the number $\mathcal{K}$ of equations gives approximately the same results. To measure the error we calculate the matrix

$$UU^\dagger - \mathbf{1}$$

which has the elements

$$K_{ik} = (\delta t)^2 \sum_j H_{ij} H^*_{kj}.$$

This matrix should be zero in an exact calculation. We calculate its Frobenius norm as a measure of the error

$$E = \left(\sum_{i,k} |K_{ik}|^2 \right)^{1/2} \tag{3.69}$$

We now consider a simple example where $d = 2$. Let

$$\zeta_0(t) = \sin(10t) + (5 + 5i)t + (2 + i) + 2\pi^{1/2}(M + iN)$$

be the path of the first zero (the term $2\pi^{1/2}(M+iN)$ is related to the toroidal structure). From the constraint of Eq. (3.47), we calculate the path of the second zero to be

$$\zeta_1(t) = 2\pi^{1/2}(1+i) - \zeta_0(t) + 2\pi^{1/2}(M'+iN').$$

We choose small time intervals δt and calculate the $F_m(0), F_m(\delta t), F_m(2\delta t)$. We solve the system

$$\begin{aligned} F_m(\delta t) &= F_m(0) + \sum_{n=0}^{1} i\delta t H_{mn} F_n(0); \\ F_m(2\delta t) &= F_m(\delta t) + \sum_{n=0}^{1} i\delta t H_{mn} F_n(\delta t). \end{aligned} \tag{3.70}$$

of four complex equations ($\mathcal{K} = 8$) with four real unknowns as follows:

We want to calculate the Hamiltonian

$$H = \begin{pmatrix} a & c+id \\ c-id & b \end{pmatrix}; \tag{3.71}$$

and the evolution operator

$$U(\delta t) = \begin{pmatrix} 1+i\delta t a & i\delta t(c+id) \\ i\delta t(c-id) & 1+i\delta t b \end{pmatrix}. \tag{3.72}$$

where a, b, c, d are real numbers.

Let

$$F_m(0) = \begin{pmatrix} x_0+iy_0 \\ x_1+iy_1 \end{pmatrix};\ F_m(\delta t) = \begin{pmatrix} x_2+iy_2 \\ x_3+iy_3 \end{pmatrix};\ F_m(2\delta t) = \begin{pmatrix} x_4+iy_4 \\ x_5+iy_5 \end{pmatrix}; \tag{3.73}$$

We here rewrite the system of Eq. (3.70) as follows:

$$\begin{pmatrix} 1+i\delta ta & i\delta t(c+id) \\ i\delta t(c-id) & 1+i\delta tb \end{pmatrix} \begin{pmatrix} x_0+iy_0 \\ x_1+iy_1 \end{pmatrix} = \begin{pmatrix} x_2+iy_2 \\ x_3+iy_3 \end{pmatrix}; \qquad (3.74)$$

$$\begin{pmatrix} 1+i\delta ta & i\delta t(c+id) \\ i\delta t(c-id) & 1+i\delta tb \end{pmatrix} \begin{pmatrix} x_2+iy_2 \\ x_3+iy_3 \end{pmatrix} = \begin{pmatrix} x_4+iy_4 \\ x_5+iy_5 \end{pmatrix}; \qquad (3.75)$$

This system of four complex equations

$$ia(x_0+iy_0)+i(c+id)(x_1+iy_1) = (x_2+iy_2)-(x_0+iy_0);$$

$$i(c-id)(x_0+iy_0)+ib(x_1+iy_1) = (x_3+iy_3)-(x_1+iy_1);$$

$$ia(x_2+iy_2)+i(c+id)(x_3+iy_3) = (x_4+iy_4)-(x_2+iy_2);$$

$$i(c-id)(x_2+iy_2)+ib(x_3+iy_3) = (x_5+iy_5)-(x_3+iy_3); \qquad (3.76)$$

and eight real equations with four unknowns

$$-ay_0-cy_1-dx_1 = x_2-x_0;$$

$$ax_0+cx_1-dy_1 = y_2-y_0;$$

$$-cy_0+dx_0-by_1 = x_3-x_1;$$

$$cx_0+dy_0+bx_1 = y_3-y_1;$$

$$-ay_2-cy_3-dx_3 = x_4-x_2;$$

$$ax_2 + cx_3 - dy_3 = y_4 - y_2;$$

$$-cy_2 + dx_2 - by_3 = x_5 - x_3;$$

$$cx_2 + dy_2 + bx_3 = y_5 - y_3. \tag{3.77}$$

We here rewrite the system of Eq. (3.77) as $AX = B$

$$\begin{pmatrix} -y_0 & -y_1 & -x_1 & 0 \\ x_0 & x_1 & -y_1 & 0 \\ 0 & -y_0 & x_0 & -y_1 \\ 0 & x_0 & y_0 & x_1 \\ -y_2 & -y_3 & -x_3 & 0 \\ x_2 & x_3 & -y_3 & 0 \\ 0 & -y_2 & x_2 & -y_3 \\ 0 & x_2 & y_2 & x_3 \end{pmatrix} \begin{pmatrix} a \\ c \\ d \\ b \end{pmatrix} = \begin{pmatrix} y_5 - y_3 \\ y_2 - y_0 \\ x_3 - x_1 \\ y_3 - y_1 \\ x_4 - x_2 \\ y_4 - y_2 \\ x_5 - x_3 \\ y_5 - y_3 \end{pmatrix}; \tag{3.78}$$

In this case we choose $\delta t = 0.01$ and evaluate the $F_m(0), F_m(0.01), F_m(0.02)$. We then solve the system in Eq. (3.78), which gives the Hamiltonian matrix

$$H_0 = \begin{pmatrix} 8.6187 & -11.8703 + 4.5382i \\ -11.8703 - 4.5382i & 19.7692 \end{pmatrix} \tag{3.79}$$

with error $E_0 = 0.07$.

A different choice of δt gives approximately the same Hamiltonian, in order to confirm that we repeat the calculation with $\delta t = 0.005$ and also $\delta t = 0.015$.

In the case of $\delta t = 0.005$ we evaluate the $F_m(0), F_m(0.005), F_m(0.01)$, after

which we then solve the system in Eq. (3.78). This gives the Hamiltonian matrix

$$H_0' = \begin{pmatrix} 9.7607 & -11.8789 + 3.9414i \\ -11.8789 - 3.9414i & 19.2609 \end{pmatrix}, \tag{3.80}$$

with error $E_0' = 0.019$.

In the case of $\delta t = 0.015$ we evaluate the $F_m(0), F_m(0.015), F_m(0.03)$. We then solve the system in Eq. (3.78). This gives the Hamiltonian matrix

$$H_0'' = \begin{pmatrix} 7.4048 & -11.7168 + 5.0944i \\ -11.7168 - 5.0944i & 19.7303 \end{pmatrix}, \tag{3.81}$$

with error $E_0'' = 0.17$.

We see that the Hamiltonians H_0, H_0' and H_0'' are approximately equal.

As expected, an increase in the time step increases the error.

The Hamiltonian is in general time-dependent, and in order to show this we have repeated the calculation of the Hamiltonian H_N for the intervals

$$(0.01N, 0.01N + 0.01), (0.01N + 0.01, 0.01N + 0.02) \text{ with } N = 2, 4, 6, 8.$$

as follows:

- We evaluate the $F_m(0.02), F_m(0.03), F_m(0.04)$ and we then solve the system in Eq. (3.78). This gives the Hamiltonian matrix

$$H_1 = \begin{pmatrix} 5.6607 & -12.8322 + 4.7287i \\ -12.8322 - 4.7287i & 17.9470 \end{pmatrix}, \tag{3.82}$$

with error $E_1 = 0.07$.

- We evaluate the $F_m(0.04), F_m(0.05), F_m(0.06)$ and we then solve the system in Eq. (3.78). This gives the Hamiltonian matrix

$$H_2 = \begin{pmatrix} 3.0297 & -11.4457 + 5.0043i \\ -11.4457 - 5.0043i & 14.1393 \end{pmatrix}, \qquad (3.83)$$

with error $E_2 = 0.05$.

- We evaluate the $F_m(0.06), F_m(0.07), F_m(0.08)$, and we then solve the system in Eq. (3.78). This gives the Hamiltonian matrix

$$H_3 = \begin{pmatrix} 2.5176 & -8.8037 + 3.2893i \\ -8.8037 - 3.2893i & 10.8301 \end{pmatrix}, \qquad (3.84)$$

with error $E_3 = 0.03$.

- We evaluate the $F_m(0.08), F_m(0.09), F_m(0.10)$ and we then solve the system in Eq. (3.78). This gives the Hamiltonian matrix

$$H_4 = \begin{pmatrix} 5.6293 & -7.0773 + 0.7992i \\ -7.0773 - 0.7992i & 7.7871 \end{pmatrix}, \qquad (3.85)$$

with error $E_4 = 0.02$.

From the above calculations, it is evident that the Hamiltonian is time-dependent.

3.8 summary

We have considered a quantum system with a $d-$dimensional Hilbert space $\mathcal{H}$, where position and momentum take vales in $\mathbb{Z}_d$. Quantum states have been represented with the analytic function of Eq. (3.29) on a torus, which has exactly d zeros and obeys the constraint of Eq. (3.47). We have considered the construction of the analytic function of state from its zeros. As the system evolves in time, the d zeros follow d paths on the torus, which define the Hamiltonian. We have also considered the inverse problem, i.e. calculated the paths $\zeta_n(t)$ of the d zeros for a given Hamiltonian.

Chapter 4

Periodic finite quantum systems

In the previous chapter we studied the time evolution of the system, and the motion of the d zeros on the torus. We saw that the d zeros follow d paths on the torus when the system evolves in time. In addition, we considered various Hamiltonians and various initial states, and numerically we calculated the d paths of the d zeros.

In this chapter, we study the periodic systems (systems with Hamiltonians with commensurate eigenvalues) and discuss some examples where two or more zeros follow the same path.

4.1 Introduction

In this chapter, we consider periodic finite quantum systems. We showed in Chapter 3 that as a system evolves in time, the d zeros follow d paths on the torus. If the eigenvalues of the Hamiltonian are rational numbers, the d paths of d zeros in general closed curves on the torus.

The chapter then moves on to give a brief introduction to the periodic system. During a period the zeros follow closed paths. We show that, in some cases, the $\mathfrak{M}$ of the zeros follow the same path. We say that this path has multiplicity $\mathfrak{M}$, which we back up with $\mathfrak{M} = 2, 3, 4, 5$ examples. We then discuss how a perturbation of the initial values of the zeros splits a path with multiplicity $\mathfrak{M}$ into $\mathfrak{M}$ different paths. Near the point where the splitting occurs, we approximate the paths of the zeros with the quadratic equation.

4.2 Periodic systems with paths with multiplicity $\mathfrak{M} = 1$

Let Ω_i (where $i = 0, ..., d-1$) be the eigenvalues of the Hamiltonian H of the system. If the ratios Ω_i/Ω_0 are rational numbers, the system is periodic. In this case the d paths of the zeros $\zeta_n(t)$ are in general closed curves on the torus.

We now present the following examples:

• We consider the Hamiltonian

$$H = \begin{pmatrix} 1 & -i \\ i & 1 \end{pmatrix} \tag{4.1}$$

which has the eigenvalues $0, 2$ and the period $T = \pi$.

Let $\zeta_0(t), \zeta_1(t)$ be the paths of the zeros. We assume that at $t = 0$

$$\zeta_0(0) = 0.39 + 2.27i; \quad \zeta_1(0) = 3.15 + 1.27i. \tag{4.2}$$

These zeros obey the constraint of Eq. (3.47) and are on a torus (i.e. they are defined modulo $(4\pi)^{1/2}$). During a period, the zeros ζ_0, ζ_1 follow closed paths.

In Fig. 4.1 we present the paths of these zeros.

• We consider the Hamiltonian

$$H = \begin{pmatrix} 1 & -i & 0 \\ i & 1 & 0 \\ 0 & 0 & 2 \end{pmatrix} \tag{4.3}$$

which has the eigenvalues $0, 2, 2$ and the period $T = \pi$.

Let $\zeta_0(t), \zeta_1(t), \zeta_2(t)$ be the paths of the three zeros. We assume that at $t = 0$

$$\zeta_0(0) = 2.01 + 2.12i; \;\; \zeta_1(0) = 2.28 + 2.47i; \;\; \zeta_2(0) = 2.21 + 1.91i. \tag{4.4}$$

These zeros obey the constraint of Eq. (3.47) and are on a torus (i.e. they

are defined modulo $(6\pi)^{1/2}$).

In Fig. 4.2 we present the paths of these zeros. During a period, the zeros ζ_0, ζ_1, ζ_2 follow a closed path. These zeros return to their original position after a period.

• We will now consider the Hamiltonian of Eq. (4.3). Let $\zeta_0(t), \zeta_1(t), \zeta_2(t)$ be the paths of the three zeros. We assume that at $t = 0$

$$\zeta_0(0) = \zeta_1(0) = \zeta_2(0) = 2.1708 + 2.1708i; \tag{4.5}$$

These zeros obey the constraint of Eq. (3.47) and are on a torus (i.e. they are defined modulo $(6\pi)^{1/2}$).

In Fig. 4.3 we present the paths of these zeros. During a period, the zeros ζ_0, ζ_1, ζ_2 follow a closed path. These zeros return to their original position after a period.

In some cases, some or all of the zeros follow the same path. If $\mathfrak{M}$ of the zeros follow the same path, we say this path has multiplicity $\mathfrak{M}$. We can now present examples with $\mathfrak{M} = 2, 3, 4, 5$.

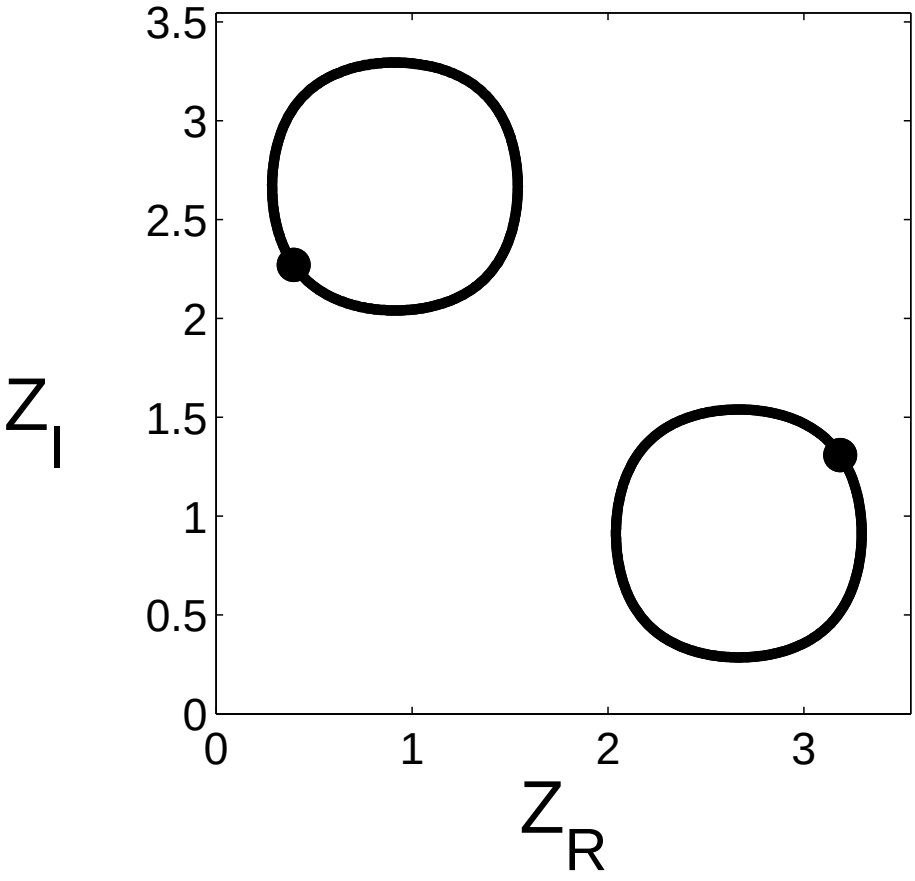

Figure 4.1: The paths of the zeros $\zeta_0(t)$, $\zeta_1(t)$ for the system with the Hamiltonian of Eq. (4.1). The zeros $\zeta_0(t)$, $\zeta_1(t)$ follow a closed path. At $t = 0$ the zeros $\zeta_0(0)$, $\zeta_1(0)$ are given in Eq. (4.2) and are indicated in the diagram. After a period T, the zeros ζ_0, ζ_1 return to their initial positions.

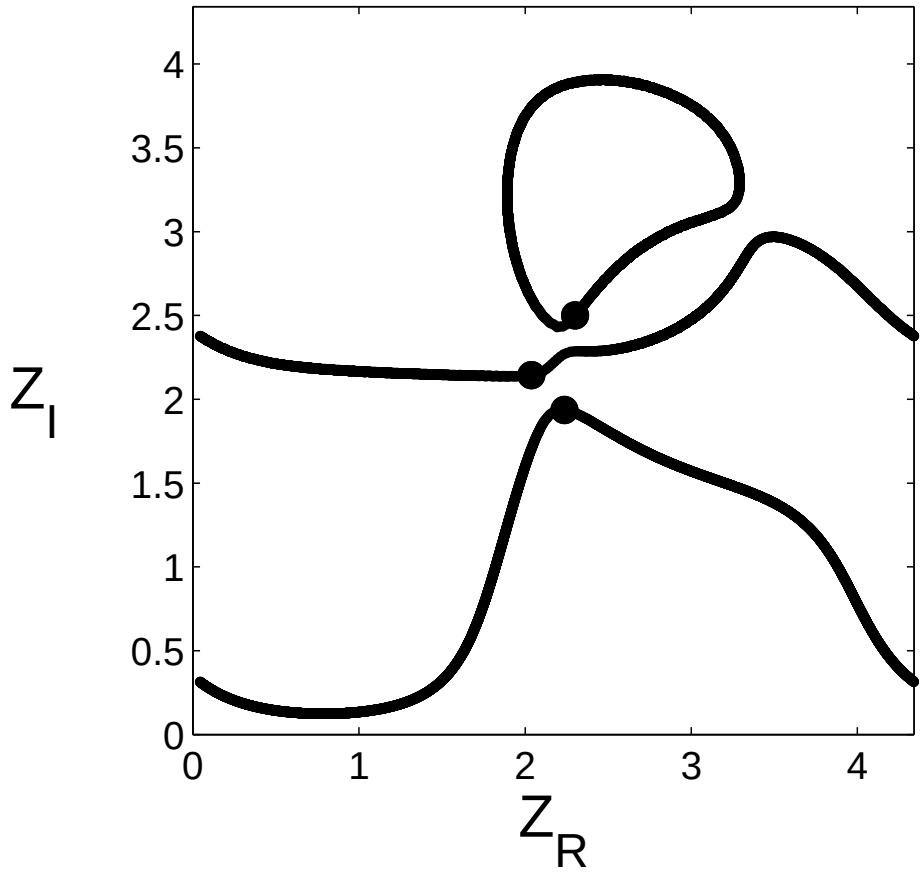

Figure 4.2: The paths of the zeros $\zeta_0(t)$, $\zeta_1(t)$, $\zeta_2(t)$ for the system with the Hamiltonian of Eq. (4.3). The zeros $\zeta_0(t)$, $\zeta_1(t)$, $\zeta_2(t)$ follow a closed path. At $t = 0$ the zeros $\zeta_0(0)$, $\zeta_1(0)$, $\zeta_2(0)$ are given in Eq. (4.4) and are indicated in the diagram. After a period T, the zeros ζ_0, ζ_1, ζ_2 return to their initial positions.

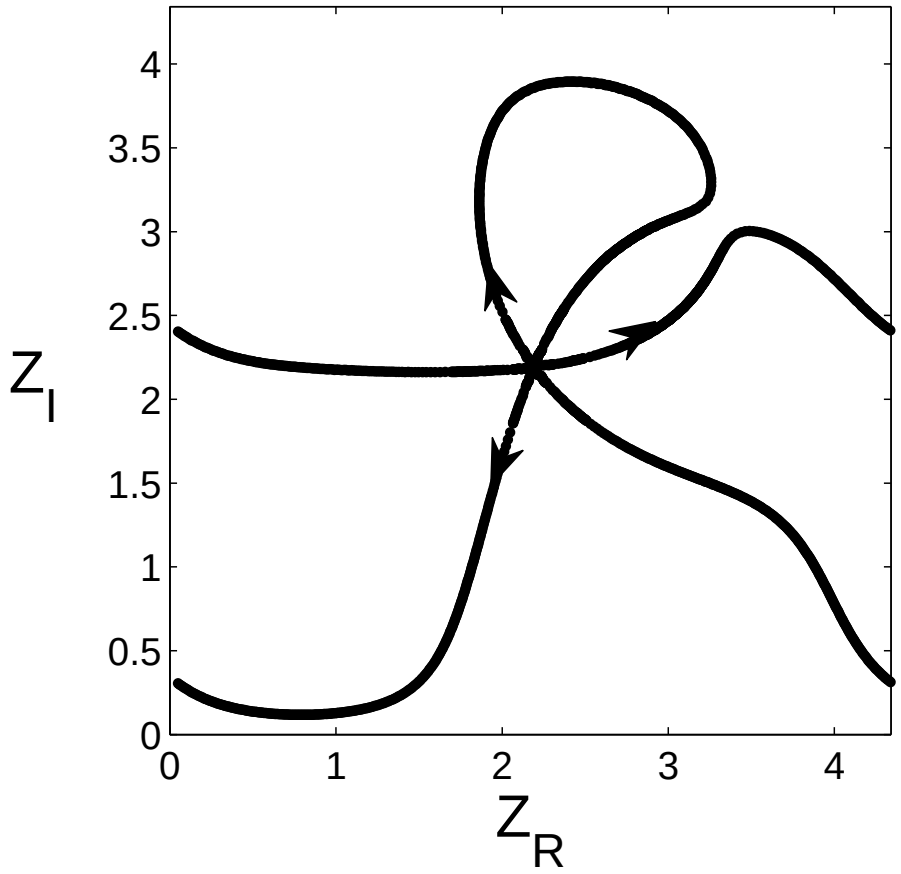

Figure 4.3: The paths of the zeros $\zeta_0(t)$, $\zeta_1(t)$, $\zeta_2(t)$ for the system with the Hamiltonian of Eq. (4.3). The zeros $\zeta_0(t)$, $\zeta_1(t)$, $\zeta_2(t)$ follow a closed path. At $t = 0$ the zeros $\zeta_0(0)$, $\zeta_1(0)$, $\zeta_2(0)$ are given in Eq. (4.5) and are indicated in the diagram. After a period T, the zeros ζ_0, ζ_1, ζ_2 return to their initial positions.

4.3 Periodic systems with paths with multiplicity $\mathfrak{M} = 2$

• We consider the Hamiltonian

$$H = \begin{pmatrix} 1 & 1 & 0 \\ 1 & 1 & 0 \\ 0 & 0 & 1 \end{pmatrix} \tag{4.6}$$

which has the eigenvalues $0, 1, 2$ and the period $T = 2\pi$. Let $\zeta_0(t), \zeta_1(t), \zeta_2(t)$ be the paths of the three zeros. We assume that at $t = 0$

$$\zeta_0(0) = 1.34 + 2.27i; \;\; \zeta_1(0) = 2.15 + 2.32i; \;\; \zeta_2(0) = 3.01 + 1.91i. \tag{4.7}$$

These zeros obey the constraint of Eq. (3.47) and are on a torus (i.e. they are defined modulo $(6\pi)^{1/2}$).

In this case, we find numerically that

$$\zeta_1(T + t) = \zeta_2(t); \quad \zeta_2(T + t) = \zeta_1(t). \tag{4.8}$$

Here, two of the zeros follow the same path (which by definition has multiplicity $\mathfrak{M} = 2$) while the third follows a different path.

In Fig. 4.4 we present the paths of these zeros. Here, after a period

$$\zeta_1(T) = \zeta_2(0); \qquad \zeta_2(T) = \zeta_1(0); \qquad \zeta_0(T) = \zeta_0(0) \tag{4.9}$$

During a period, the zero ζ_0 follows a closed path, whilst the other two

zeros exchange positions after a period. These zeros return to their original position after 2 periods

$$\zeta_1(2T) = \zeta_1(0); \quad \zeta_2(2T) = \zeta_2(0). \tag{4.10}$$

• We now consider the Hamiltonian of Eq. (4.6).

Let $\zeta_0(t), \zeta_1(t), \zeta_2(t)$ be the paths of the three zeros. We assume that at $t = 0$

$$\zeta_0(0) = 0.26 + 2.95i; \quad \zeta_1(0) = 2.16 + 2.22i; \quad \zeta_2(0) = 4.09 + 1.34i; \tag{4.11}$$

which obey the constraint of Eq. (3.47).

Here, we find numerically that

$$\zeta_0(T + t) = \zeta_2(t); \quad \zeta_2(T + t) = \zeta_0(t). \tag{4.12}$$

In this case, two of the zeros follow the same path (which by definition has multiplicity $\mathfrak{M} = 2$) while the third follows a different path.

In Fig. 4.5 we present the paths of these zeros. In this case, after a period

$$\zeta_0(T) = \zeta_2(0); \quad \zeta_2(T) = \zeta_0(0); \quad \zeta_1(T) = \zeta_1(0). \tag{4.13}$$

The zero ζ_1 follows a closed path during a period, while the other two zeros exchange positions after a period. These zeros return to their original position

after 2 periods.

$$\zeta_1(2T) = \zeta_1(0); \quad \zeta_2(2T) = \zeta_2(0). \tag{4.14}$$

- We consider the Hamiltonian

$$H = \begin{pmatrix} 1 & -i & 0 \\ i & 1 & 0 \\ 0 & 0 & 2 \end{pmatrix} \tag{4.15}$$

which has the eigenvalues $0, 2, 2$, and the period is $T = \pi$.

Let $\zeta_0(t), \zeta_1(t), \zeta_2(t)$ be the paths of the three zeros. We assume that at $t = 0$

$$\zeta_0(0) = 2.01 + 2.33i; \;\; \zeta_1(0) = 1.46 + 2.62i; \;\; \zeta_2(0) = 3.10 + 1.62i; \tag{4.16}$$

which obey the constraint of Eq. (3.47). Here, we find numerically that

$$\zeta_1(T + t) = \zeta_2(t); \quad \zeta_2(T + t) = \zeta_1(t). \tag{4.17}$$

In this case, two of the zeros follow the same path (which by definition has multiplicity $\mathfrak{M} = 2$) while the third follows a different path.

In Fig. 4.6 we present the paths of these zeros. In this case, after a period

$$\zeta_1(T) = \zeta_2(0); \quad \zeta_2(T) = \zeta_1(0). \tag{4.18}$$

During a period, the zero ζ_0 follows a closed path. The other two zeros

exchange position after a period. These zeros return to their original position after 2 periods.

$$\zeta_1(2T) = \zeta_1(0); \quad \zeta_2(2T) = \zeta_2(0). \tag{4.19}$$

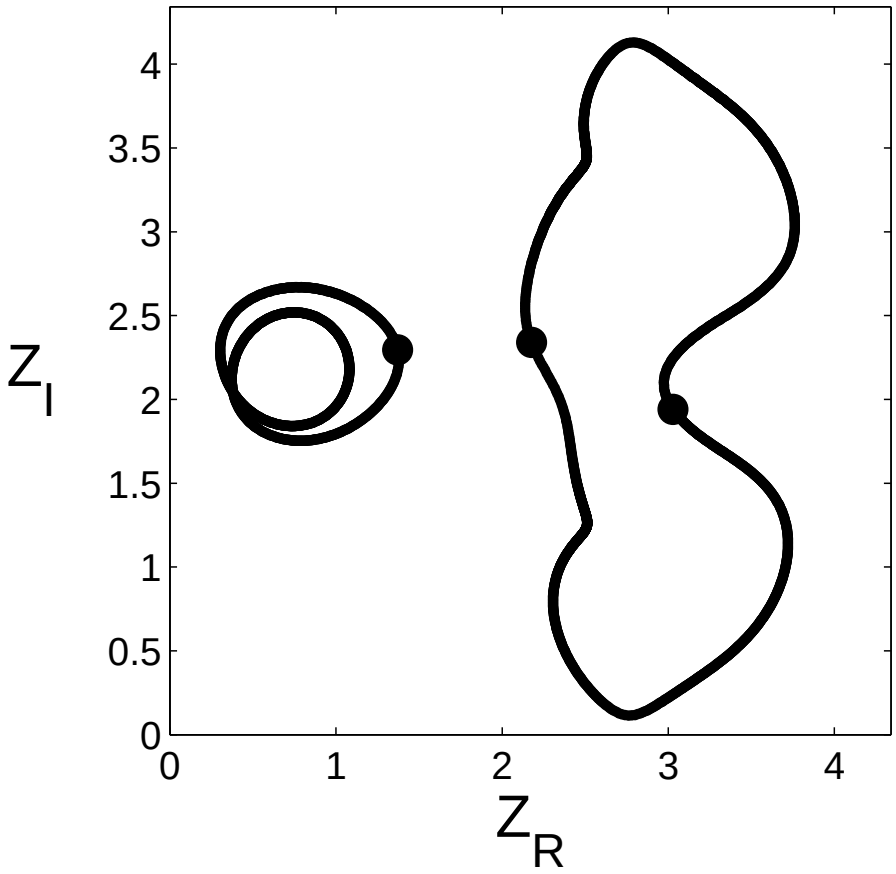

Figure 4.4: The paths of the zeros $\zeta_0(t)$, $\zeta_1(t)$, $\zeta_2(t)$ for the system with the Hamiltonian of Eq. (4.6). The zeros $\zeta_1(t)$, $\zeta_2(t)$ follow the same path while the zero $\zeta_0(t)$ follows a different path. At $t = 0$, the zeros $\zeta_0(0)$, $\zeta_1(0)$, $\zeta_2(0)$ are given in Eq. (4.7) and are indicated in the diagram. After a period T, the zeros ζ_1, ζ_2 exchange positions, as described in Eq. (4.9), while ζ_0 returns to its initial position.

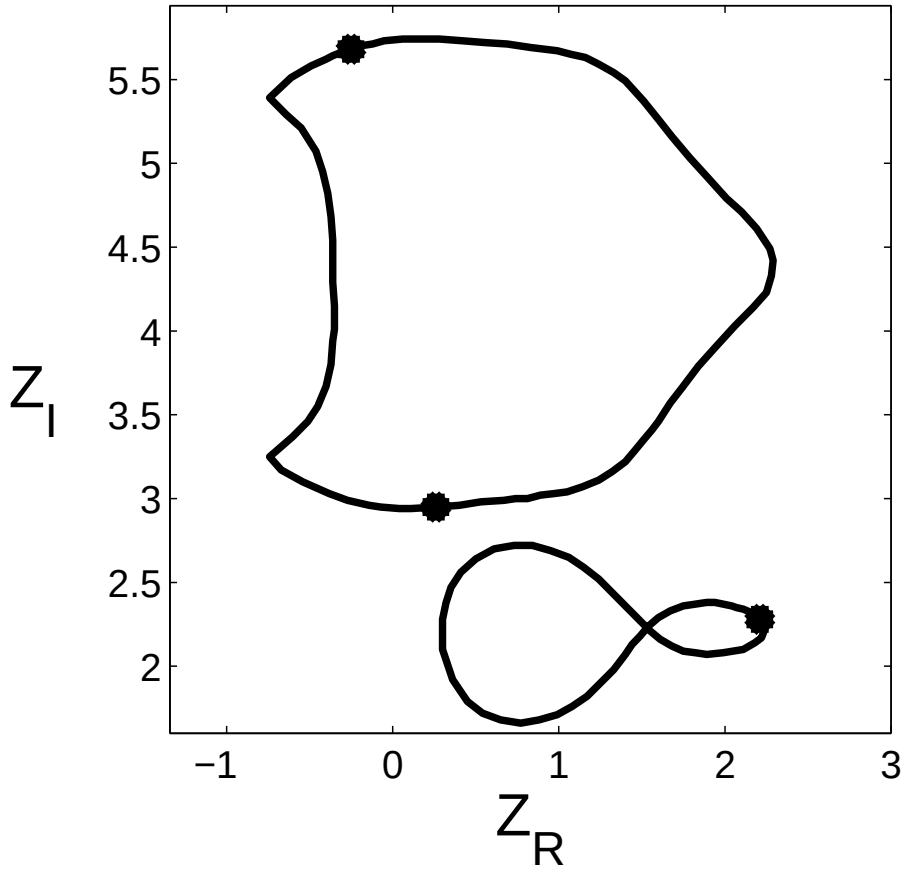

Figure 4.5: The paths of the zeros $\zeta_0(t)$, $\zeta_1(t)$, $\zeta_2(t)$ for the system with the Hamiltonian of Eq. (4.6). The zeros $\zeta_0(t)$, $\zeta_2(t)$ follow the same path while the zero $\zeta_1(t)$ follows a different path. At $t = 0$, the zeros $\zeta_0(0)$, $\zeta_1(0)$, $\zeta_2(0)$ are given in Eq. (4.11) and are indicated in the diagram. After a period T, the zeros ζ_0 and ζ_2 exchange positions, as described in Eq. (4.13), while ζ_1 returns to its initial position.

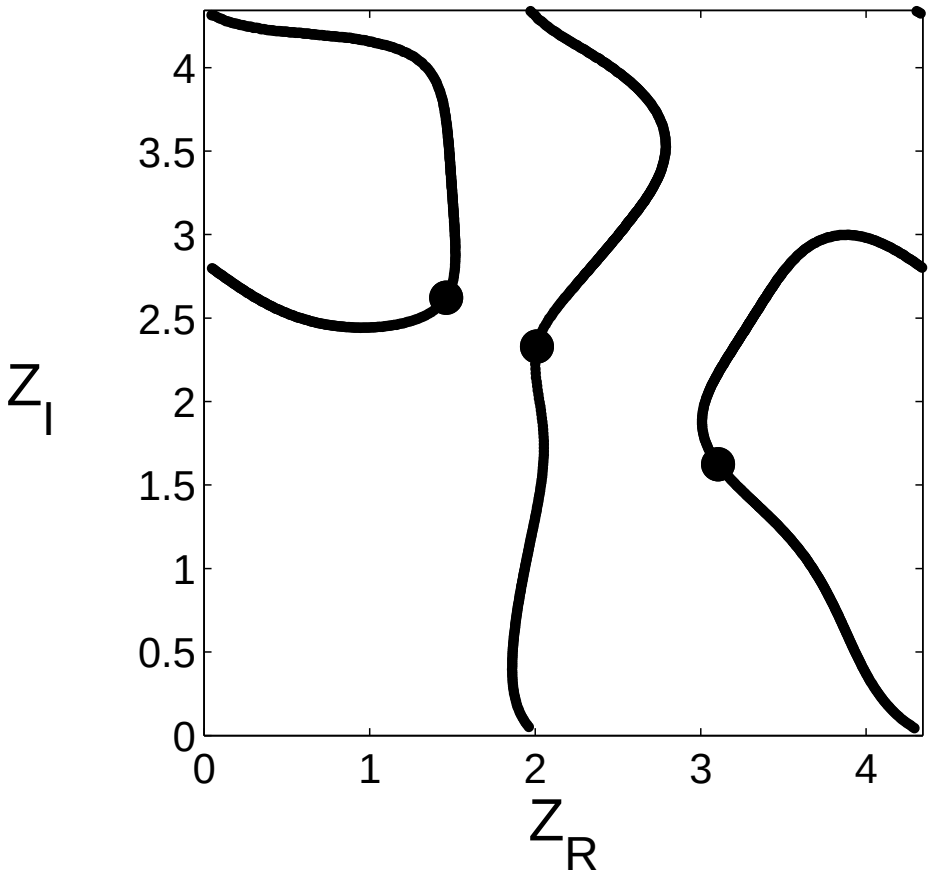

Figure 4.6: The paths of the zeros $\zeta_0(t)$, $\zeta_1(t)$, $\zeta_2(t)$ for the system with the Hamiltonian of Eq. (4.15). The zeros $\zeta_1(t)$, $\zeta_2(t)$ follow the same path while the zero $\zeta_0(t)$ follows different paths. At $t = 0$, the zeros $\zeta_0(0)$, $\zeta_1(0)$, $\zeta_2(0)$ are given in Eq. (4.16) and indicated in the diagram. After a period T, the zeros ζ_1, ζ_2 exchange positions, as described in Eq. (4.18), while $\zeta_0(t)$ returns to its initial position.

4.3.1 Splitting of a path with multiplicity $\mathfrak{M} = 2$ into two different paths

In this section, we show that a small perturbation in the initial values of the zero splits the path with multiplicity $\mathfrak{M} = 2$ into two paths.

• We now consider the Hamiltonian of Eq. (4.6).

We consider two cases where the zeros at $t = 0$ are slightly different from each other. In the first case,

$$\zeta_0(0) = 1.40 + 2.33i; \;\; \zeta_1(0) = 2.15 + 2.32i; \;\; \zeta_2(0) = 2.95 + 1.85i; \qquad (4.20)$$

and in the second case,

$$\zeta_0(0) = 1.46 + 2.39i; \;\; \zeta_1(0) = 2.15 + 2.32i; \;\; \zeta_2(0) = 2.89 + 1.79i. \qquad (4.21)$$

In the case of Eq. (4.20), we get

$$\zeta_1(T + t) = \zeta_2(t); \qquad \zeta_2(T + t) = \zeta_1(t), \qquad (4.22)$$

and therefore these zeros follow the same path with multiplicity $\mathfrak{M} = 2$. The third zero follows its own path, which is shown in Fig. 4.7 (broken line).

In the case of Eq. (4.21), each zero follows its own path (continuous lines in Fig. 4.7).

It is established that a small perturbation in the initial values of the zeros splits the path with multiplicity $\mathfrak{M} = 2$ into two paths.

Near the point where the splitting occurs, we approximate the paths of

the zeros with the quadratic equation

$$Ax^2 + Bxy + Cy^2 + Dx + Ey + F = 0, \tag{4.23}$$

which is an approximation of part of these paths. It is well known that the graph of a quadratic equation in two variables is always a conic section, where:

if $B^2 - 4AC < 0$, the equation represents an ellipse,

if $B^2 - 4AC = 0$, the equation represents a parabola, and

if $B^2 - 4AC > 0$, the equation represents a hyperbola.

In the case of Eq. (4.20), this is an ellipse (and has a single branch), while in the case of Eq. (4.21) it is a hyperbola and has two branches (we remind the reader that it is on a torus).

More generally, we consider the case where the zeros at $t = 0$ are

$$\begin{aligned} \zeta_0(0) &= (1.40 + \lambda) + (2.33 + \mu)i; \quad \zeta_1(0) = 2.15 + 2.32i; \\ \zeta_2(0) &= (2.95 - \lambda) + (1.85 - \mu)i, \end{aligned} \tag{4.24}$$

and define

$$\Delta = B^2 - 4AC. \tag{4.25}$$

In Fig. 4.8 we present the sign of Δ as a function of λ, μ. The toroidal structure is taken into account in deriving these values.

The case of Eq. (4.20) corresponds to the point $(0, 0)$ (point B in the figure), and the case of Eq. (4.21) corresponds to the point $(0.06, 0.06)$

(point A in the figure).

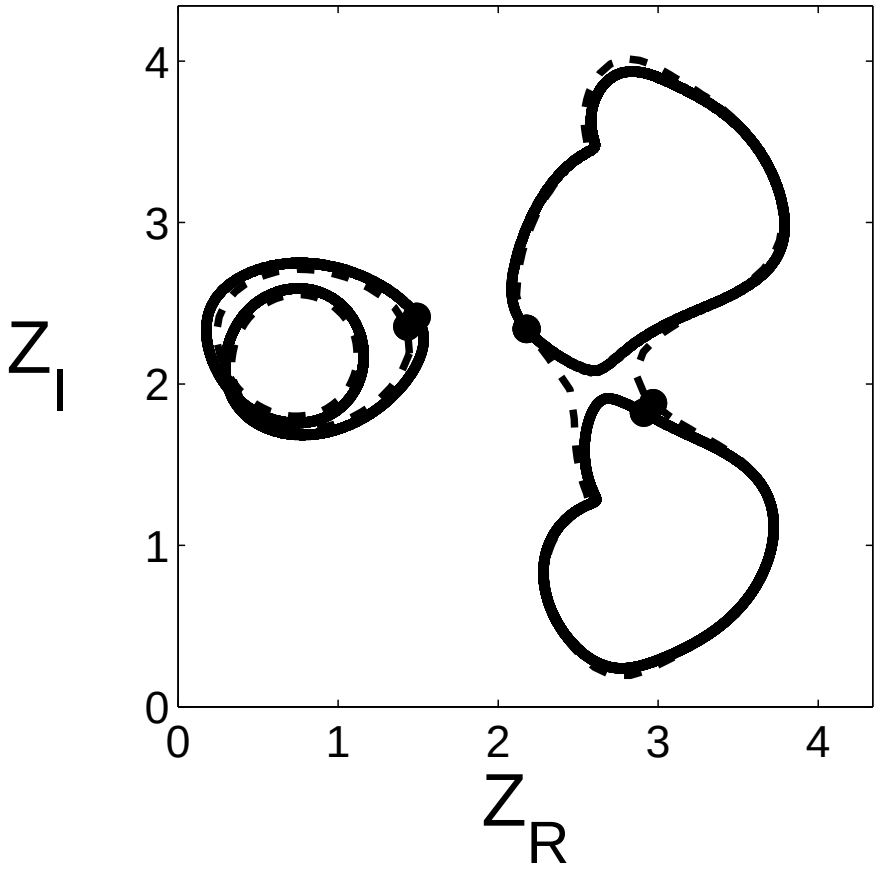

Figure 4.7: The path of the zeros $\zeta_0(t)$, $\zeta_1(t)$, $\zeta_2(t)$ for the system with the Hamiltonian of Eq. (4.6). In the case of the initial zeros of Eq. (4.20), the zeros ζ_1, ζ_2 follow the same path while the third zero follows its own path (broken line). In the case of the slightly different initial zeros of Eq. (4.21), each zero follows its own path (continuous lines).

- We consider the Hamiltonian

$$H = \begin{pmatrix} 1 & -i & 0 \\ i & 1 & 0 \\ 0 & 0 & 2 \end{pmatrix} \tag{4.26}$$

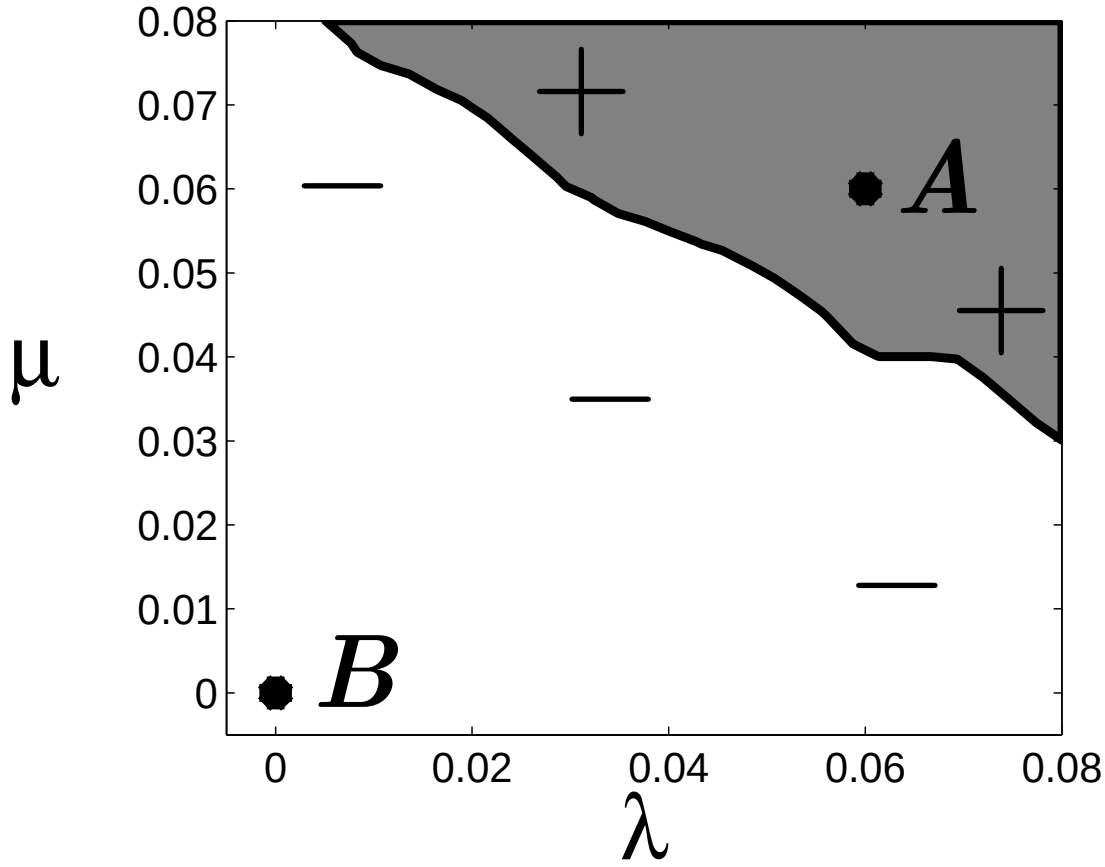

Figure 4.8: The sign of Δ as a function of λ, μ.

which has the eigenvalues $0, 2, 2$, and the period is $T = \pi$.

We present two cases where the zeros at $t = 0$ are slightly different from each other. In the first case

$$\zeta_0(0) = 2.19 + 2.19i; \;\; \zeta_1(0) = 1.39 + 3.40i; \;\; \zeta_2(0) = 2.93 + 0.91i; \qquad (4.27)$$

and in the second case,

$$\zeta_0(0) = 2.12 + 2.12i; \;\; \zeta_1(0) = 1.39 + 3.40i; \;\; \zeta_2(0) = 3 + 0.98i. \qquad (4.28)$$

In the case of Eq. (4.27) we get

$$\zeta_0(T + t) = \zeta_1(t); \qquad \zeta_1(T + t) = \zeta_0(t), \qquad (4.29)$$

which means that $\zeta_0(t)$ and $\zeta_1(t)$ follow the same path with multiplicity $\mathfrak{M} = 2$. The third zero follows its own path, which is shown in Fig. 4.9 (continuous line).

In the case of Eq. (4.28), each zero follows a different path (broken lines in Fig.4.9).

It is evident that a small perturbation in the initial values of the zeros splits the path with multiplicity $\mathfrak{M} = 2$ into two paths.

We now approximate the paths of the zeros with the quadratic equation near the point where the splitting occurs.

$$Ax^2 + Bxy + Cy^2 + Dx + Ey + F = 0, \qquad (4.30)$$

which is an approximation of part of these paths.

In the case of Eq. (4.27), this is an ellipse (and has a single branch), whereas in the case of Eq. (4.28) it is a hyperbola (and has two branches).

More generally, we consider the case where the zeros at $t = 0$ are

$$\begin{aligned} \zeta_0(0) &= (2.12 + \lambda) + (2.12 + \mu)i; \quad \zeta_1(0) = 1.39 + 3.40i; \\ \zeta_2(0) &= (3.00 - \lambda) + (0.98 - \mu)i. \end{aligned} \tag{4.31}$$

In Fig. 4.10 we show the sign of Δ as a function of λ, μ.

The case of Eq. (4.27) corresponds to the point $(0.07, 0.07)$ (point A in the figure), and the case of Eq.(4.28) corresponds to the point $(0, 0)$ (point B in the figure).

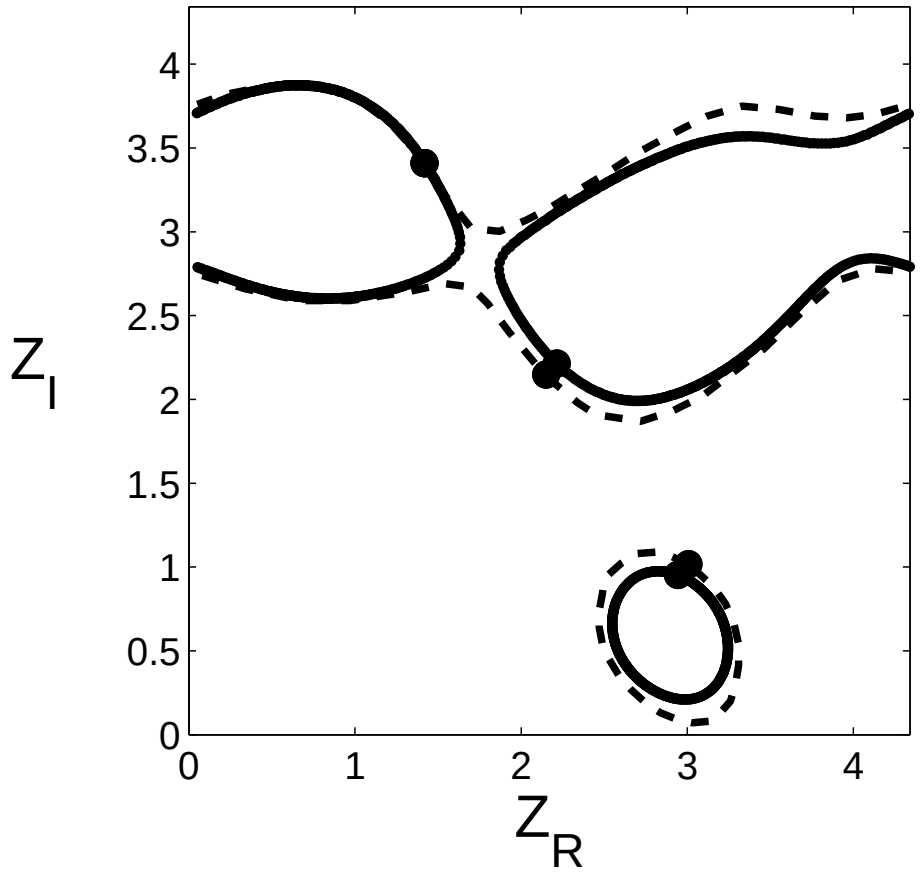

Figure 4.9: The path of the zeros $\zeta_0(t)$, $\zeta_1(t)$, $\zeta_2(t)$ for the system with the Hamiltonian of Eq. (4.26). In the case of the initial zeros of Eq. (4.27), the zeros ζ_0, ζ_1 follow the same path and the third zero follows its own path (continuous lines). In the case of the slightly different initial zeros of Eq. (4.28), each zero follows its own path (broken lines).

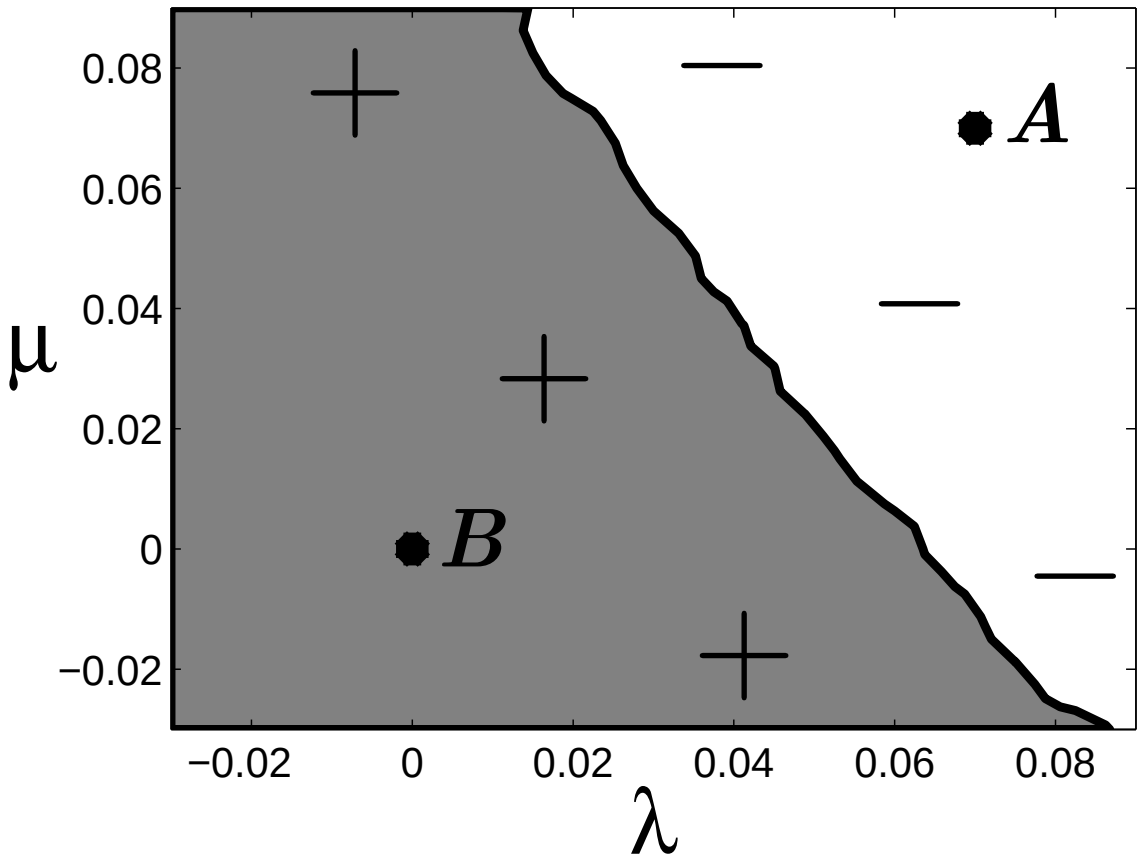

Figure 4.10: The sign of Δ as function of λ, μ.

4.4 Periodic systems with paths with multiplicity $\mathfrak{M} = 3$.

• We consider the Hamiltonian

$$H = \begin{pmatrix} 1 & 1 & 0 \\ 1 & 1 & 0 \\ 0 & 0 & 1 \end{pmatrix} \tag{4.32}$$

which has the eigenvalues $0, 1, 2$ and the period $T = 2\pi$.

Let $\zeta_0(t), \zeta_1(t), \zeta_2(t)$ be the paths of the three zeros. We assume that at $t = 0$

$$\zeta_0(0) = 2.03 + 2.03i; \;\; \zeta_1(0) = 2.02 + 2.51i; \;\; \zeta_2(0) = 2.51 + 2.02i. \tag{4.33}$$

These zeros obey the constraint of Eq. (3.47) and they are on a torus (i.e., they are defined modulo $(6\pi)^{1/2}$).

Numerically, we find that

$$\zeta_0(T + t) = \zeta_1(t); \;\; \zeta_1(T + t) = \zeta_2(t); \;\; \zeta_2(T + t) = \zeta_0(t). \tag{4.34}$$

The three zeros follow the same path.

In Fig. 4.11 we show the path of these zeros (for clarity, we show three paths, which are the same due to the periodicity).

We see that after a period

$$\zeta_0(T) = \zeta_1(0); \;\; \zeta_1(T) = \zeta_2(0); \;\; \zeta_2(T) = \zeta_0(0). \tag{4.35}$$

It is established that after a period T, each zero moves to the original position of another zero. Therefore, within a period a single zero does not follow a closed path, although the three zeros together do follow this route. After three periods, each zero returns to its original position

$$\zeta_i(3T) = \zeta_i(0) \text{ where } i = 0, 1, 2.$$

• We consider the Hamiltonian

$$H = \begin{pmatrix} 1 & -i & 0 \\ i & 1 & 0 \\ 0 & 0 & 1 \end{pmatrix} \tag{4.36}$$

which has the eigenvalues $0, 1, 2$ and the period $T = 2\pi$.

We assume that at $t = 0$ the zeros are given by Eq. (4.11).

Numerically, we find that

$$\zeta_0(T + t) = \zeta_2(t); \;\; \zeta_2(T + t) = \zeta_1(t); \;\; \zeta_1(T + t) = \zeta_0(t). \tag{4.37}$$

In Fig. 4.12 we show the path of these zeros.

We find that after a period

$$\zeta_0(T) = \zeta_2(0); \;\; \zeta_2(T) = \zeta_1(0); \;\; \zeta_1(T) = \zeta_0(0) \tag{4.38}$$

This shows that after a period T, each zero moves to the original position of another zero. Therefore, within a period, although the three zeros together do follow a closed path, a single zero does not follow this route.

After three periods, each zero returns to its original position

$$\zeta_i(3T) = \zeta_i(0) \text{ where } i = 0, 1, 2.$$

• We consider the Hamiltonian of Eq. (4.26) with the initial zeros of Eq. (4.11).

Numerically, we find that

$$\zeta_0(T+t) = \zeta_1(t); \;\; \zeta_1(T+t) = \zeta_2(t); \;\; \zeta_2(T+t) = \zeta_0(t). \tag{4.39}$$

In Fig. 4.13 we present the path of these zeros.

After a period

$$\zeta_0(T) = \zeta_1(0); \;\; \zeta_1(T) = \zeta_2(0); \;\; \zeta_2(T) = \zeta_0(0). \tag{4.40}$$

As in the previous example, the zeros exchange position after a period.

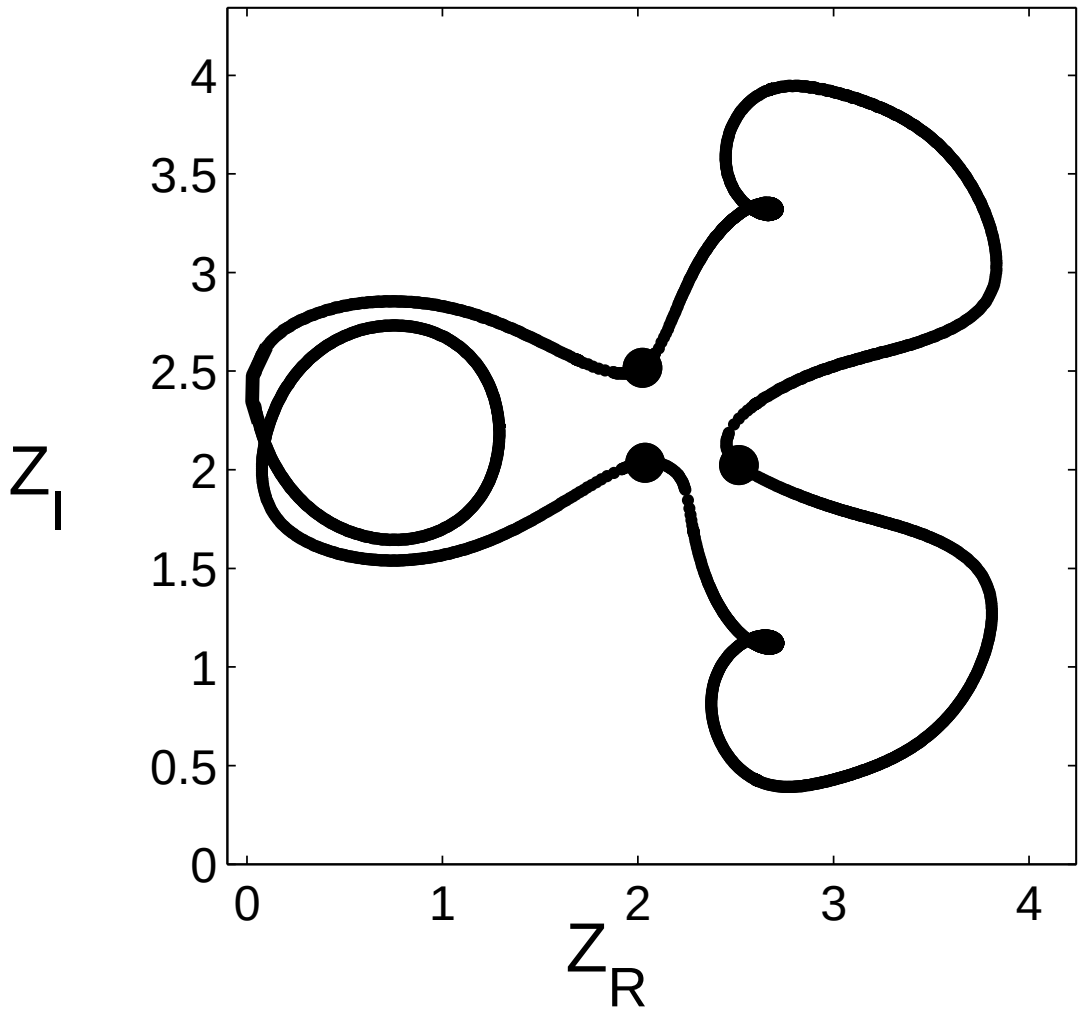

Figure 4.11: The path of the zeros $\zeta_0(t)$, $\zeta_1(t)$, $\zeta_2(t)$ for the system with the Hamiltonian of Eq. (4.32). All zeros follow the same path. At $t = 0$ the zeros $\zeta_0(0)$, $\zeta_1(0)$, $\zeta_2(0)$ are given in Eq. (4.33) and are indicated in the diagram. After a period T, the zeros exchange positions as described in Eq. (4.35)

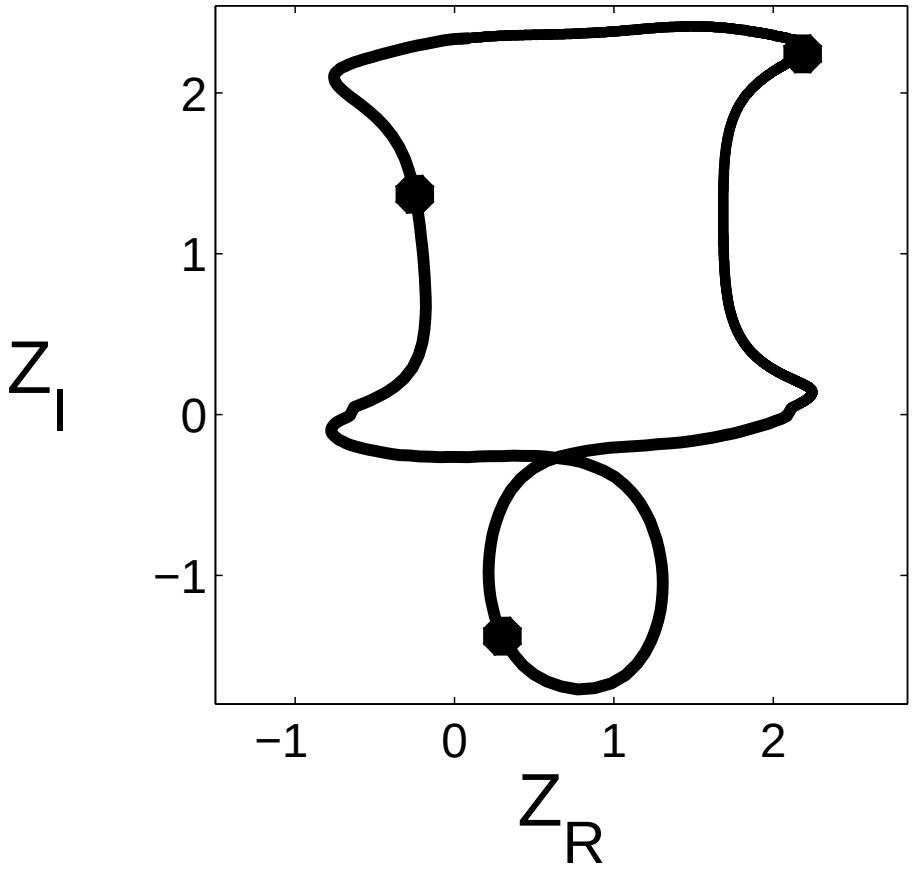

Figure 4.12: The path of the zeros $\zeta_0(t)$, $\zeta_1(t)$ and $\zeta_2(t)$ for the system with the Hamiltonian of Eq. (4.36). All zeros follow the same path. At $t = 0$, the zeros $\zeta_0(0)$, $\zeta_1(0)$, $\zeta_2(0)$ are given in Eq. (4.11) and are indicated in the diagram. After a period T, the zeros exchange positions as described in Eq. (4.38).

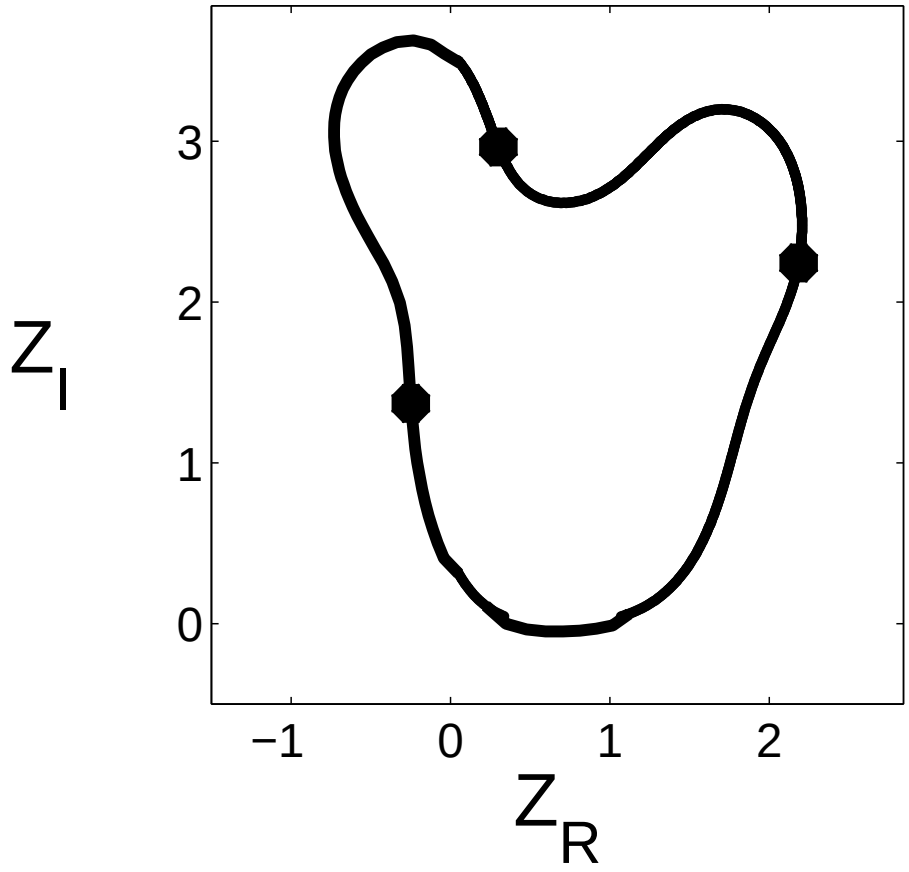

Figure 4.13: The path of the zeros $\zeta_0(t)$, $\zeta_1(t)$ and $\zeta_2(t)$ for the system with the Hamiltonian of Eq. (4.26). All zeros follow the same path. At $t = 0$, the zeros $\zeta_0(0)$, $\zeta_1(0)$, $\zeta_2(0)$ are given in Eq. (4.11) and are indicated in the diagram. After a period T, the zeros exchange positions as described in Eq. (4.40).

4.4.1 Splitting of a path with multiplicity $\mathfrak{M} = 3$ into two different paths with multiplicities $\mathfrak{M} = 2$ and $\mathfrak{M} = 1$.

In this section, we show that a small perturbation in the initial values of the zeros splits the path with multiplicity $\mathfrak{M} = 3$ into two paths with multiplicities $\mathfrak{M} = 2$ and $\mathfrak{M} = 1$.

We consider the Hamiltonian of Eq. (4.26) as well as two cases where the zeros at $t = 0$ are in the first case

$$\zeta_0(0) = 0.26 + 2.95i; \;\; \zeta_1(0) = 4.41 + 1.66i; \;\; \zeta_2(0) = 1.84 + 1.90i; \quad (4.41)$$

and in the second case

$$\zeta_0(0) = 0.26 + 2.95i; \;\; \zeta_1(0) = 4.46 + 1.71i; \;\; \zeta_2(0) = 1.79 + 1.85i. \quad (4.42)$$

In the case of Eq. (4.41), we get

$$\zeta_0(T + t) = \zeta_2(t); \quad \zeta_2(T + t) = \zeta_1(t); \;\; \zeta_1(T + t) = \zeta_0(t). \quad (4.43)$$

The three zeros follow the same path with multiplicity $\mathfrak{M} = 3$, which shown in Fig. 4.14 (broken line).

In the case of Eq. (4.42) the zeros ζ_2, ζ_1 follow the same path and the third zero ζ_0 follows a different path (continuous lines in Fig. 4.14).

It is evident that a small perturbation in the initial values of the zeros splits the path with multiplicity $\mathfrak{M} = 3$ into two paths with multiplicities

$\mathfrak{M} = 2$ and $\mathfrak{M} = 1$.

Near the point where the splitting occurs, we approximate the paths of the zeros with the quadratic equation

$$Ax^2 + Bxy + Cy^2 + Dx + Ey + F = 0 \tag{4.44}$$

Clearly, this is an approximation of part of these paths.

In the case $\Delta = B^2 - 4AC < 0$ we get an ellipse, and in the case $\Delta > 0$ we get a hyperbola (two branches). The case of Eq. (4.41) corresponds to an ellipse which has a single branch, while the case of Eq. (4.42) corresponds to a hyperbola which has two branches.

More generally, we consider the case where the zeros at $t = 0$ are

$$\begin{aligned} \zeta_0(0) &= (4.41 + \lambda) + (1.66 + \mu)i; \;\; \zeta_1(0) = 0.26 + 2.95i \\ \zeta_2(0) &= (1.84 - \lambda) + (1.90 - \mu)i \end{aligned} \tag{4.45}$$

In Fig. 4.15 we present the sign of Δ as a function of λ, μ.

The toroidal structure is taken into account in deriving these values. The case of Eq. (4.41) corresponds to the point $(0, 0)$ (point A in the figure), and the case of Eq. (4.42) corresponds to the point $(0.05, 0.05)$ (point B in the figure).

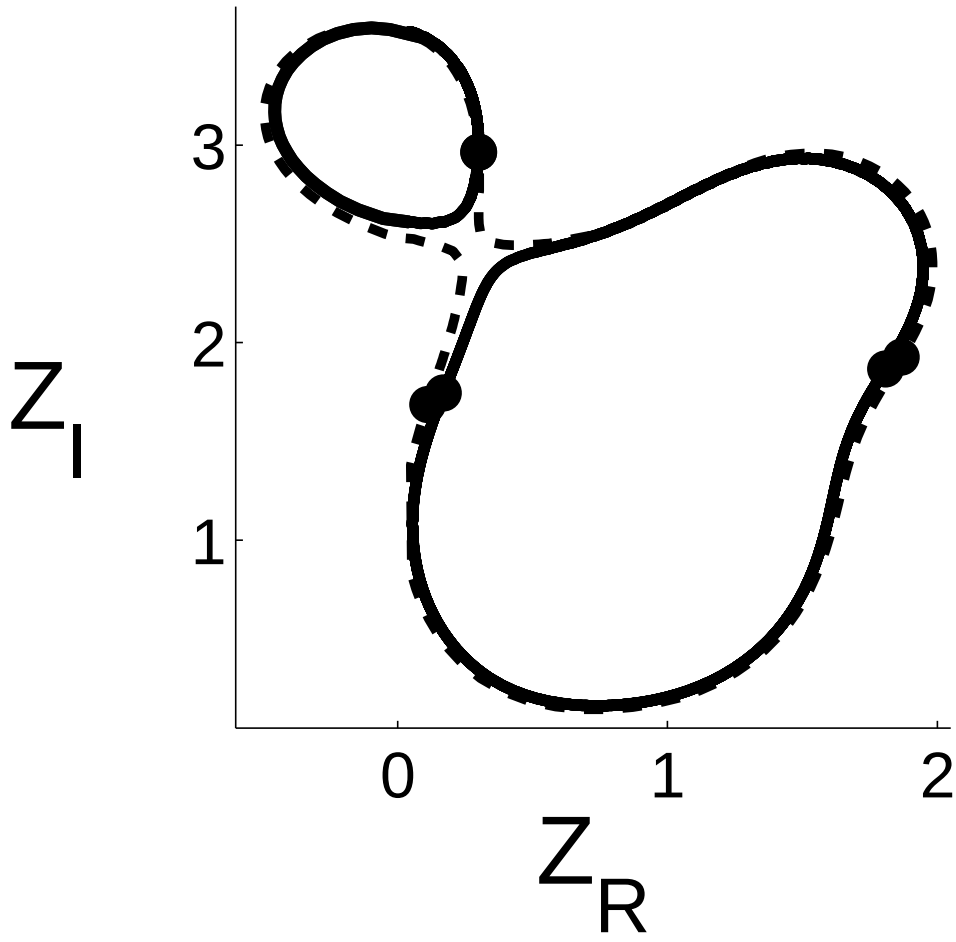

Figure 4.14: The path of the zeros $\zeta_0(t)$, $\zeta_1(t)$, $\zeta_2(t)$ for the system with the Hamiltonian of Eq. (4.26). In the case of the initial zeros of Eq. (4.41), the zeros $\zeta_0, \zeta_1, \zeta_2$ follow the same path (broken line). In the case of the slightly different initial zeros of Eq. (4.42), the zeros ζ_1, ζ_2 follow the same path and the ζ_0 follows its own path (continuous lines).

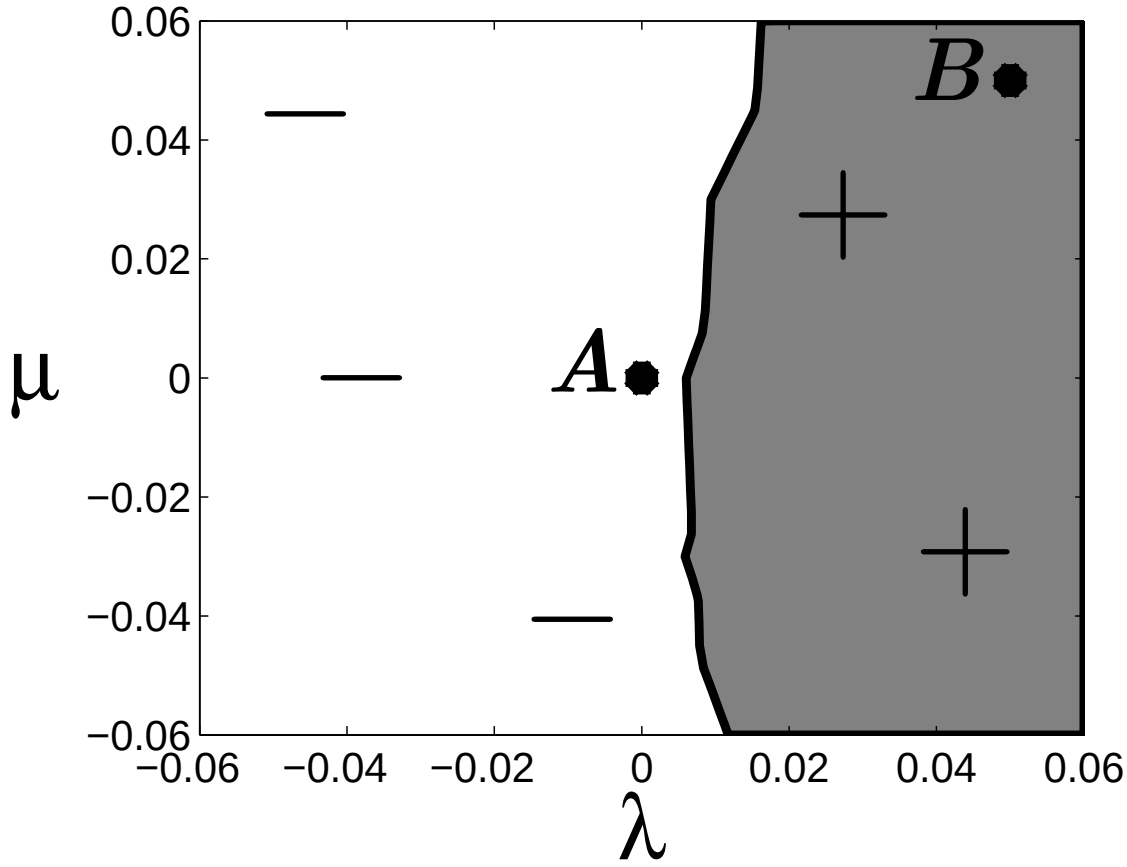

Figure 4.15: The sign of Δ as a function of λ, μ.

4.5 Periodic systems with paths with multiplicity $\mathfrak{M} = 4$.

We consider the Hamiltonian

$$H = \begin{pmatrix} 1 & -i & 0 & 0 & 0 \\ i & 1 & 0 & 0 & 0 \\ 0 & 0 & 2 & 0 & 0 \\ 0 & 0 & 0 & 2 & 0 \\ 0 & 0 & 0 & 0 & 2 \end{pmatrix} \tag{4.46}$$

which has the eigenvalues 0 (with multiplicity 1) and 2 (with multiplicity 4). The period $T = \pi$.

Let $\zeta_0(t), \zeta_1(t), \zeta_2(t), \zeta_3(t), \zeta_4(t)$ be the paths of the five zeros. We assume that at $t = 0$

$$\begin{aligned} &\zeta_0(0) = 0.3 + 3.66i; \quad \zeta_1(0) = 1.61 + 2.72i; \quad \zeta_2(0) = 3.03 + 4.83i; \\ &\zeta_3(0) = 4.89 + 0.81i; \quad \zeta_4(0) = 4.29 + 2.11i. \end{aligned} \tag{4.47}$$

These zeros obey the constraint of Eq. (3.47) and are on a torus (i.e. they are defined modulo $(10\pi)^{1/2}$).

In this case, we find numerically that

$$\begin{aligned} &\zeta_0(T + t) = \zeta_1(t); \quad \zeta_1(T + t) = \zeta_3(t); \\ &\zeta_3(T + t) = \zeta_4(t); \quad \zeta_4(T + t) = \zeta_0(t). \end{aligned} \tag{4.48}$$

Here, four of the zeros follow the same path (which by definition has multiplicity $\mathfrak{M} = 4$) and the fifth one follows a different path.

In Fig. 4.16 we present the path of these zeros.

We note that after a period

$$\begin{aligned} &\zeta_0(T) = \zeta_1(0); \quad \zeta_1(T) = \zeta_3(0); \\ &\zeta_3(T) = \zeta_4(0); \quad \zeta_4(T) = \zeta_0(0). \end{aligned} \tag{4.49}$$

During a period, the zero ζ_2 follows a closed path while the other four zeros exchange positions after a period, and then return to their original positions after 4 periods

$$(\zeta_i(4T) = \zeta_i(0) \text{ where } i = 0, 1, 3, 4); \quad \zeta_2(T) = \zeta_2(0).$$

Another example is the Hamiltonian

$$H = \begin{pmatrix} 1 & -i & 0 & 0 \\ i & 1 & 0 & 0 \\ 0 & 0 & 2 & 0 \\ 0 & 0 & 0 & 2 \end{pmatrix} \tag{4.50}$$

which has the eigenvalues 0 (with multiplicity 1) and 2 (with multiplicity 3). The period $T = \pi$.

Let $\zeta_0(t), \zeta_1(t), \zeta_2(t), \zeta_3(t)$ be the paths of the four zeros. We assume that at $t = 0$

$$\zeta_0(0) = 0.65 + 2.61i; \quad \zeta_1(0) = 2.11 + 4.30i;$$
$$\zeta_2(0) = 3.71 + 1.03i; \quad \zeta_3(0) = 3.64 + 2.16i. \tag{4.51}$$

These zeros obey the constraint of Eq. (3.47) and are on a torus (i.e. they are defined modulo $(8\pi)^{1/2}$).

In this case, we find numerically that

$$\zeta_0(T+t) = \zeta_1(t); \quad \zeta_1(T+t) = \zeta_2(t);$$
$$\zeta_2(T+t) = \zeta_3(t); \quad \zeta_3(T+t) = \zeta_0(t). \tag{4.52}$$

Here, all zeros follow the same path (which by definition has multiplicity $\mathfrak{M} = 4$).

In Fig. 4.17 we present the path of these zeros.

We note that after a period

$$\zeta_0(T) = \zeta_1(0); \quad \zeta_1(T) = \zeta_2(0);$$
$$\zeta_2(T) = \zeta_3(0); \quad \zeta_3(T) = \zeta_0(0). \tag{4.53}$$

This shows that after a period T, each zero moves to the original position of another zero. Therefore, within a period, a single zero does not follow a closed path, although the four zeros together do follow this route. Each zero returns to its original position after 4 periods

$$(\zeta_i(4T) = \zeta_i(0) \text{ where } i = 0, 1, 2, 3).$$

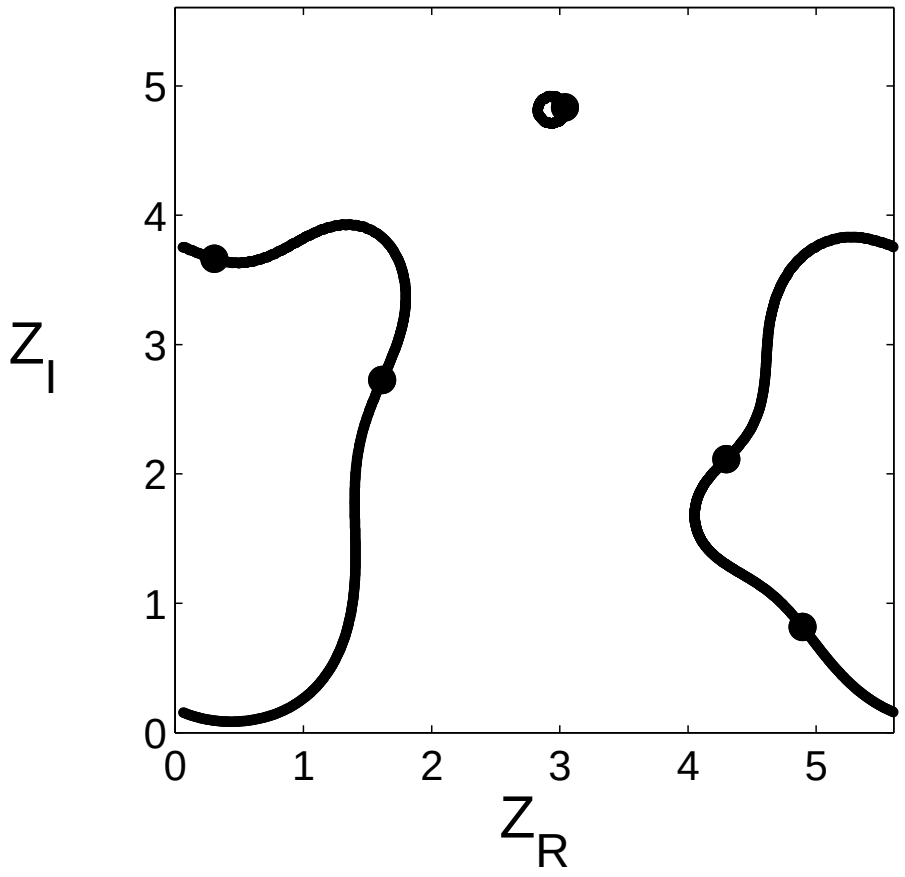

Figure 4.16: The path of the zeros $\zeta_0(t), \zeta_1(t), \zeta_2(t), \zeta_3(t), \zeta_4(t)$ for the system with the Hamiltonian of Eq. (4.46). The zeros $\zeta_0(t), \zeta_1(t), \zeta_3(t), \zeta_4(t)$ follow the same path and the zero $\zeta_2(t)$ follows a different path. At $t = 0$, the zeros $\zeta_0(0)$, $\zeta_1(0)$, $\zeta_2(0)$, $\zeta_3(0)$ and $\zeta_4(0)$ are given in Eq. (4.47) and are indicated in the diagram. After a period T, the zeros ζ_0, ζ_1, ζ_3 and ζ_4 exchange positions as described in Eq. (4.49), while ζ_2 returns to its initial position.

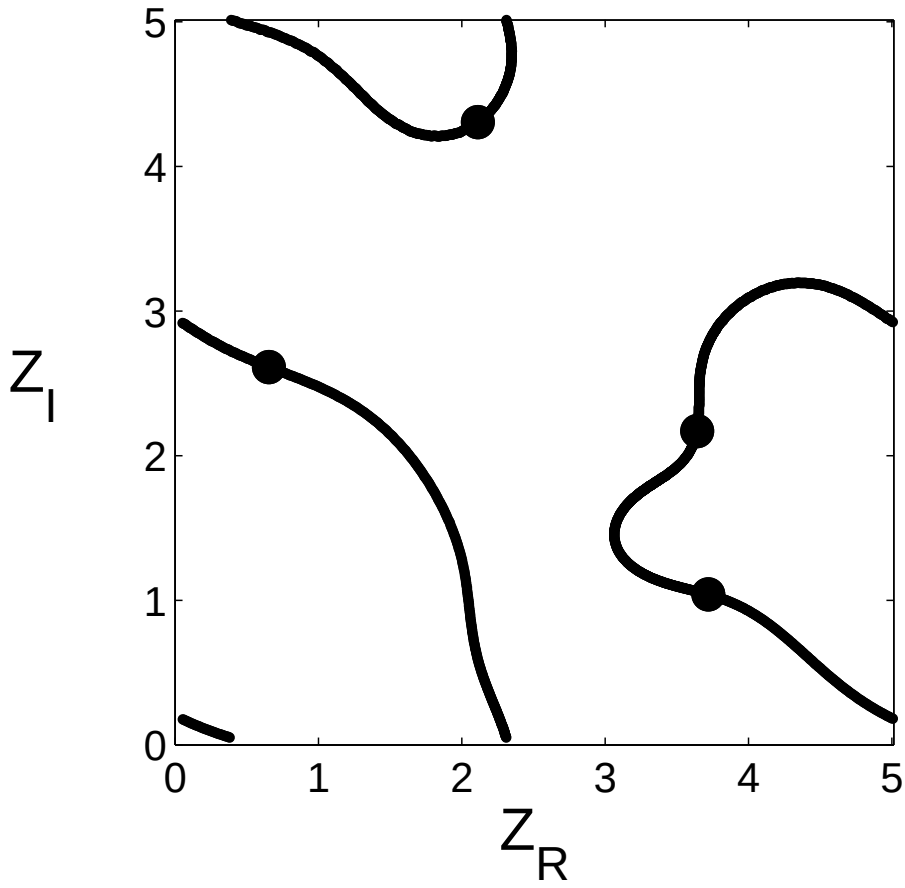

Figure 4.17: The path of the zeros $\zeta_0(t), \zeta_1(t), \zeta_2(t), \zeta_3(t)$ for the system with the Hamiltonian of Eq. (4.50). All zeros follow the same path. At $t = 0$, the zeros $\zeta_0(0)$, $\zeta_1(0)$, $\zeta_2(0)$ and $\zeta_3(0)$ are given in Eq. (4.51) and are indicated in the diagram. After a period T, the zeros exchange positions as described in Eq. (4.53).

4.5.1 Splitting of a path with multiplicity $\mathfrak{M} = 4$ into two different paths with multiplicities $\mathfrak{M} = 2$.

In this section, we show that a small perturbation in the initial values of the zero splits the path with multiplicity $\mathfrak{M} = 4$ into two paths with multiplicities $\mathfrak{M} = 2$.

We consider the Hamiltonian

$$H = \begin{pmatrix} 1 & -i & 0 & 0 \\ i & 1 & 0 & 0 \\ 0 & 0 & 2 & 0 \\ 0 & 0 & 0 & 2 \end{pmatrix} \tag{4.54}$$

which has the eigenvalues 0 (with multiplicity 1) and 2 (with multiplicity 3). The period $T = \pi$.

We take two cases where the zeros at $t = 0$ are, for the first case,

$$\begin{aligned} \zeta_0(0) &= 0.65 + 2.61i; \quad \zeta_1(0) = 2.11 + 4.3i; \\ \zeta_2(0) &= 3.71 + 1.03i; \quad \zeta_3(0) = 3.54 + 2.06i; \end{aligned} \tag{4.55}$$

and in the second case

$$\begin{aligned} \zeta_0(0) &= 0.75 + 2.71i; \quad \zeta_1(0) = 2.11 + 4.3i; \\ \zeta_2(0) &= 3.71 + 1.03i; \quad \zeta_3(0) = 3.44 + 1.96i. \end{aligned} \tag{4.56}$$

These zeros obey the constraint of Eq. (3.47) and are on a torus (i.e. they

are defined modulo $(8\pi)^{1/2}$).

In the case of Eq. (4.55) we get

$$\begin{aligned} &\zeta_0(T+t) = \zeta_1(t); \quad \zeta_1(T+t) = \zeta_2(t); \\ &\zeta_2(T+t) = \zeta_3(t); \quad \zeta_3(T+t) = \zeta_0(t); \end{aligned} \tag{4.57}$$

and all zeros follow the same path with multiplicity $\mathfrak{M} = 4$, which is shown in Fig. 4.18 (continuous line).

In the case of Eq. (4.56) we get

$$\zeta_0(T+t) = \zeta_3(t); \quad \zeta_3(T+t) = \zeta_0(t); \tag{4.58}$$

and

$$\zeta_1(T+t) = \zeta_2(t); \quad \zeta_2(T+t) = \zeta_1(t). \tag{4.59}$$

This is shown in Fig. 4.18 (broken lines).

It is evident that a small perturbation in the initial values of the zero splits the path with multiplicity $\mathfrak{M} = 4$ into two paths with multiplicities $\mathfrak{M} = 2$.

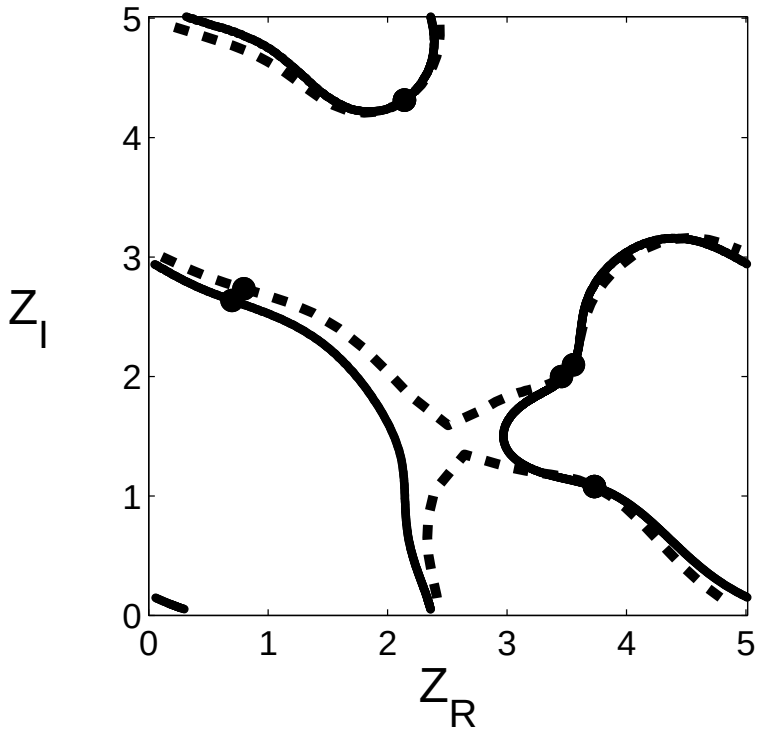

Figure 4.18: The path of the zeros $\zeta_0(t), \zeta_1(t), \zeta_2(t), \zeta_3(t)$ for the system with the Hamiltonian of Eq. (4.54). In the case of the initial zeros of Eq. (4.55), the zeros $\zeta_0(t), \zeta_1(t), \zeta_2(t), \zeta_3(t)$) follow the same path (continuous line). In the case of the slightly different initial zeros of Eq. (4.56), the zeros $\zeta_0(t), \zeta_3(t)$ follow the same path and the zeros $\zeta_1(t), \zeta_2(t)$ follow another path (broken lines).

4.6 Periodic systems with paths with multiplicity $\mathfrak{M} = 5$.

We consider the Hamiltonian of Eq. (4.46)

Let $\zeta_0(t), \zeta_1(t), \zeta_2(t), \zeta_3(t), \zeta_4(t)$ be the paths of the five zeros. We assume that at $t = 0$

$$\zeta_0(0) = 0.3 + 3.66i; \quad \zeta_1(0) = 1.61 + 2.72i; \quad \zeta_2(0) = 3.5 + 2.9i;$$
$$\zeta_3(0) = 3.83 + 4.03i; \quad \zeta_4(0) = 4.89 + 0.81i. \tag{4.60}$$

These zeros obey the constraint of Eq. (3.47) and are on a torus (i.e. they are defined modulo $(10\pi)^{1/2}$).

In this case, we find numerically that

$$\zeta_0(T + t) = \zeta_1(t); \quad \zeta_1(T + t) = \zeta_4(t); \quad \zeta_4(T + t) = \zeta_2(t);$$
$$\zeta_2(T + t) = \zeta_3(t); \quad \zeta_3(T + t) = \zeta_0(t). \tag{4.61}$$

Here, all zeros follow the same path (which by definition has multiplicity $\mathfrak{M} = 5$).

In Fig. 4.19 we present the path of these zeros.

We note that after a period

$$\zeta_0(T) = \zeta_1(0); \quad \zeta_1(T) = \zeta_4(0); \quad \zeta_4(T) = \zeta_2(0);$$
$$\zeta_2(T) = \zeta_3(0); \quad \zeta_3(T) = \zeta_0(0). \tag{4.62}$$

This shows that after a period T, each zero moves to the original position of another zero. Therefore, within a period, a single zero does not follow a closed path, although the five zeros together do follow this route. Each zero returns to its original position after 5 periods

$$(\zeta_i(5T) = \zeta_i(0) \text{ where } i = 0, 1, 2, 3, 4).$$

Another example is the Hamiltonian

$$H = \begin{pmatrix} 1 & -i & 0 & 0 & 0 \\ i & 1 & 0 & 0 & 0 \\ 0 & 0 & 2 & 0 & 0 \\ 0 & 0 & 0 & 2 & 0 \\ 0 & 0 & 0 & 0 & 4 \end{pmatrix} \tag{4.63}$$

which has the eigenvalues 0 (with multiplicity 1), 2 (with multiplicity 3) and 4 (with multiplicity 1). The period $T = \pi$.

Let $\zeta_0(t), \zeta_1(t), \zeta_2(t), \zeta_3(t), \zeta_4(t)$ be the paths of the five zeros.

We assume that at $t = 0$

$$\zeta_0(0) = 0.3 + 3.66i; \quad \zeta_1(0) = 1.61 + 2.72i; \quad \zeta_2(0) = 3.03 + 4.83i;$$
$$\zeta_3(0) = 4.89 + 0.81i; \quad \zeta_4(0) = 4.29 + 2.11i. \tag{4.64}$$

These zeros obey the constraint of Eq. (3.47) and are on a torus (i.e. they are defined modulo $(10\pi)^{1/2}$).

In this case, we find numerically that

$$\begin{aligned}&\zeta_0(T+t)=\zeta_1(t);\quad \zeta_1(T+t)=\zeta_3(t);\quad \zeta_3(T+t)=\zeta_4(t);\\&\zeta_4(T+t)=\zeta_2(t);\quad \zeta_2(T+t)=\zeta_0(t).\end{aligned}\tag{4.65}$$

Here, all zeros follow the same path (which by definition has multiplicity $\mathfrak{M}=5$).

In Fig. 4.20 we present the path of these zeros. We note that after a period

$$\begin{aligned}&\zeta_0(T)=\zeta_1(0);\quad \zeta_1(T)=\zeta_3(0);\quad \zeta_3(T)=\zeta_4(0);\\&\zeta_4(T)=\zeta_2(0);\quad \zeta_2(T)=\zeta_0(0).\end{aligned}\tag{4.66}$$

This shows that after a period T, each zero moves to the original position of another zero. Therefore, within a period, a single zero does not follow a closed path, although the five zeros together do follow this route. Each zero returns to its original position after 5 periods

$$(\zeta_i(5T)=\zeta_i(0) \text{ where } i=0,1,2,3,4).$$

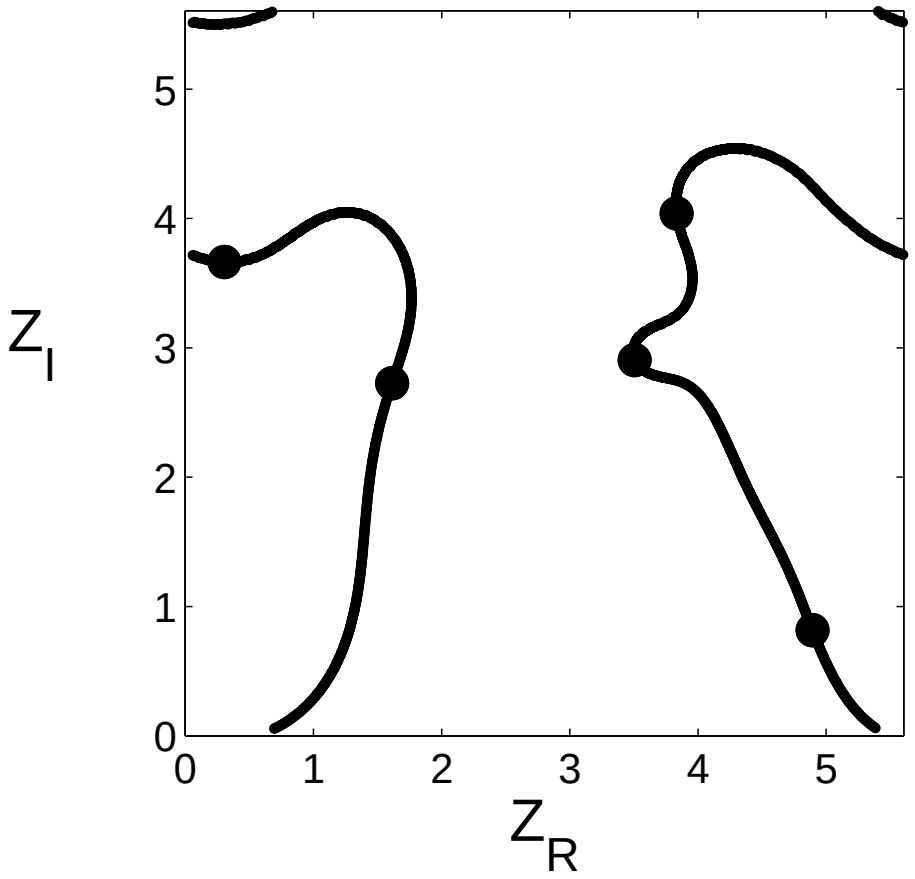

Figure 4.19: The path of the zeros $\zeta_0(t), \zeta_1(t), \zeta_2(t), \zeta_3(t), \zeta_4(t)$ for the system with the Hamiltonian of Eq. (4.46). All zeros follow the same path. At $t = 0$, the zeros $\zeta_0(0)$, $\zeta_1(0)$, $\zeta_2(0)$, $\zeta_3(0)$ and $\zeta_4(0)$ are given in Eq. (4.60) and are indicated in the diagram. After a period T, the zeros exchange positions as described in Eq. (4.62).

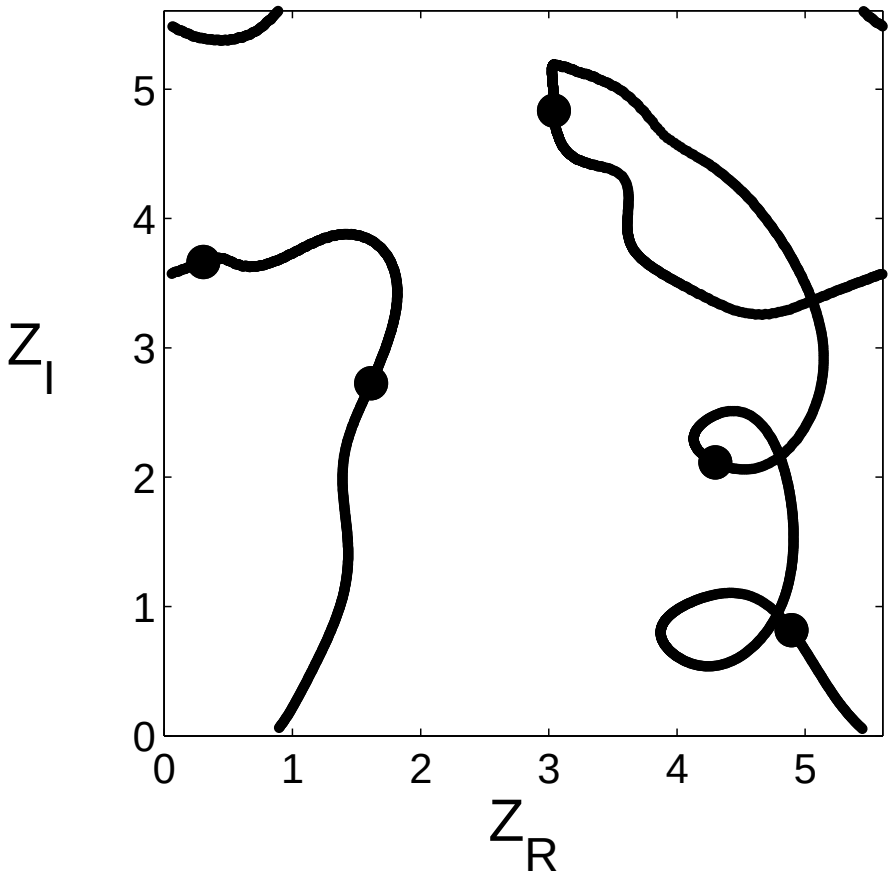

Figure 4.20: The path of the zeros $\zeta_0(t), \zeta_1(t), \zeta_2(t), \zeta_3(t), \zeta_4(t)$ for the system with the Hamiltonian of Eq. (4.63). All zeros follow the same path. At $t = 0$, the zeros $\zeta_0(0)$, $\zeta_1(0)$, $\zeta_2(0)$, $\zeta_3(0)$ and $\zeta_4(0)$ are given in Eq. (4.64) and are indicated in the diagram. After a period T, the zeros exchange positions as described in Eq. (4.66).

4.6.1 Splitting of a path with multiplicity $\mathfrak{M} = 5$ into two different paths with multiplicities $\mathfrak{M} = 4$ and $\mathfrak{M} = 1$.

In this section, we show that a small perturbation in the initial values of the zero splits the path with multiplicity $\mathfrak{M} = 5$ into two paths with multiplicities $\mathfrak{M} = 4$ and $\mathfrak{M} = 1$.

We consider the Hamiltonian

$$H = \begin{pmatrix} 1 & -i & 0 & 0 & 0 \\ i & 1 & 0 & 0 & 0 \\ 0 & 0 & 2 & 0 & 0 \\ 0 & 0 & 0 & 2 & 0 \\ 0 & 0 & 0 & 0 & 2 \end{pmatrix} \tag{4.67}$$

which has the eigenvalues 0 (with multiplicity 1) and 2 (with multiplicity 4). The period $T = \pi$.

We take two cases where the zeros at $t = 0$ are, for the first case,

$$\zeta_0(0) = 0.3 + 3.66i; \quad \zeta_1(0) = 1.26 + 2.37i; \quad \zeta_2(0) = 3.5 + 2.9i;$$
$$\zeta_3(0) = 3.83 + 4.03i; \quad \zeta_4(0) = 5.1 + 1.02i; \tag{4.68}$$

and in the second case

$$\zeta_0(0) = 0.3 + 3.66i; \quad \zeta_1(0) = 1.06 + 2.17i; \quad \zeta_2(0) = 3.5 + 2.9i;$$
$$\zeta_3(0) = 3.83 + 4.03i; \quad \zeta_4(0) = 5.3 + 1.22i. \tag{4.69}$$

These zeros obey the constraint of Eq. (3.47) and are on a torus (i.e. they are defined modulo $(10\pi)^{1/2}$).

In the case of Eq. (4.68) we get

$$\zeta_0(T+t) = \zeta_1(t); \quad \zeta_1(T+t) = \zeta_4(t); \quad \zeta_4(T+t) = \zeta_2(t);$$
$$\zeta_2(T+t) = \zeta_3(t); \quad \zeta_3(T+t) = \zeta_0(t). \tag{4.70}$$

and all zeros follow the same path with multiplicity $\mathfrak{M} = 5$, which is shown in Fig. 4.21 (broken line).

In the case of Eq.(4.69) we get

$$\zeta_0(T+t) = \zeta_1(t); \quad \zeta_1(T+t) = \zeta_4(t);$$
$$\zeta_4(T+t) = \zeta_3(t); \quad \zeta_3(T+t) = \zeta_0(t). \tag{4.71}$$

and the zero ζ_2 follows its own path (continuous lines in Fig. 4.21).

It is established that a small perturbation in the initial values of the zero splits the path with multiplicity $\mathfrak{M} = 5$ into two paths with multiplicities $\mathfrak{M} = 4$ and $\mathfrak{M} = 1$.

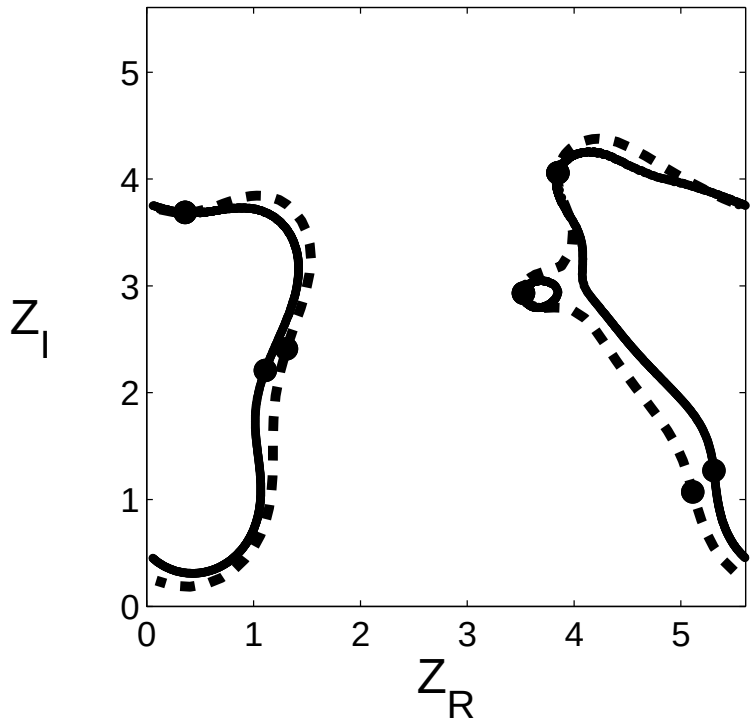

Figure 4.21: The path of the zeros $\zeta_0(t), \zeta_1(t), \zeta_2(t), \zeta_3(t), \zeta_4(t)$ for the system with the Hamiltonian of Eq. (4.67). In the case of the initial zeros of Eq. (4.68), the zeros $\zeta_0(t), \zeta_1(t), \zeta_2(t), \zeta_3(t), \zeta_4(t)$ follow the same path (broken line). In the case of the slightly different initial zeros of Eq. (4.69), the zeros $\zeta_0(t), \zeta_1(t), \zeta_3(t), \zeta_4(t)$ follow the same path and the ζ_2 follows its own path (continuous lines).

4.7 summary

In this chapter we studied periodic finite quantum systems, in which the d paths of the zeros $\zeta_n(t)$ are in general closed curves on the torus. We have seen that, in some cases, the $\mathfrak{M}$ of the d zeros follow the same path, in which case we can say that this path has multiplicity $\mathfrak{M}$. We also considered a few examples which showed that after a period the zeros exchange their positions. Furthermore, we demonstrated that the zeros obey relations like (4.12), (4.34),(4.48) and (4.61), and, after a period, they exchange their positions (Eqs(4.13), (4.35)), (4.49) and (4.62). We discussed how a perturbation of the initial values of the zeros splits a path with multiplicity $\mathfrak{M}$ into $\mathfrak{M}$ different paths. In addition, we highlighted that a small perturbation in the initial values of the zero splits the path with multiplicity $\mathfrak{M} = 2$ into two paths, while a small perturbation in the initial values of the zero splits the path with multiplicity $\mathfrak{M} = 3$ into two paths with multiplicities $\mathfrak{M} = 2$ and $\mathfrak{M} = 1$. In addition, we approximated the paths of the zeros with the quadratic equation near the point where the splitting occurs.

Chapter 5

Symplectic transformations and Zeros

In chapter 3, we have studied the analytic function of Eq. (3.29) on a torus, which has exactly d zeros and obeys the constraint of Eq. (3.47). We have seen that, as the system evolves in time, the d zeros follow d paths on the torus, which define the Hamiltonian.

In chapter 4, we studied periodic finite quantum systems. We have seen that, in some cases, the $\mathfrak{M}$ of the d zeros follow the same path. We have considered a few examples which showed that after a period the zeros exchange their positions.

In this chapter, we give a brief introduction to Symplectic transformations into the $\mathbb{Z}_d \times \mathbb{Z}_d$ phase space of a finite quantum system [20, 66]. We then move on to study the effect of Symplectic transformations of the basis on the zeros.

5.1 Introduction

The unitary transformation is a one-to-one function between two Hilbert spaces. Let A be a Hermitian matrix, and let U be a unitary transformation. It is well known that the matrix $UAU^{\dagger}$ is a Hermitian and has the same eigenvalues as A.

A unitary transformation is equivalent to a change of basis that transforms one basis into another.

In this chapter, we study the effect of a change in the basis on the zeros. As an example we consider the Symplectic transformations of a finite quantum system, which we back up with $d = 3, 5$ examples.

5.2 Symplectic transformations

We now introduce Symplectic transformations into the $\mathbb{Z}_d \times \mathbb{Z}_d$ phase space of a finite quantum system.

As such, we consider the unitary transformations

$$\begin{aligned} X^{'} &= SXS^{\dagger} = X^{\kappa}Z^{\lambda}\omega(2^{-1}\kappa\lambda) = D(\lambda,\kappa); \\ Z^{'} &= SZS^{\dagger} = X^{\mu}Z^{\nu}\omega(2^{-1}\mu\nu) = D(\nu,\mu); \end{aligned} \tag{5.1}$$

where $\lambda, \kappa, \mu, \nu$ are integers in $\mathbb{Z}_d$ and obey the relation

$$\kappa\nu - \lambda\mu = 1(mod(d)), \tag{5.2}$$

and $\omega(\alpha) = exp(i2\pi\alpha/d)$.

To calculate the operator $S(\kappa, \lambda, \mu)$, we calculate the (normalised) eigenvectors of the matrix

$$\langle X; m|Z^{'}|X; n\rangle = \omega(2^{-1/2}\nu\mu + n\nu)\delta(m, n + \mu). \tag{5.3}$$

These eigenvectors are the states $|X^{'}; m\rangle$(up to phase factors). Now we calculate the phases by starting with the eigenvector $|X^{'}; 0\rangle$, for which we can choose any phase.

We use the equation

$$(X^{'})^m|X^{'}; 0\rangle = |X^{'}; m\rangle, \tag{5.4}$$

where

$$\langle X; m|X^{'}|X; n\rangle = \omega(2^{-1/2}\kappa\lambda + n\lambda)\delta(m, n + \kappa).$$

The $|X^{'}; m\rangle$ calculated in Eq. (5.4) should differ from the $|X^{'}; m\rangle$ calculated as eigenvectors of the matrix $\langle X; m|Z^{'}|X; n\rangle$ only by a phase factor.

The operator S is given in a matrix

$$S(n, m) = \langle X; m|S|X; n\rangle.$$

We can now present examples with $d = 3, 5$.

• We consider a three-dimensional Hilbert space ($d = 3$) and $S(\kappa, \lambda, \mu) = S(1, -1, -1)$ which leads (by Eqs. (5.1) to the transformations

$$\begin{aligned} X^{'} &= SXS^{\dagger} = XZ^{-1}\omega(-\frac{1}{2}); \\ Z^{'} &= SZS^{\dagger} = X^{-1}Z^2\omega(-1). \end{aligned} \tag{5.5}$$

We calculate the matrix

$$\langle X; m|Z'|X; n\rangle =$$

$$\begin{pmatrix} 0 & -0.5 + 0.8660i & 0 \\ 0 & 0 & 1 \\ -0.5 - 0.8660i & 0 & 0 \end{pmatrix} \tag{5.6}$$

The (normalised) eigenvectors of the matrix in the Eq. (5.6) are

$$\begin{pmatrix} 0.5774 & 0.5774 & 0.5774 \\ -0.2887 - 0.5i & -0.2887 + 0.5i & 0.5774 \\ -0.2887 - 0.5i & 0.5774 & -0.2887 + 0.5i \end{pmatrix} \tag{5.7}$$

We now calculate the matrix

$$\langle X; m|X'|X; n\rangle =$$

$$\begin{pmatrix} 0 & 0 & 0.5 + 0.8660i \\ 0.5 - 0.8660i & 0 & 0 \\ 0 & -1 & 0 \end{pmatrix} \tag{5.8}$$

Then we calculate the phases by starting with the eigenvector $|X^{'};0\rangle$, for which we choose

$$|X';0\rangle \;=\; \begin{pmatrix} 0.5774 \\ -0.2887+0.5i \\ 0.5774 \end{pmatrix} \tag{5.9}$$

We use the matrix $X^{'}$ in Eq. (5.8) to calculate

$$(X')^m|X';0\rangle = |X';m\rangle; \quad m=1,2.$$

The operator S is given in a matrix $S(n,m)$. The matrix elements $S(n,m)$ are given in Table 5.1.

	$m=0$	$m=1$	$m=2$
$n=0$	z_1	$-z_2^*$	z_1
$n=1$	z_2	$-z_2$	z_1
$n=2$	z_1	$-z_2$	z_2

Table 5.1: The coefficients $S(n,m)$ for the transformations of Eq. (5.5). Here $z_1 = 0.5774$; $z_2 = -0.2887 + 0.5i = z_1\omega(1)$; $\omega(1) = \exp(i2\pi/3)$.

- We consider a five-dimensional Hilbert space ($d = 5$) and $S(1,2,3)$, which leads (by Eqs. (5.1)) to the transformations

$$X' = SXS^\dagger = XZ^2\omega(1);$$
$$Z' = SZS^\dagger = X^3Z^2\omega(3). \tag{5.10}$$

We calculate the matrix

$$\langle X; m|Z'|X; n\rangle =$$

$$\begin{pmatrix} 0 & 0 & -0.8090 + 0.5878i & 0 & 0 \\ 0 & 0 & 0 & 0.3090 - 0.9511i & 0 \\ 0 & 0 & 0 & 0 & 0.3090 + 0.9511i \\ -0.8090 - 0.5878i & 0 & 0 & 0 & 0 \\ 0 & 1 & 0 & 0 & 0 \end{pmatrix} \tag{5.11}$$

The (normalised) eigenvectors of the matrix in the Eq. (5.11) are

$$\begin{pmatrix} 0.4472 & 0.1382 - 0.4253i & 0.1382 + 0.4253i & 0.1382 + 0.4253i & -0.3618 - 0.2629i \\ 0.1382 + 0.4253i & -0.3618 - 0.2629i & .4472 & 0.1382 + 0.4253i & 0.4472 \\ 0.1382 + 0.4253i & 0.1382 - 0.4253i & -0.3618 - 0.2629i & .4472 & 0.1382 + 0.4253i \\ 0.4472 & 0.4472 & 0.4472 & -0.3618 - 0.2629i & 0.1382 + 0.4253i \\ -0.3618 - 0.2629i & .4472 & 0.1382 + 0.4253i & 0.4472 & 0.4472 \end{pmatrix}$$

We Now calculate the matrix

$$\langle X; m|X'|X; n\rangle =$$

$$\begin{pmatrix} 0 & 0 & 0 & 0 & 0.3090 - 0.9511i \\ 0.3090 + 0.9511i & 0 & 0 & 0 & 0 \\ 0 & -0.8090 - 0.5878i & 0 & 0 & 0 \\ 0 & 0 & 1 & 0 & 0 \\ 0 & 0 & 0 & -0.8090 + 0.5878i & 0 \end{pmatrix} \tag{5.13}$$

Then we calculate the phases by starting with the eigenvector $|X^{'}; 0\rangle$, for which we choose

$$|X'; 0\rangle \;=\; \omega^2 \begin{pmatrix} 0.1382 + 0.4253i \\ 0.4472 \\ -0.3618 - 0.2629i \\ 0.4472 \\ 0.1382 + 0.4253i \end{pmatrix} = \begin{pmatrix} -0.3618 - 0.2628i \\ -0.3618 + 0.2629i \\ 0.4472 \\ -0.3618 + 0.2629i \\ -0.3618 - 0.2628i \end{pmatrix}; \tag{5.14}$$

We use the matrix $X^{'}$ in Eq. (5.13) to calculate $(X')^m\ |X'; 0\rangle = \ |X'; m\rangle; \quad m = 1, 2, 3, 4.$

The operator S is given in a matrix $S(n, m)$. The matrix elements $S(n, m)$ are given in Table 5.2.

	m= 0	m= 1	m=2	m=3	m=4
n= 0	z_3	z_3^*	z_3	z_2^*	z_2^*
n= 1	z_3^*	z_2	z_3	z_2	z_3^*
n=2	z_1	z_1	z_3^*	z_2^*	z_3^*
n=3	z_3^*	z_1	z_1	z_3^*	z_2^*
n=4	z_3	z_2	z_3^*	z_3^*	z_2

Table 5.2: The coefficients $S(n, m)$ for the transformations of Eq. (5.10). Here $z_1 = 0.4472$; $z_2 = 0.1382 - 0.4253i = z_1\omega(-1)$; $z_3 = -0.3618 - 0.2629i = z_1\omega(-2)$; $\omega(1) = \exp(i2\pi/5)$.

5.3 The effect of a change in the basis on the zeros: Example with Symplectic transformations

The transformation with operator S on the analytic function $f(z)$

$$f(z) = \pi^{-1/4} \sum_{m=0}^{d-1} F_m \, \vartheta_3 \left[\pi m d^{-1} - z\pi^{1/2}(2d)^{-1/2}; id^{-1} \right] \qquad (5.15)$$

can be expressed as

$$Sf(z) \longrightarrow \pi^{-1/4} \sum_{m=0}^{d-1} S_{ml} F_l \, \vartheta_3 \left[\pi m d^{-1} - z\pi^{1/2}(2d)^{-1/2}; id^{-1} \right]. \qquad (5.16)$$

We denote as ζ_n the zeros of function $f(z)$ and we denote as η_n the zeros of function

$$g(z) = \pi^{-1/4} \sum_{m=0}^{d-1} S_{ml} F_l \, \vartheta_3 \left[\pi m d^{-1} - z\pi^{1/2}(2d)^{-1/2}; id^{-1} \right]. \qquad (5.17)$$

In order to provide some examples, we demonstrate the distributions of zeros for three different cases

• We consider a three-dimensional Hilbert space ($d = 3$) and The operator S in Table 5.1.

We assume that the initial zeros of $f(z)$ are

$$\zeta_0(0) = 1.5 + 2.5i; \quad \zeta_1(0) = 2.5 + 3i; \quad \zeta_2(0) = 2.51 + 1.01i. \qquad (5.18)$$

Then the initial zeros of $g(z)$ are

$$\eta_0(0) = 1.15 + 0.93i; \quad \eta_1(0) = 1.95 + 3.71i; \quad \eta_2(0) = 3.46 + 1.93i. \quad (5.19)$$

In Fig. 5.1 we present the zero of $f(z)$ (circles) and the zeros of $g(z)$ (triangles).

• We consider a five-dimensional Hilbert space ($d = 5$) and The operator S in Table 5.2.

We assume that the initial zeros of $f(z)$ are

$$\zeta_0(0) = 0.66 + 1.64i; \quad \zeta_1(0) = 1.68 + 4.39i; \quad \zeta_2(0) = 3.52 + 1.07i;$$
$$\zeta_3(0) = 2.91 + 2.99i; \quad \zeta_4(0) = 5.36 + 4.04i. \quad (5.20)$$

Then the initial zeros of $g(z)$ are

$$\eta_0(0) = 0.71 + 2.22i; \quad \eta_1(0) = 2.65 + 2.32i; \quad \eta_2(0) = 1.99 + 4.88i;$$
$$\eta_3(0) = 4.13 + 3.87i; \quad \eta_4(0) = 4.66 + 0.84i. \quad .(5.21)$$

In Fig. 5.2 we present the zero of $f(z)$ (circles) and the zeros of $g(z)$ (triangles).

• We consider a five-dimensional Hilbert space ($d = 5$) and The operator S in Table 5.2.

We assume that the initial zeros of $f(z)$ are

$$\zeta_0(0) = \zeta_1(0) = \zeta_2(0) = \zeta_3(0) = \zeta_4(0) = 2.8025 + 2.8025i. \quad (5.22)$$

Then the initial zeros of $g(z)$ are

$$\eta_0(0) = 0.46 + 2.43i; \quad \eta_1(0) = 1.72 + 5.04i; \quad \eta_2(0) = 2.97 + 2.11i;$$
$$\eta_3(0) = 3.61 + 0.57i; \quad \eta_4(0) = 5.36 + 3.97i. \qquad .(5.23)$$

In Fig. 5.3 we present the zero of $f(z)$ (circle) and the zeros of $g(z)$ (triangles).

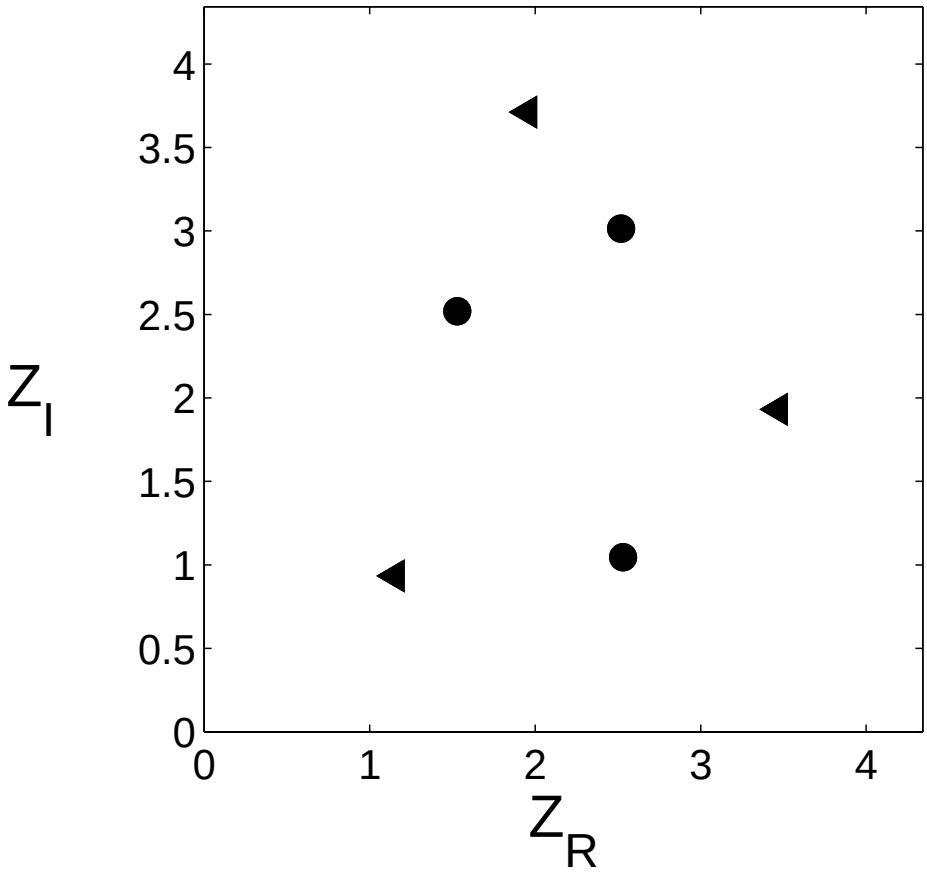

Figure 5.1: The zero of $f(z)$(circles). At $t = 0$, the zeros $\zeta_0(0)$, $\zeta_1(0)$ and $\zeta_2(0)$ are given in Eq. (5.18). The zeros of $g(z)$(triangles). At $t = 0$, the zeros $\eta_0(0)$, $\eta_1(0)$ and $\eta_2(0)$ are given in Eq. (5.19).

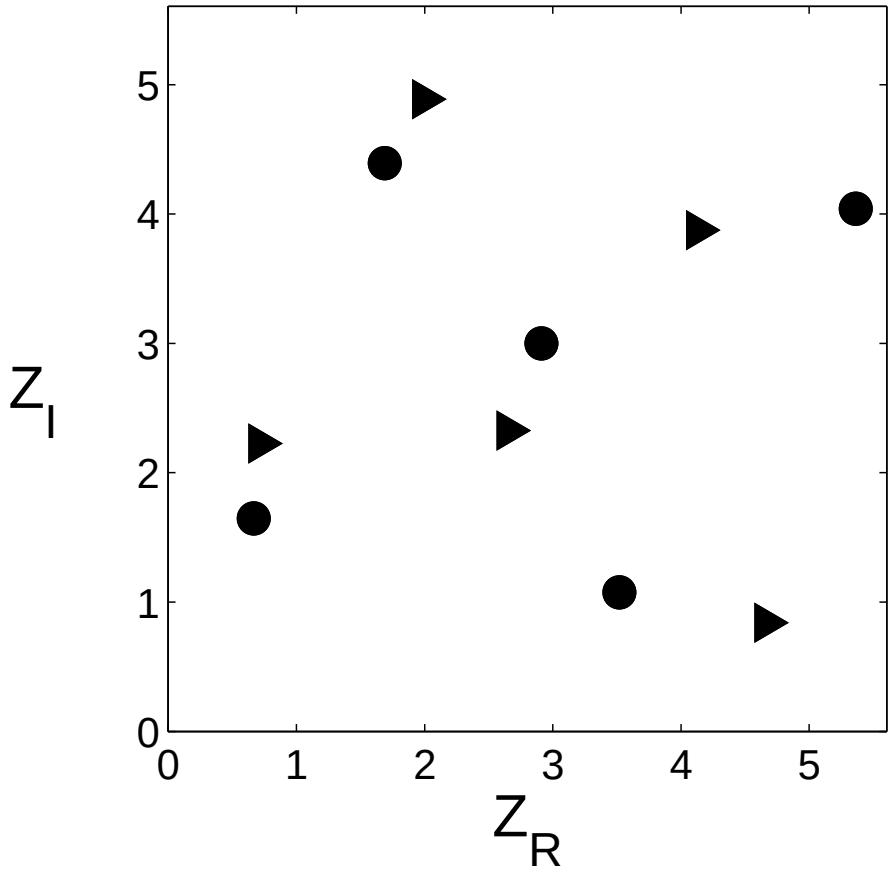

Figure 5.2: The zero of $f(z)$(circles). At $t = 0$, the zeros $\zeta_0(0)$, $\zeta_1(0)$, $\zeta_2(0)$,$\zeta_3(0)$ and $\zeta_4(0)$ are given in Eq. (5.20). The zeros of $g(z)$(triangles). At $t = 0$, the zeros $\eta_0(0)$, $\eta_1(0)$, $\eta_2(0)$,$\eta_3(0)$ and $\eta_4(0)$ are given in Eq. (5.21).

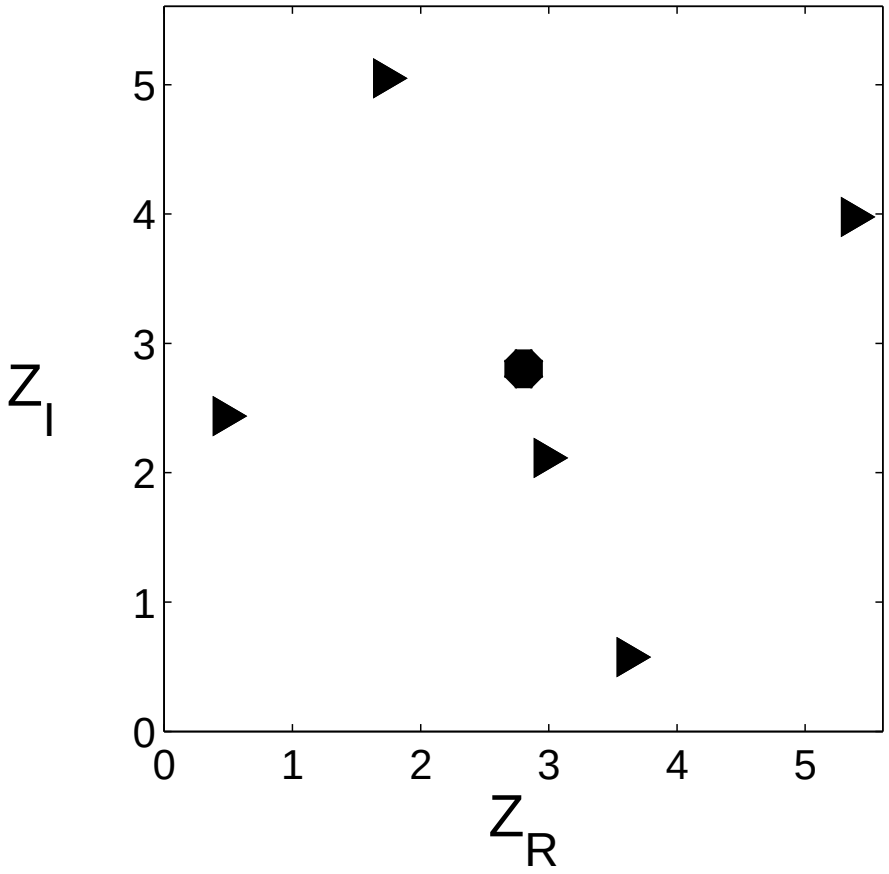

Figure 5.3: The zero of $f(z)$(circle). At $t = 0$, the zeros $\zeta_0(0)$, $\zeta_1(0)$, $\zeta_2(0)$,$\zeta_3(0)$ and $\zeta_4(0)$ are given in Eq. (5.22). The zeros of $g(z)$(triangles). At $t = 0$, the zeros $\eta_0(0)$, $\eta_1(0)$, $\eta_2(0)$,$\eta_3(0)$ and $\eta_4(0)$ are given in Eq. (5.23).

5.4 summary

In this chapter we studied the Symplectic transformations into the $\mathbb{Z}_d \times \mathbb{Z}_d$ phase space of a finite quantum system. In addition, to highlight some examples, we calculated the operator $S(\kappa, \lambda, \mu)$ for the cases $d = 3$ and $d = 5$.

Furthermore, we considered the effect of Symplectic transformations of the basis on the zeros. A unitary transformation is equivalent to a change of basis that transforms one basis into another. various examples have been given. We note here that further work is required, on the effect of a change in the basis on the paths of the zeros.

Chapter 6

Conclusion

In the present work we considered quantum systems with positions and momenta in $\mathbb{Z}_d$. Extensive work was carried out on the zeros of analytic representation of finite quantum systems in terms of Theta functions on a torus. Quantum states were represented with the analytic function of Eq. (3.29) on a torus. This analytic function, which has exactly d zeros, obeyed the constraint of Eq. (3.47). These zeros define uniquely the quantum state. We stress here that the zeros in analytic representations in systems with an infinite dimensional Hilbert space (e.g. in the Bargmann representation) do not define uniquely the quantum state. The d paths $\zeta_n(t)$ of the zeros, however, define completely the finite quantum system. We gave several examples of the distributions of zeros of analytic functions, and studied the time evolution of the system and the motion of the d zeros on the torus. As the system evolves in time, the d zeros follow d paths on the torus, which define the Hamiltonian. We gave various examples of the paths $\zeta_n(t)$ of the zeros, for various Hamiltonians. We also considered the inverse problem, where

the paths $\zeta_n(t)$ of the $d-1$ zeros were given (the path of the last zero is determined by the constraint of eq. (3.47)), and we calculated the Hamiltonian. The work shows that the paths of the zeros provide an alternative description for standard quantum formalism for finite quantum systems. In periodic systems, the d paths of the zeros $\zeta_n(t)$ are in general closed curves on the torus. Furthermore, we considered the case where $\mathfrak{M}$ of the zeros follow the same path. We say that this path has multiplicity $\mathfrak{M}$. We also considered the case of paths with multiplicity $\mathfrak{M}$, and presented examples with $\mathfrak{M} = 1, 2, 3, 4, 5$. It was established that the zeros satisfy relations like (4.12), (4.34),(4.48) and (4.61). Moreover, after a period the zeros exchange their positions (Eqs. (4.13), (4.35), (4.49) and (4.62)). We also discussed how a perturbation of the initial values of the zeros splits a path with multiplicity $\mathfrak{M}$ into $\mathfrak{M}$ different paths. It was evidenced that a small perturbation in the initial values of the zero splits the path with multiplicity $\mathfrak{M} = 2$ into two paths and a small perturbation in the initial values of the zero splits the path with multiplicity $\mathfrak{M} = 3$ into two paths with multiplicities $\mathfrak{M} = 2$ and $\mathfrak{M} = 1$. Furthermore, we highlighted that a small perturbation in the initial values of the zero splits the path with multiplicity $\mathfrak{M} = 4$ into two paths with multiplicities $\mathfrak{M} = 2$ and a small perturbation in the initial values of the zero splits the path with multiplicity $\mathfrak{M} = 5$ into two paths with multiplicities $\mathfrak{M} = 4$ and $\mathfrak{M} = 1$. In addition, we approximated the paths of the zeros with the quadratic equation near the point where the splitting occurs.

Finally, we briefly introduced the Symplectic transformations into the $\mathbb{Z}_d \times \mathbb{Z}_d$ phase space of a finite quantum system. We also studied the effect of Symplectic transformations of the the basis on the zeros.

6.1 Further Work

The work may be extended to study the effect of a change in the basis on the paths of the zeros using Symplectic transformations. The work may be also be extended to study the effect of a change in the basis on the paths of the zeros using various unitary transformations.

List of Figures

List of Tables

References

Bibliography

[1] A. M. Perelomov. Generalized Coherent States and Their Applications. Springer-Verlag, Berlin, 1986.

[2] A. Vourdas. Analytic representations in quantum mechanics. J. Phys. A: Math. Gen., 39:R65, 2006.

[3] A. Vourdas and R. F. Bishop. Thermal coherent states in the Bargmann representation. Phys. Rev. A, 50:3331, 1994.

[4] V. Bargmann. On a Hilbert space of analytic functions and an associated integral transform Part I. Commun. Pure Appl. Math., 14:187, 1961.

[5] V. Bargmann. On a Hilbert space of analytic functions and an associated integral transform Part II. Commun. Pure Appl. Math., 120:1, 1967.

[6] S. Schweber. On the application of Bargmann Hilbert spaces to dynamical problems. Ann. Phys., 41:205, 1967.

[7] A. Vourdas. The completeness of sequences of coherent state. J. Opt. B,5:S413, 2003.

[8] J. Kurchan, P. Leboeuf, and M. Saraceno. Semiclassical approximations in the coherent-state representation. Phys. Rev. A, 40:6800, 1989.

[9] A. Voros. Wentzel-Kramers-Brillouin method in the Bargmann representation. Phys. Rev. A, 40:6814, 1989.

[10] J. H. Hannay. Chaotic analytic zero points: exact statistics for those of a random spin state. J. Phys. A: Math. Gen., 29:L101, 1996.

[11] J. H. Hannay. The chaotic analytic function. J. Phys. A:Math. Gen., 31:L755, 1998.

[12] N. L. Balazs and A. Voros. Chaos on the pseudosphere. Phys. Rep., 143:109, 1986.

[13] P. Leboeuf and A. Voros. Chaos-revealing multiplicative representation of quantum eigenstates. J. Phys. A, 23:1765, 1990.

[14] P. Leboeuf. Phase space approach to quantum dynamics. J. Phys. A: Math. Gen., 24:4575, 1991.

[15] M. B. Cibils, Y. Cuche, P. Leboeuf, and W. F. Wreszinski. Zeros of the Husimi functions of the spin-boson model. Phys. Rev. A, 46:4560, 1992.

[16] J. M. Tualle and A. Voros, Chaos. Normal modes of billiards portrayed in the stellar (or nodal) representation. Solitons and Fractals. 5:1085, 1995

[17] S. Nonnenmacher and A. Voros. Chaotic eigenfunctions in phase space. J. Phys. A, 30:L677, 1997.

[18] H. J. Korsch, C. Múller, and H. Wiescher. On the zeros of the Husimi distribution. J. Phys. A:Math. Gen., 30:L677, 1997.

[19] F. Toscano and A. M. O. de Almeida. Geometrical approach to the distribution of the zeros for the Husimi function. J. Phys. A:Math. Gen., 32:6321, 1999.

[20] A. Vourdas. Finite quantum systems. Rep. Prog. Phys., 67:267, 2004.

[21] S. Zhang and A. Vourdas. Analytic representation of finite quantum systems. J. Phys. A: Math. Gen., 37:8349, 2004.

[22] S. Zhang and A. Vourdas. Analytic representation of finite quantum systems. J. Phys. A: Math. Gen., 38:1197, 2005(corrigendum).

[23] C. Gerry and P. Knight. Introductory Quantum Optics. Cambridge University Press, 2005.

[24] R. J. Glauber. The quantum theory of optical coherence. Phys. Rev., 130:2529, 1963.

[25] R. J. Glauber. Coherent and incoherent states of the radiation field. Phys. Rev., 131:2766, 1963.

[26] E. C. G. Sudarshan. Equivalence of semiclassical and quantum mechanical descriptions of statistical ligth beams. Phys. Rev. lett., 10:277, 1963.

[27] J. R. klauder and E. C. G. Sudarshan. Coherent States. World Scientific, Singapore, 1985.

[28] J. R. Klauder and E. C. G. Sudarshan. Fundamentals of Quantum Optics. New York: Benjamin, 1968.

[29] D. F. Walls and G. Milburn. Quantum Optics. Springer, Berlin, 1994.

[30] W. Vogel and D. G. Welsch. Lectures on Quantum Optics. Akademie-Verlag, Berlin, 1990.

[31] W. P. Schleich. Quantum Optics in Phase Space. Wiley, Berlin, 2001.

[32] E. Wigner. On the quantum correction for thermodynamic equilibrium. Phys. Rev., 40:749, 1932.

[33] H. Groenewold. On the principles of elementary quantum mechanics. Physica, 12:405, 1946.

[34] J. E. Moyal. Quantum mechanics as a statistical theory. Proc. Cambridge Philos. Soc., 45:99, 1949.

[35] Y. S. Kim and M. E. Noz. Phase Space Picture of Quantum Mechanics. Worlf Scientific, 1991.

[36] C. Zachos. Deformation quantization: Quantum mechanics lives and works in phase-space. Int. J. Mod. Phys. A, 17:297, 2002.

[37] R. P. Boas. Entire Functions. Academic Press, New York, 1954.

[38] B. Ja Levin. Distribution of Zeros of Entire Functions. American Mathematical Society, Providence, Rhode Island 1964.

[39] B. J. Levin, Lecture on Entire Functions. Rhode Island: American Mathematical Society, 1996.

[40] A. Vourdas. The growth Bargmann functions and the completeness of sequences of coherent states. J. Phys. A: Math. Gen., 30:4867, 1997.

[41] I. Segal. Mathematical characterization of the physical vacuum for a linear Bose-Einstein field. Illinois. J. Math., 6:500, 1962.

[42] J. R. Klauder. Continuous-representation theory. I. Postulates of Continuous-representation. J. Math. Phys., 4:1055, 1963.

[43] Y. Kano. A new phase-space distribution function in the statistical theory of the electromagnetic field. J. Math. Phys., 6:1913, 1965.

[44] C. L. Matha and E. Sudarshan. Relation between quantum and semicalssical description of optical coherence. Phys. Rev. B, 138:274, 1965.

[45] H. Weyl. The Theory of Group and Quantum Mechanics. New York: Dover, 1950.

[46] J. Schwinger. Unitary operator bases. Proc. Natl. Acad. Sci. USA, 46:570,1960.

[47] J. Schwinger. Quantum Kinematics and Dynamics. New York: Benjamin, 1970.

[48] F. A. Buot. Method for calculating TrH^n in solid-state theory. Phys. Rev. B, 10:3700, 1974.

[49] O. Coherent, Ph. Combe, M. Sirugue, and M. Sirugue-Collin. Astochastic treatment of the dynamics of an integer spin. J. Phys. A, 21:2875, 1988.

[50] U. Leonhardt. Quantum-state tomograhy and discrete wigner function. Phys. Rev. lett., 74:4101, 1995.

[51] J. Hannay and M. V. Berry. Quantization of linear maps on a torus-fresnel diffraction by a periodic grating. Physica D, 1:267, 1980.

[52] C. Miquel, J. P. Paz, and M. Saraceno. Quantum computers in phase space. Phys. Rev. A, 65:062309, 2002.

[53] C. Miquel at al. Interpretation of tomography and spectroscopy as dual forms of quantum computation. Nature, 418:59,2002.

[54] J. A. Vaccaro and D. T. Pagg. Wigner function for number and phase. Phys. Rev. A, 41:5156, 1990.

[55] A. Vourdas. Transformations in the angle-angular-momentum phase space. Phys. Rev. A, 43:1564, 1991.

[56] A. Vourdas. The angle-angular momentum quantum phase space. J. Phys. Rev. A, 29:4275, 1996.

[57] G. G. Athanasiu, E. G. Floratos, and S. Nicolis. Holomorphic quantization on the torus and finite quantum mechanics. J. Phys. A, 29:6737, 1996.

[58] W. K. Wootters. A wigner-function formulation of finite-state quantum mechanics. Ann. Phys., 176:1, 1987.

[59] D. Galetti and A. F. R. de Toledo Piza. An extended weyl-wigner transformation for special finite spaces. Physcia A, 149:267, 1988.

[60] K. S. Gibbons, M. J. Hoffman, and W. K. Wootters. Discrete phase space baced on finite fields. Phys. Rev. A, 70:062101, 2004.

[61] S. Zhang. Quantum Phase Space Methods and Their Applications. PhD thesis, University of Bradford, UK, August 2005.

[62] G. G. Athanasiu and E. G. Floratos. Coherent states in finite quantum mechanics. Nuclear Physics B, 425:343, 1994.

[63] J. Tolar and G. Chadzitaskos. Quantization on Z_M and coherent states over $Z_M \times Z_M$. J. Phys. A, 30:2509, 1997.

[64] I. S. Gradshteyn and I. M. Ryzhik. Table of Integrals, Series, and Products. Acadamic Press, Inc., 1994.

[65] D. Mumford. Tata Lectures on Theta I, II. Birkhauser, 1983.

[66] L. Wang, H. Al Hadhrami, and A. Vourdas. Symplectic transformations and entanglement in multipartite finite systems. Eur. Phys. J. D, 49:265, 2008.

[67] M. Tubani, A. Vourdas, and S. Zhang. Zeros in analytic representations of finite quantum systems on a torus. To appear, 2010.

[68] J. P. Keating, F. Mezzadri, and J. M. Robbins. Quantum boundary conditions for torus maps. Nonlinearty, 12:579, 1999.